Universität Trier

FACHBEREICH I – PSYCHOBIOLOGIE

RAPID, NON-GENOMIC EFFECTS OF CORTISOL ON THE FUNCTIONING OF THE HUMAN BRAIN

DISSERTATION ZUR ERLANGUNG DES DOKTORGRADES DER NATURWISSENSCHAFTEN (DR. RER. NAT.)

AUTOR:

DIPL.-PSYCH. FLORIAN STRELZYK

GUTACHTER:

PROF. DR. MED. HARTMUT SCHÄCHINGER

DR. RER. NAT. EWALD NAUMANN

TRIER, APRIL 2011

THE PRESENTED RESEARCH IN THIS THESIS WAS CONDUCTED AT THE:

DIVISION OF CLINICAL PHYSIOLOGY

INSTITUTE OF PSYCHOBIOLOGY – UNIVERSITY OF TRIER

&

PSYCHOPHYSIOLOGICAL LABORATORY

DEPARTMENT OF PSYCHOLOGY – UNIVERSITY OF TRIER

– AFFILIATION OF THE SUPERVISORS –

PROF. DR. MED. HARTMUT SCHÄCHINGER

DIVISION OF PHYSIOLOGY – INSTITUTE OF PSYCHOBIOLOGY – UNIVERSITY OF TRIER

DR. RER. NAT. EWALD NAUMANN

PSYCHOPHYSIOLOGICAL LABORATORY - DEPARTMENT OF PSYCHOLOGY – UNIVERSITY OF TRIER

THE RESEARCH PRESENTED HERE WAS SUPPORTED BY THE

INTERNATIONAL RESEARCH TRAINING GROUP "PSYCHONEUROENDOCRINOLOGY OF STRESS: FROM MOLECULES AND GENES TO AFFECT AND COGNITION".

FUNDED BY THE GERMAN RESEARCH FOUNDATION (DEUTSCHE FORSCHUNGSGESELLSCHAFT - DFG),

GRANT: GRK 1389/1.

TO MY WIFE, MY DEAREST FRIEND

What's the earth with all its art, verse, music, worth - Compared with love, found, gained, and kept?

Robert Browning

English poet (1812 - 1889)

ACKNOWLEDGEMENTS

This dissertation would not have been possible without the guidance and support of several individuals who in one way or another have contributed to the preparation and completion of the work and words of this thesis.

First and foremost, I offer my sincerest gratitude to both of my supervisors, Dr. Ewald Naumann and Prof. Dr. Hartmut Schächinger, who supported me throughout the work of my entire thesis with their patience and expert knowledge while allowing me the room to work unhindered and independently. I received the best of their (not always matching) advice which, more often than not, forced me to make up my own mind rather than solely adapting an already thought through opinion. Thank you for the methodological discussions, the trust, and the mentoring - one simply could not wish for better supervisors!

I would also like to thank Dr. Michael Hermes for both his work on the arterial spin labeling technique and for his technical advice that gave my work an early head start. I am also indebted to Dr. Steffen Richter and Dr. Monika Kölsch, who used their personal free time to provide study-related medical screenings and supervisions before and during the data acquisition, without which my pharmacological studies would not have been possible. As well, I would like to thank Helmut Peifer and Dr. Immo Curio for solving technical problems, and most of the study *ground work* would not have been possible without my student assistants Nicol Siegmund, Ricarda Bergmann, and Nicole Weber.

I am also grateful to Prof. Dr. Stefan Debener and his entire department at the University of Oldenburg for openly accepting me into their group and enhancing my scientific understanding by igniting my enthusiasm for topics previously unknown.

In my daily work, I have been blessed with a friendly and cheerful group of fellow colleagues, all of whom I want to thank for the countless lunch breaks and conversations that gave me many much needed breaks during my work.

Above all, I would like to thank my wife for her personal support and great patience at all times, followed by my parents and family who have given me their unequivocal support throughout - my mere expression of thanks does not suffice!

GENERAL ABSTRACT

Cortisol is a stress hormone that acts on the central nervous system in order to support adaptation and time-adjusted coping processes. Whereas previous research has focused on slow emerging, genomic effects of cortisol likely mediated by protein synthesis, there is only limited knowledge about rapid, non-genomic cortisol effects on *in vivo* neuronal cell activity in humans. Three independent placebo-controlled studies in healthy men were conducted to test effects of 4 mg cortisol on central nervous system activity, occurring within 15 minutes after intravenous administration. Two of the studies (N = 26; N = 9) used continuous arterial spin labeling as a magnetic resonance imaging sequence, and found rapid bilateral thalamic perfusion decrements. The third study (N = 14) revealed rapid cortisol-induced changes in global signal strength and map complexity of the electroencephalogram. The observed changes in neuronal functioning suggest that cortisol may act on the thalamic relay of non-relevant background as well as on task specific sensory information in order to facilitate the adaptation to stress challenges. In conclusion, these results are the first to coherently suggest that a physiologically plausible amount of cortisol profoundly affects functioning and perfusion of the human CNS *in vivo* by a rapid, non-genomic mechanism.

TABLE OF CONTENTS

INDEX OF FIGURES

INDEX OF TABLES

INDEX OF ABBREVIATIONS

AEP	Auditory evoked potential
ACTH	Adrenocorticotropic hormone
Ag-AgCl	Silver-silver-chloride
ANCOVA	Analyses of covariance
ANOVA	Analyses of variance
ANS	Autonomic nervous system
ASL	Arterial spin labeling
BMI	Body mass index
BOLD	Blood oxygen level dependence
CASL	Continuous arterial spin labeling
CBF	Cerebral blood flow
CI	Confidence interval
cm	Centimeter
CNS	Central nervous system
CRH	Corticotropin-releasing hormone
df	Degrees of freedom
dB	Decibel
EEG	Electroencephalogram
EPI	Echo planar imaging
ERP	Event related potential
FA	Factorial analysis
FFT	Fast Fourier analysis
fMRI	Functional magnetic resonance imaging
FOV	Field of view
g	Gram
GE	Gradient echo
GFP	Global field power
GMD	Global map dissimilarity
GR	Glucocorticoid receptor

h	Hours
HPA	Hypothalamic-pituitary-adrenocortical
Hz	Hertz
IC	Independent component
ICA	Independent component analysis
kOhm	Kilo ohm
ln	Natural logarithm
min	Minutes
ml	Milliliter
ml/100g/min	Milliliter per 100g per minute
MNI	Montrèal Neurological Institute
MR	Mineralocorticoid receptors
MRI	Magnetic resonance imaging
nmol/l	Nano mol per liter
PCA	Principle component analysis
PET	Positron emission tomography
PVN	Paraventricular nucleus of the hypothalamus
PVT	Paraventricular nucleus of the thalamus
rCBF	Regional cerebral blood flow
ROI	Region of interest
s	Seconds
SC	Saliva cortisol
SD	Standard deviation
T	Tesla
T_1	Longitudinal relaxation time
T_2	Transversal relaxation time
TE	Echo time
TR	Repetition time
µV	Microvolt
VEP	Visual evoked potential

INTRODUCTION AND OBJECTIVES OF THE THESIS

CHAPTER I

1.1 INTRODUCTION

When people talk about the *stress* in their lives it is usually understood by those around them what they mean. Finding a common definition of stress however, had been an enduring challenge since Hans Selye first coined the term for biology in his "General Adaptive Syndrome" in the mid-1930s (e.g. Selye, 1936, 1950). Since then, research on what stress is and how it can influence a person's life has progressed significantly. Today, stress is broadly defined as, "an actual or anticipated disruption of homeostasis or an anticipated threat to well-being" (Ulrich-Lai & Herman, 2009). This definition points out that stress has been found to be inherently biological and yet holds many psychological components. Biological (e.g., pain, extreme temperatures, injuries, etc.) or psychological (e.g. fear, anxiety, uncertainty, etc.) stressors both trigger physiological responses in order to support coping processes. Therefore, physiological correlates of stress (such as its endocrine responses) have been increasingly used in order to study changes in psychological phenomena and vice versa. One of the most commonly used physiological markers to assess whether or not a situation (or the anticipation thereof) elicits stress is to measure changes in the secretion of glucocorticoids.

Glucocorticoids are adrenal steroid hormones that are increasingly released during stress. They modulate a variety of psychobiological processes to support adaptation and coping to challenging situations. Many experimental investigations have focused on how glucocorticoids affect the functioning of the central nervous system (CNS) via genomic mechanisms. However, even with mounting evidence for the existence of rapid, non-genomic glucocorticoid mechanisms (recent reviews: Evanson, Herman, Sakai, & Krause, 2010; Groeneweg, Karst, de Kloet, & Joels, 2011; Haller, Mikics, & Makara, 2008) little is known about their *in vivo* functional effects on the human CNS.

1.1.1 Glucocorticoids

Glucocorticoid secretion originates from neuroendocrinological feed-back and feed-forward mechanisms of the hypothalamic-pituitary-adrenocortical (HPA) axis (Figure 1.1.1, left) which, together with the sympatho-adrenomedullary axes of the autonomic nervous system (ANS), is the primary system for reinstating and maintaining homeostasis

during stress. A breach in homeostasis can be characterized by its origin - bottom-up (physiological) brainstem mediated stress signals (e.g. pain, inflammation, extreme temperatures) or top-down (psychological) regulatory processes that involve the limbic forebrain (e.g. perceived or anticipated challenges) - yet both may result in (almost) identical neuro-endocrinological responses (Figure 1.1.1, right). The HPA axis is activated after the exposure to stress signals (i.e. stressors) that trigger hypophysiotrophic neurons in the paraventricular nucleus of the hypothalamus which secrete a number of releasing hormones, such as the corticotropin-releasing hormone (CRH) and arginine vasopressin

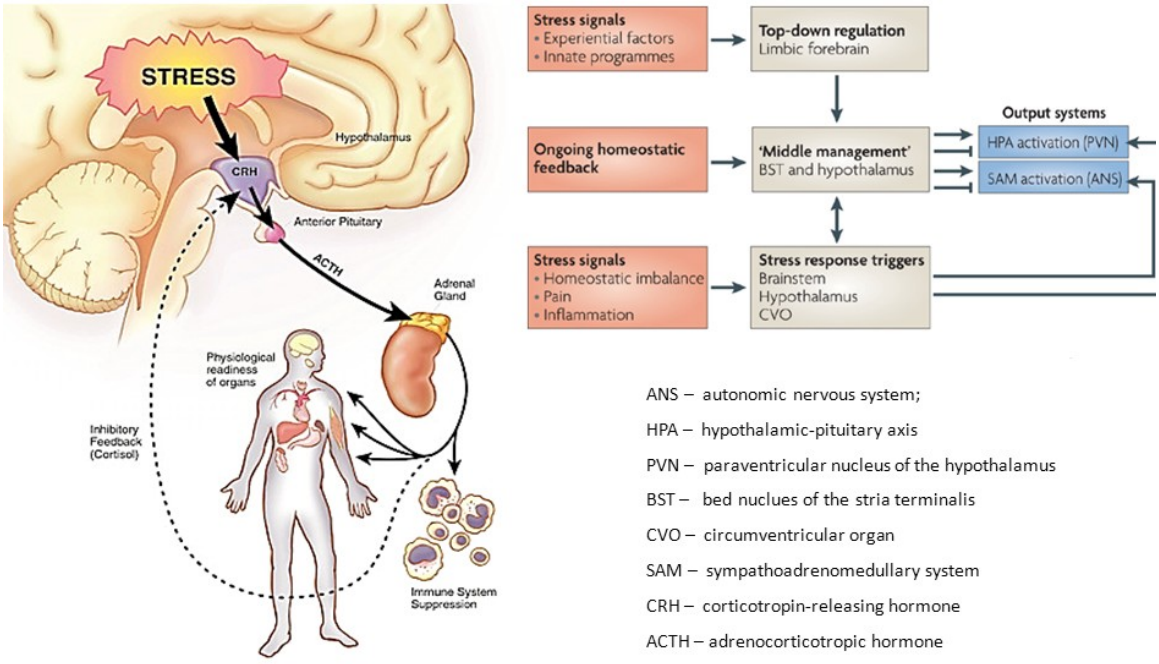

Figure 1.1.1 The endocrine stress response

Left: Depiction of hypothalamic-pituitary-adrenocortical (HPA) axis (Dryden & Fitch, 2000). **Right:** General scheme of acute stress regulation pathways. Stressors activate brainstem and/or forebrain limbic structures. The brainstem generates rapid HPA axis and ANS responses through direct projections to hypophysiotrophic neurons in the PVN or to preganglionic autonomic neurons. Forebrain limbic regions, by contrasts, have no direct connections with the HPA axis or the ANS and require intervening synapses before they can access autonomic or neuroendocrine neurons (top-down regulation). Most of these intervening neurons are located in hypothalamic nuclei that are also responsive to homeostatic status, providing a mechanism by which the descending limbic information can be modulated according to the body's physiological status ('middle management') (illustration and description adapted from: Ulrich-Lai & Herman, 2009).

(AVP), into the portal circulation of the median eminence. These releasing hormones act on the anterior pituitary in order to promote secretion of the adrenocorticotropic hormone (ACTH), which itself acts on the inner adrenal cortex and initiates the release and syntheses of glucocorticoids. Freely available glucocorticoids in the bloodstream promote the mobilization of stored energy and potentiate a number of sympathetically mediated effects, such as peripheral vasoconstriction (descriptions of HPA-axis adapted from, Ulrich-Lai & Herman, 2009). Glucocorticoids also divert energy supplies to challenged tissues and are believed to control the excitability of neuronal networks (de Kloet, Oitzl, & Joels, 1999).

The circulating glucocorticoids (cortisol in humans, corticosterone in rodents) affect the entire body including the CNS via binding to glucocorticoid receptors (GR) and mineralocorticoid receptors (MR). Both receptors act as ligand-activated transcription factors and induce slowly emerging changes in gene transcription (De Kloet, Vreugdenhil, Oitzl, & Joels, 1998) that alter protein expression, structure, and functioning of affected cells (for more detailed information about genomic cortisol mechanisms, see e.g. de Kloet, Joels, & Holsboer, 2005; Dedovic, Duchesne, Andrews, Engert, & Pruessner, 2009; McEwen & Sapolsky, 1995; Sapolsky, 1996). The MR binds glucocorticoids with a high affinity and is strongly bound even during low glucocorticoid secretion. The GR has approximately a tenth of the affinity of MRs and is extensively bound only at high levels of glucocorticoid secretion, such as during acute stress responses (de Kloet, et al., 1999). The GR is thought to be the main mediator of the (several minutes) *delayed*, genomic glucocorticoid action during stress responses. On the contrary, non-genomic effects of glucocorticoids are thought to occur within seconds to minutes after glucocorticoid release (Groeneweg, et al., 2011; Makara & Haller, 2001). Indeed, it is believed that any rapid effect that occurs within less than 15 minutes after glucocorticoid infusion cannot be mediated by changes in protein expressions (Mikics, Kruk, & Haller, 2004).

1.1.2 Non-genomic effects of glucocorticoids

The knowledge about rapid, non-genomic glucocorticoid action in the CNS is scarce and originates primarily from *in vitro* studies and animal models (e.g. Coirini, Marusic, De Nicola, Rainbow, & McEwen, 1983; De Kloet, Veldhuis, Wagenaars, &

Bergink, 1984; Ferris & Stolberg, 2010; Mikics, et al., 2004), with a few *in vivo* studies in humans (e.g. Kuehl et al., 2010; Lovallo, Robinson, Glahn, & Fox, 2009; Richter et al., 2011).

1.1.2.1 Criteria for the identification non-genomic glucocorticoid effects

Makara and Haller (2001) apply several criteria to differentiate genomic from non-genomic mechanisms that they derived from the knowledge of classical genomic mechanisms of glucocorticoids. As a simple heuristic, they argue that any glucocorticoid effects that do not match the particularities of genomic mechanisms should be considered to be another (i.e. non-genomic) mechanism. They introduce four criteria to judge whether or not effects are due to non-genomic glucocorticoid mechanisms:

(i) The temporal criterion. Genomic glucocorticoid mechanisms involve a number of time consuming steps. The translocation (10 - 30 minutes; Nishi et al., 1999; Robertson, Schulman, Karnik, Alnemri, & Litwack, 1993) of the ligand bound receptors to the nucleus and the translation and transcription (5 - 120 minutes; Cullinan, Herman, Battaglia, Akil, & Watson, 1995; Hsieh & Watanabe, 2000; Ikeda, Nakajima, Osborne, Mies, & Nowak, 1994) are the most time demanding. These time-frames suggest that the genomic effects may not become notable before at least 15 minutes have passed. In addition, it has been reported that glucocorticoid effects that are mediated through genomic inhibition require considerably longer than 15 minutes (Webster & Cidlowski, 1999). Furthermore, these relatively fast genomic effects may be exceptional, since a number of more common genomic effects are expressed after hours or even weeks after a stressful encounter (Joels & de Kloet, 1994; Makara & Haller, 2001). A final important temporal distinction of non-genomic effects involves their washout time, which is considerably shorter than for genomic actions. Since non-genomic effects depend on the interaction between the ligand and targeted substrates, their effects disappear after the dissociation of the involved molecules. As a consequence, the rapid termination of glucocorticoid effects also seems to indicate non-genomic mechanisms (Makara & Haller, 2001).

(ii) The MR/GR independence criterion. Genomic glucocorticoid effects are closely linked to their cytoplasmic receptors – the mineralocorticoid and the glucocorticoid receptor – and only their ligand complex actually activates genomic mechanisms. Thus,

genomic glucocorticoid actions can be interrupted by blocking these receptors (Joels & de Kloet, 1994). Therefore, if after blocking MR and GR the glucocorticoid effect remains intact, some other (i.e. non-genomic) mechanism must have been activated.

(iii) The genome-independence criterion. The ultimate result of genomic glucocorticoid action is either the syntheses of proteins or their blockage (in case of glucocorticoid induced gene inhibition). Thus, glucocorticoid effects cannot be genomically mediated if their effects remain unchanged after eliminating the genomic components.

(iv) The plausible physiological dose criterion. Glucocorticoid effects that occur at concentrations that exceed the physiological abilities of an organism may be interesting, but they are also irrelevant for assessing the role of glucocorticoids in controlling neural functions. Therefore, experimental manipulations resulting in brain concentrations higher than physiologically plausible should be considered irrelevant from a functional point of view (regardless if they occur rapidly or not).

Taken together, if effects (1) occur earlier than 15 minutes, (2) are not affected by MR/GR blockade, (3) do not require a genetic apparatus, and (4) are elicited by a physiologically plausible dose, then they cannot be mediated by the genomic mechanism. Generally, Makara and Haller (2001) argue that the fulfillment of just one of the first three criteria is sufficient for excluding the involvement of genomic mechanisms, e.g. effects occurring within seconds or a few minutes cannot be mediated by genomic mechanisms. Only in a few other cases do the authors propose that more than one criterion should be fulfilled (e.g. resistance to protein synthesis blockade can be used as an argument only if the process is very rapid, and/or is also resistant to MR/GR blockade).

1.1.2.2 Findings from 'in vitro' studies and animal models

The activation of stress-related neuronal networks that is caused by the perception of a threatening situation triggers the signaling cascade of the HPA axis, and plasma glucocorticoid levels begin to increase after 3 minutes. By 20 minutes, concentrations have approached maximal values (Dallman, 2005). During the first initial moments after its release, within milliseconds to minutes, rapid glucocorticoid signaling already acts on target tissues that have been found to include pons, hypothalamus,

midbrain, and limbic system. In addition, the actions of glucocorticoids influence the activity in various motor systems that are involved in the stress response. These rapid glucocorticoid actions in animal models involve increased locomotion activity, food intake, ingestion of carbohydrates, vocalization, memory, aggressive behavior, decreased sexual clasping, and ACTH secretion (cited in: Dallman, 2005).

Haller and colleagues (2008), in their review on the existing physiological evidence, propose that rapid, non-genomic glucocorticoid mechanisms are able to modify cell functioning (and ultimately the above-mentioned behaviors) by their ability to affect: "(1) membrane lipids (e.g. membrane fluidity), (2) membrane proteins (e.g. ion channels and neurotransmitter receptors), (3) intracytoplasmic proteins (e.g. mitogen- activated protein kinases, phospholipases, etc.), and (4) protein–protein interactions (e.g. secondary effects mediated by the components of the glucocorticoid receptor complex). […] (5) The [activation of the genomic] glucocorticoid transporter […]."

Derived from the above mentioned functional abilities and suggestive evidence, Haller and colleagues (2008) further propose that the purpose of non-genomic glucocorticoid actions may be to: (1) induce genomic effects, (2) affect genomic mechanisms via non-genomic action, and (3) assert influence on mechanisms that are not affected through genomic mechanisms. However, which of these purposes may turn out to be the most relevant for the adaptation to stressful situations still has to be established in further research.

The current state of the animal model literature indicates that non-genomic mechanisms of glucocorticoids influence a wide array of behavioral responses by affecting cell functioning in a large number of tissues and organs (through influencing a wide variety of intracellular processes). It is important to note that genomic and non-genomic mechanisms are not separated; instead they often act together and complementary (Haller, et al., 2008). Rapid, non-genomic effects are, therefore, an important contributor to understand the adaptation to stressors and the reinstitution of homeostasis. However, even with the large number of recent findings, non-genomic mechanisms of glucocorticoids are still poorly understood, especially in regards to their (psychophysiological) role in the human stress response.

1.1.2.3 Current findings in humans

Despite their far-reaching implications for understanding the rapid adaptation to stress, the neurophysiological correlates of the above mentioned behavioral effects in animal models have not been investigated much in humans. The reason for this may be that in addition to the above mentioned criteria for identifying non-genomic glucocorticoid effects (section 1.2.1) in humans, rapid non-genomic effects can only be studied by applying intravenous infusions. This additional criterion significantly increases the required efforts that are needed to assure the proper legal and ethical framework for running these studies in humans. To this point, only three *in vivo* studies (Kuehl, et al., 2010; Lovallo, et al., 2009; Richter, et al., 2011) have recently applied intravenous glucocorticoid infusions in humans, and only two of them have also implemented the application of appropriate doses that do not exceed physiologically plausible amounts. The following paragraphs provide more detailed information about these studies and will conclude with possible pit-falls that may compromise the detection of rapid glucocorticoid mechanisms.

In 24 healthy men, Kuehl and colleagues (2010) investigated the effects of rapid cortisol action on eyeblink conditioning after they had first stabilized the basal HPA axis activity through metyrapone (750 mg) and then intravenously infused 2 mg of cortisol (hydrocortisone). Under these (perfectly) optimized experimental conditions, accelerated learning in a trace eyeblink conditioning paradigm occurred within minutes (< 10 minutes) after cortisol administration, compared to placebo. In addition, these cortisol effects were only limited to the conditioned eyeblink responses, and there were no significant differences between the cortisol and placebo groups in any other of the eyeblink measures (e.g. spontaneous blink rate, alpha responses, non-adaptive CRs, or reactivity during familiarization). Importantly, these results suggest that rapid, non-genomic glucocorticoid (i.e. cortisol) effects can be reliably measured in humans in vivo.

Richter and colleagues (2011) were the first to demonstrate a rapid (< 15 minutes) but quickly recovering disruption of sensorimotor gating, measured with prepulse inhibition of startle in a sample of 30 healthy men, after the intravenous infusion of 1 mg of cortisol (hydrocortisone). The authors argue that the disruption of prepulse inhibition suggests a generally diminished capacity for sensorimotor gating, which in turn would

increase the ability to process threatening startle stimuli. Furthermore, a crucial practical implication was made that supports the importance of the above mentioned temporal criteria from Makara and Haller (2001) - that is: The rapid non-genomic cortisol effect and its rapid recovery suggests that stress effects on sensorimotor gating should be evaluated soon after stress induction (i.e. cortisol infusion). Experimental paradigms that pass a certain critical window in which the non-genomic effect occurs may not reveal such effects.

Just one study, by Lovallo and colleagues (2009), has assessed the effects of intravenous infusion of cortisol (10 mg; equals a dose that exceeds the physiological range) on hemodynamic changes of the brain, yet rapid (i.e. likely non-genomic) cortisol effects were not found. Instead, in 21 participants (11 women), decreases in the standard deviations relative to placebo were reported after about 25 minutes, with its maximum at about 35 minutes, for the hippocampus and the amygdala. These results match experimental findings for genomic glucocorticoid actions (van Stegeren, 2009), but why were there no rapid effects that are in line with the results of the two previously mentioned studies?

The lack of rapid cortisol effects in the third presented study suggests that an intravenous infusion may be a mandatory but not necessarily a sufficient requirement for unveiling rapid, non-genomic glucocorticoid (i.e. cortisol) mechanisms in humans. In fact, the lack of such effects implies the importance of accurately controlling for confounding (i.e. error variance inducing) variables, such as physiologically plausible infusion doses or the heterogeneity of the sample. After all, the particular strength of the above mentioned studies in vitro and with animal models (that reliably uncovered non-genomic glucocorticoid actions) is their ability to precisely control for confounding variables. Such strict controls regarding the samples seem to have been met by the first two above described studies in humans. The third study, however, used a heterogeneous sample (age range: 18 – 55 years; mixed gender; not controlled for smoking or time of data acquisition), and a non-physiological dose of cortisol, which makes it entirely possible that rapid effects may have gone undetected.

In summary, two recent studies in humans that applied intravenous infusion were able to uncover rapid, non-genomic, and stress relevant effects of cortisol. Due to their

type and nature, these effects must have a functional expression in the CNS. However, a first imaging study that would have potentially been able to uncover cortisol induced hemodynamic changes in the brain found no such effects. There is, therefore, a gap between the theoretically implied functional changes in the brain and the empirical evidence. It seems likely that this discrepancy can be overcome by applying carefully designed experimental procedures (e.g.: diminishing confounding variables, physiological infusion doses, etc.) and appropriate physiological measurements (e.g.: magnetic resonance imaging and electrophysiological measurements).

1.2 OBJECTIVE

The increasing amount of evidence for a rapid, non-genomic mode of neuronal action raises many new questions that Groeneweg and colleagues (2011) pin point in their most recent review: “Where in the brain do these rapid effects take place? What are the functional consequences for cognition and neuroendocrine control? And, importantly, how are these rapid corticosteroid actions integrated with other components of the stress response?”

The aim of three independent, placebo-controlled, and double-blinded intravenous infusion studies (presented in this thesis) was, to determine if experimental manipulations similar to naturally occurring cortisol boosts (4 mg hydrocortisone; hydrocortisone is the pharmaceutical term for synthetically produced cortisol with equal binding characteristics; from this point on infusions/interventions with hydrocortisone will be referred to as *cortisol*) may exert measurable, non-genomic effects on the human brain. With this objective, it was possible to pursue answers to the questions about where rapid, non-genomic glucocorticoid effects take place, and what the functional consequences of their mechanisms might be. Consequently, if effect sites for rapid non-genomic effects are identified, the involved receptors and neuronal pathways responsible for these effects may be more readily apparent and, therefore, testable for future research. In understanding their true attributes, rapid glucocorticoid actions may in fact turn out to be the missing link in the ability to more fully understand the normal human

stress response and eventually its pathological extremes (e.g.: post-traumatic stress disorder, or chronic depressive disorders).

The first of the three studies that was particularly aimed to explore if and where rapid, non-genomic cortisol mechanisms can actually be identified using magnet resonance imaging (MRI), will be presented in Chapter II. The above mentioned work of Lovallo and colleagues (2009) already suggested that the challenge in this may be to adequately control the experimental setting in order to assure that rapid effects are indeed tested under optimal conditions. This includes not only the application of intravenous infusions, but also measurements on a homogeneous and strictly controlled sample of participants in which any (psychophysiological) stress inducing situation is to be avoided. Besides implementing experimental procedures that would assure an adequate experimental setting, Study 1 also used a unique imaging sequence that allowed the quantification of absolute cerebral blood flow (perfusion) during resting conditions. This imaging sequence has a superior spatial localization of experimental effects compared to more commonly used MRI-sequences.

The second study, presented in Chapter III, was designed to confirm and replicate the main findings of Study 1 in an independent, but equally well controlled sample. The replication of hemodynamic effects in Study 2, in a separate group of participants, increases the reliability of the resulting interpretations and, therefore, increases its scientific value.

The third and final study in this thesis, presented in Chapter IV, was designed to confirm the existence of glucocorticoid induced and rapid functional correlates in the electroencephalogram (EEG) by assessing the spectral power of spontaneous oscillations and global markers of signal strength and topographical map complexity. In Study 3, equal care was taken to assure that the acquisition conditions were optimal for uncovering electrophysiological aspects of the hemodynamic effects of the first and second study.

Together, these studies provide evidence for the existence of rapid, non-genomic glucocorticoid actions in the human CNS.

RAPID EFFECTS OF CORTISOL ON THE PERFUSION OF THE HUMAN BRAIN

Chapter II

ABSTRACT

The stress hormone cortisol acts on the central nervous system in order to support adaptation and time-adjusted coping processes. There is only limited knowledge about rapid, non-genomic cortisol effects on *in vivo* neuronal activity in humans. Therefore, a placebo-controlled and double-blinded study in healthy men (N=26) was conducted to test effects of 4 mg cortisol on central nervous system activity, occurring within 15 minutes after intravenous administration. Since neuronal activity is very energy consuming and dependent on the supply of freshly oxygenated blood, the assessment of cerebral blood flow is well suited to indicate cortisol induced changes of such activity. Cerebral blood flow was assessed using continuous arterial spin labeling as a magnetic resonance imaging sequence, and rapid bilateral perfusion decrements in the thalamus and caudate nucleus were found. Other regions affected by the cortisol infusion were located in the frontal, occipital, and parietal lobe. The observed changes in neuronal functioning suggest (for the first time) that cortisol may act on the thalamic relay and that a physiologically plausible amount of cortisol profoundly affects perfusion of the human central nervous system *in vivo* by a rapid, non-genomic mechanism.

2.1 INTRODUCTION

The stress hormone cortisol acts on the human brain in order to support adaptation and time-adjusted coping processes to present or anticipated stressors. Despite mounting evidence from *in vitro* studies and animal models, there is only limited knowledge about rapid, non-genomic cortisol effects on *in vivo* neuronal activity in humans. Therefore, a placebo-controlled and double-blinded study in healthy men (N=26) was conducted to test effects of 4 mg cortisol on CNS activity occurring within 15 minutes after intravenous administration. Since neuronal activity is very energy consuming and dependent on the supply of freshly oxygenated blood, the assessment of hemodynamic measurements can quantify cortisol induced changes in neuronal metabolism.

Investigations of rapid hemodynamic cortisol effects on the CNS (studies in rodents and humans) have so far used blood oxygenation level dependent (BOLD) MRI sequences (e.g. Ferris & Stolberg, 2010; Lovallo, et al., 2009). At least in humans, this has not led to neuroimaging results for rapid cortisol effects (see Section 1.1.2.3 in Chapter I). BOLD uses deoxyhemoglobin as an endogenous contrast enhancing agent that serves as the source of the MRI signal (Goense & Logothetis, 2010). However, differences in MRI sequences and measurement parameters are known to influence the observed effects. For example, the overall consensus is that (1) gradient-echo BOLD (as used by Lovallo and colleagues (2009)) represents mostly a venous signal, which becomes more strongly weighted toward smaller venules and capillaries as the field strength increases, (2) spin-echo BOLD (as used in Ferris and Stolberg (2010)) represents mostly a capillary signal, the cerebral blood volume (CBV) signal is thought to represent smaller vessels (arteries and veins) and capillaries, and (3) the cerebral blood flow (CBF) signal is thought to represent mostly arterioles and capillaries (Goense & Logothetis, 2010).

The specificity of the BOLD response to local neural activation depends on the blood flow regulation that is believed to correspond with neuronal activation (Goense & Logothetis, 2010). The neurovascular response is regulated through smooth muscles and has recently been observed to be mediated by astrocytes (around capillaries), which due to their key location between vasculature and neurons are believed to contribute to changes in the CBF, and ultimately the BOLD signal (Goense & Logothetis, 2010). The

BOLD signal, however, cannot easily assess slow increasing and long lasting changes in neural activity during repetitive measurements over long periods of time (Z. Wang et al., 2008) and it is inferior in regards to its functional localization abilities (see section 2.2.3.1). Such changes, however, are well assessed by measuring cerebral blood flow (CBF) directly.

The imaging sequence of Study 1 is therefore aimed at investigating cortisol related effects on absolute CBF which also enables the assessment of longer lasting changes in neural processes, such as may be evoked by preparatory cortisol mediated coping mechanisms.

Absolute CBF is traditionally acquired utilizing expensive and invasive positron emission tomography (PET), which is limited in the duration of each measurement session due to the risk of over saturating the tissue with exogenously applied tracer substances. Therefore, CBF measurements in Study 1 were implemented using the non-invasive MRI based continuous arterial spin labeling (CASL) sequence (Williams, Detre, Leigh, & Koretsky, 1992) that avoided the disadvantages of PET (first and foremost the use of ionizing radiation). Similar to PET, CASL allows the quantification of CBF in physiological units (ml/100g/min) - both at rest as well as during activation. Section 2.2.3.1 in this Chapter will provide more in depth information about the CASL imaging sequence.

It has been reported that in women, CBF in the hippocampus was positively correlated with perceived stress during the task, while it was negatively correlated with perceived stress in men (J. Wang et al., 2007). These gender effects of stress interventions, however, are not yet understood but may originate from differences in cognitive processing or differences in gender specific physiological mechanisms. Therefore, Study 1 only investigated healthy young men in order to avoid unknown interactions with the menstrual cycle or gender specific stress processing. This also increased the statistical power compared to a mixed gender study, while keeping the required number of participants relatively low. In addition, special care was taken (during a strict screening process) to ensure a homogeneous and healthy sample of participants, and special attention was paid to avoid any (psychological) stress related arousal.

2.2 METHODS

2.2.1 Participants

Twenty-six right-handed healthy men participated (mean age = 25.54 years, SD = 2.94 years). Prior to the MRI measurements, all participants underwent a screening interview to determine if they were suitable for MR imaging. Informed consent was obtained for all participants. Exclusion criteria included cerebrovascular or cardiovascular diseases, psychiatric disorders, medication (including glucocorticoid containing substances), smoking at any point in life, other than normal body mass index (BMI), as well as any acute or chronic diseases. The study was approved by the ethics committee of Rhineland-Palatinate and was in accordance with the ethical guidelines of the Declaration of Helsinki.

2.2.2 Experimental procedure

In Study 1, participants were measured once, in a between-subjects design and were randomly assigned to either cortisol (N = 13) or placebo (N = 13) groups. Participants arrived one hour prior to the start of the MRI measurement and were lying down until entering the MRI-scanner room to ensure physical relaxation during waiting. Upon arrival, an additional medical exam assured their overall fitness on the measuring day, and a flexible IV line was placed into their right arm, which remained there until the end of the experiment. The one hour long waiting period before the start of the experiment was intended to reduce potential carry-over stress effects related to the initial pain induced by placing the intravenous infusion line. Subsequently, participants were asked to complete a number of questionnaires that obtained their general sleeping habits and their current

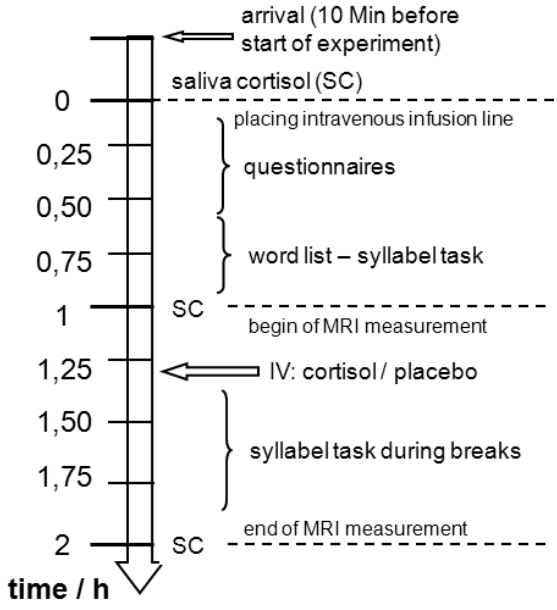

Figure 2.2.1 Overview of the general experimental procedure of Study 1

psychological state. Thirty minutes prior to MRI acquisition, all participants practiced a word discrimination task to familiarize them for a similar task in the scanner. One hour after placing the IV line, the participants entered the MRI-scanner room and were comfortably placed for the MRI-measurements, and an extension for the intravenous infusion line was attached to enable the intervention from outside the MRI-scanner room, unaware to the participant. MRI measurements lasted about one hour with four experimental measurement blocks (independent variable MEASUREMENT BLOCK) that were intermitted by three-minute long breaks. The infusion of cortisol (4mg) or physiological saline solution (placebo) (independent variable INTERVENTION) was administered from outside the scanner room in a double-blind fashion during the first break. During the two remaining breaks, participants were asked to perform the word discrimination task to keep them engaged in the experiment. The task required participants to determine if pre-recorded, audibly presented nouns had either one or two syllables (e.g. two syllables: "Thema"; one syllable: "Plan"), by button-presses of their right or left hand. The nouns were chosen to be non-emotional, non-arousing, non-descriptive, low in valence, and low in concreteness in order to avoid emotional arousal or cognitive ruminations during the CASL measurements. Participants received the pre-recorded nouns through a MRI compatible headset. After the MRI-measurement was finished, the participants completed final questionnaires, were compensated for their participation (50€), and were informed about whether they had received cortisol or placebo (see Figure 2.2.1).

2.2.3 MRI measurements

Regional cerebral blood flow (rCBF) was acquired by applying CASL – see Figure 2.2.2 – which reduces between-subject variability in activation amplitude, improves signal-to-noise ratio in regions with high static susceptibility gradients, and provides superior functional localization as compared to BOLD fMRI (Z. Wang, et al., 2008). Due to the short decay rate of the endogenous tracer, CASL measurements may be repeated many times and in short intervals. CASL allows the non-invasive quantification of rCBF in physiological units (ml/100g/min), both at rest as well as during activation. Reproducibility of CASL results has also been verified (Hermes et al., 2007).

2.2.3.1 Advantages of CASL

Absolute cerebral blood flow can be measured using magnet resonance imaging by employing arterial blood water as an endogenous, non-invasive blood flow tracer. The labeling of inflowing arterial blood, known as arterial spin labeling (ASL), is achieved through radio frequency pulses. Current applications of the ASL techniques include continuous ASL (Detre, Leigh, Williams, & Koretsky, 1992), which was used for the present study, flow-sensitive alternating inversion recovery (FAIR) (S. G. Kim, 1995; Kwong et al., 1995), and various others (Edelman et al., 1994; Wong, Buxton, & Frank, 1998). The radio frequency pulses for CASL are applied just below the imaging field of view (FOV) - the labeling plane in CASL is located 6 cm below the center of the FOV. The difference between succeeding pictures with and without a preceding labeling pulse is then used to quantify the absolute CBF (Figure 2.2.2).

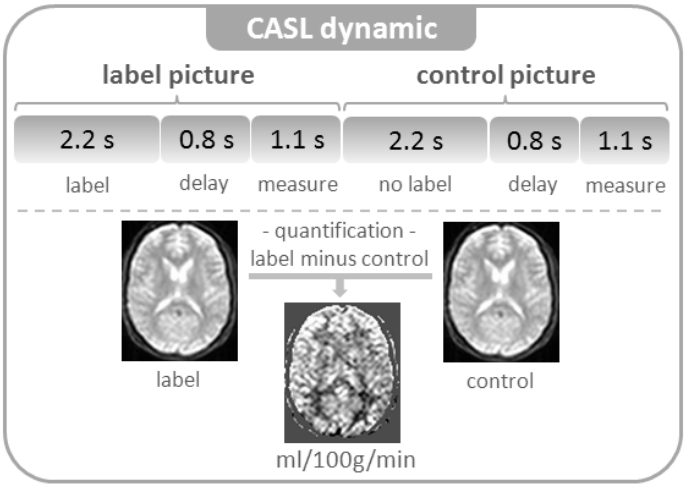

Figure 2.2.2 Simplification of a continuous arterial spin labeling (CASL) dynamic

A CASL dynamic is one pair of consecutive volume-scan acquisitions that consists of scans that were acquired after a label pulse (label picture) and scans that were acquired after the absence of a label pulse (control picture). In the subsequent quantification algorithm, the control pictures are then (among other transformations) subtracted from the labeling picture. The result is an image that contains *just* the portion of the MR-signal that can be attributed to the labeled arterial blood. Since the amount of labeling is known, this image also expresses the cerebral blood flow in the absolute physiological unit of ml per 100g of tissue per minute (ml/100g/min).

The first advantage of the CASL technique lies within the properties of the labeling itself. Most of the labeled water molecules extract into the surrounding tissues and the remainders of the labeled molecules lose most of their label by the time they reach the draining veins (S. G. Kim, Jin, & Fukuda, 2010). In fact, the labeling decays (i.e. relaxes) with the T_1 of blood and has a very short half-life. Therefore, CASL measurements can be obtained non-invasively over a very long period of time without saturating the tissue with any exogenously applied tracing substances (such as radioactive tracers that have to be intravenously infused during positron emission tomography) which would compromise signal quality.

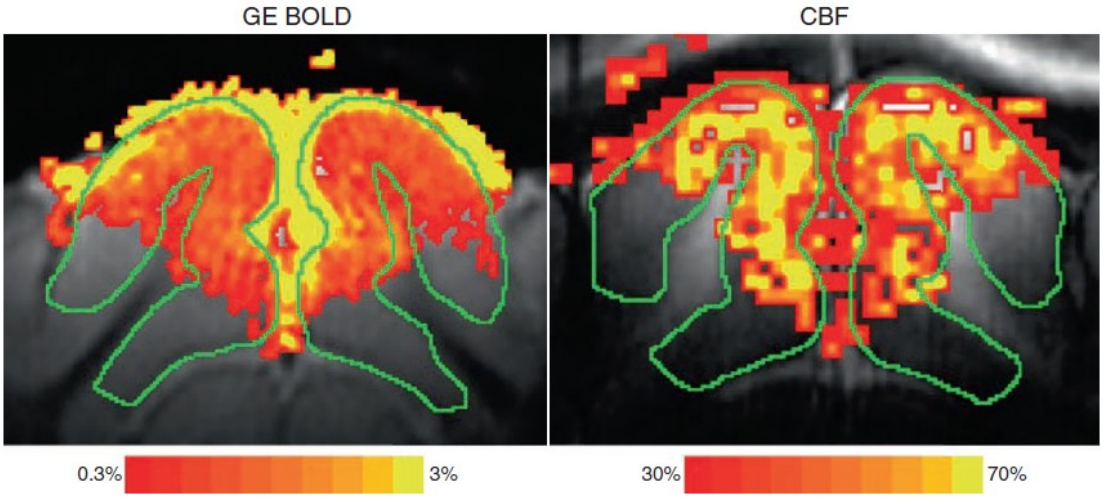

Figure 2.2.3 GE BOLD and CBF fMRI maps of a cat brain during visual stimulation overlaid on anatomical EPI images

Gray matter areas are outlined in green. The highest BOLD signal effects are observed at the surface of the cortex in the draining veins, while the highest CBF effects occur at the middle of the cortex in the capillaries (S. G. Kim, et al., 2010).

The second, and for psychophysiological studies main, advantage of CASL is that due to the short-decay of the labeling, CBF signals predominantly originate from the capillaries and the arterial vessels (T. Kim & Kim, 2005; Lee, Silva, & Kim, 2002; Ye et al., 1997). As a result, their spatial specificity is superior compared to GE BOLD techniques (Duong, Kim, Ugurbil, & Kim, 2001). For example, signal changes in more commonly used BOLD are predominantly located at draining veins as Figure 2.2.3 illustrates. Perfusion-based fMRI techniques are more specific to tissues and, therefore, are superior to GE

BOLD fMRI. In addition, ASL techniques, in general, are not as sensitive to baseline signal drifts, since slow non-activation-related signal changes are more easily removed by the pair-wise subtraction and ASL is also more stable to low-frequency stimulation as compared to BOLD. For that reason, ASL fMRI techniques are the method of choice for superior functional localization during repetitive measurements over long periods of time (S. G. Kim, et al., 2010).

The third and most practical advantage of CASL sequences is their ability to obtain CBF measurements in absolute physiological units (ml/100g/min). Other than BOLD fMRI sequences, whose particular strength it is to determine high resolution neuronal (relative) signal changes between rapidly alternating and often externally induced stimuli, CASL measurements are even meaningful in the absence of such stimulation. In fact, their particular strength is to determine neuronal activation under resting conditions without the need for externally induced (evoked) activity. CASL is able to even detect very slow signal drifts under resting conditions which cannot be easily achieved with BOLD fMRI.

In summary, CASL sequences are the method of choice for non-event related experimental settings in which it is important to precisely localize even low-frequency changes of neuronal baseline activation. This makes CASL ideal for the investigation of pharmacological glucocorticoid effects under resting conditions.

2.2.3.2 Acquisition

Imaging was performed on a clinical 1.5T scanner (Intera, Philips Medical Systems, Best, The Netherlands) with a send/receive coil provided by the manufacturer. The imaging sequences and procedures were conducted as reported by Hermes and colleagues (2009), with the exception of sequence order, scanning time, and individual M_0 measurements. Interleaved label and control images were acquired using a single-shot spin echo EPI sequence. Thirteen slices covering the whole brain were acquired [FOV = 230 mm, matrix = 64 × 64, slice thickness = 8 mm, 1 mm gap, bandwidth = 78.4 kHz, flip angle = 90°, TR/TE = 4.125/42 ms] and reconstructed to a 128 × 128 matrix. The labeling plane was placed 60mm beneath the center of the imaging slices (labeling duration=2.2s, labeling amplitude=35mG, labeling gradient=0.25G/cm). The postlabeling delay varied from 0.8 to 1.8s because each slice was acquired at a slightly different time. CBF was

measured in four consecutive CASL measurement blocks. Each of the four measuring blocks consisted of 46 individual CASL acquisitions (i.e. dynamics; scan duration: 6:50 minutes - rounded up and referred to as 7:00 minutes from here on) and was acquired while the participants kept their eyes open (see Figure 2.2.4).

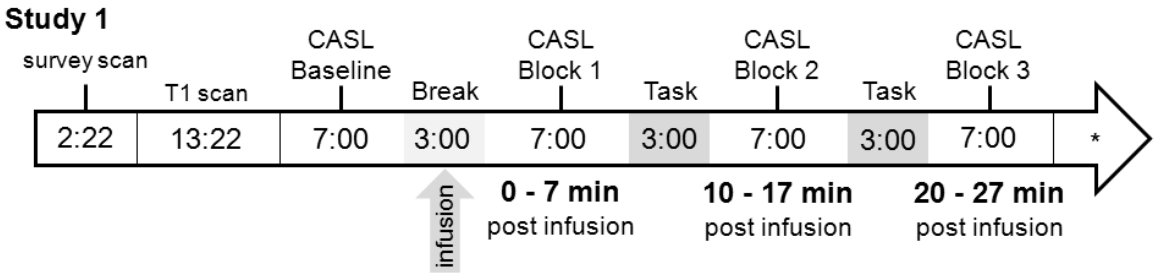

Figure 2.2.4 Order of measurements and duration (in minutes) of Study 1

(*) The experimental measurements were succeeded by an M_0 measurement (3:25 minutes) and a T_2-weighted anatomical measurement (2:54 minutes) to further control for physiological abnormalities. The time that each participant spent in the MR-scanner was about 58 minutes in total. After all MRI measurements were finished, the participants provided their final saliva sample for the manipulation check.

In order to familiarize the participant to the scanner environment, a T_1-weighted sequence (fast field echo, 160 slices, FOV = 256 × 192 mm, matrix = 256 × 256, slice thickness = 1 mm, TR/TE = 11.9 / 3.3 ms, duration: 13:22 min) was acquired prior to the CASL measurements. After the CASL measurements, a T_2-weighted image was acquired in order to control for neurological abnormalities (scan duration: 2:43 min). After the T_2-weighted image, a series of 46 M_0-images were acquired to determine the equilibrium magnetization (scan duration: 3:25 min). The same imaging parameters as in the CASL sequence (same TR, TE, etc.) were used for the M_0 measurements, except that the labeling was completely turned off.

2.2.3.3 Data Processing

Offline data processing of CASL and T_1 images was performed with the Statistical Parametric Mapping Software (SPM8, Welcome Department of Imaging Neuroscience, London UK, implemented in MATLAB 2008, The MathWorks Inc., Natick, MA, USA), using

the methods as described by Hermes and colleagues (2007) – see Figure 2.2.5 for an overview of the processing steps. First, the data was checked for gross artifacts. Since the lowest slice showed heavy low-intensity artifacts in all subjects, all voxels in this slice were set to zero and thereby excluded from CBF quantification. Next, the label, control, and M_0 images were motion corrected. During these steps no interpolation was applied to the data, but a set of parameters was estimated, which was applied later on. Then the parameters for normalization were estimated based on the T_1 image (with the default bounding box of SPM8) and transferred to the label, control, and M_0 images. The template for normalization was the MNI 152 participant average brain (Montrèal Neurological Institute). Then, the T_1 image as well as the label, control, and M_0 images were resampled using a fourth degree B-spline interpolation, which applied the parameters derived from realignment, reorientation, and normalization. The CASL images were resampled to a voxel size of 1.8×1.8×9mm and the T_1 images to 1×1×1mm. Following these steps, label and non-label images were separately averaged for each of the four CASL acquisition blocks. The M_0 images were also averaged separately. The label, non-label, and M_0 averages were used to quantify CBF following the quantification model proposed by Alsop and Detre (1996):

$$CBF = \frac{(M_C - M_L) \cdot \lambda}{2M_0 \cdot \alpha \cdot T_{1t} \cdot exp\left(-\frac{\delta}{T_{1a}}\right)\left[exp\left(\frac{min(\delta - w, 0)}{T_{1t}}\right) - exp\left(-\frac{w}{T_{1t}}\right)\left(1 - \frac{T_{1t,RF}}{T_{1t}}\right)\right]} \quad (1)$$

where CBF is the cerebral blood flow in ml/100 g/min; M_L is the tissue magnetization in the label pictures; λ is the brain-blood partition coefficient of water which was set to 0.98 for gray matter and 0.82 for white matter (Herscovitch & Raichle, 1985; Roberts, Rizi, Lenkinski, & Leigh, 1996); M_0 is the equilibrium magnetization; α is the labeling efficiency (α = 0.71) (Friston, Ashburner, et al., 1995); T_{1t} is the T_1 of brain tissue which was set to 1 s for gray matter and 0.6 s for white matter; δ is the assumed arterial transit time from the labeling plane to the imaged slice (δ = 1.2 s); T_{1a} is the T_1 of arterial blood (T_{1a} = 1.4 s); w is the post-labeling delay (Alsop & Detre, 1996) which varies from 0.8 to 1.8 s because each slice is acquired at a slightly different time; $T_{1t,RF}$ is the T_1 of brain tissue in the

presence of the labeling pulse which was set to 0.75 s for gray matter (Oguz et al., 2003) and 0.45 s for white matter. These parameters are identical to the ones used by Hermes and colleagues (2007).

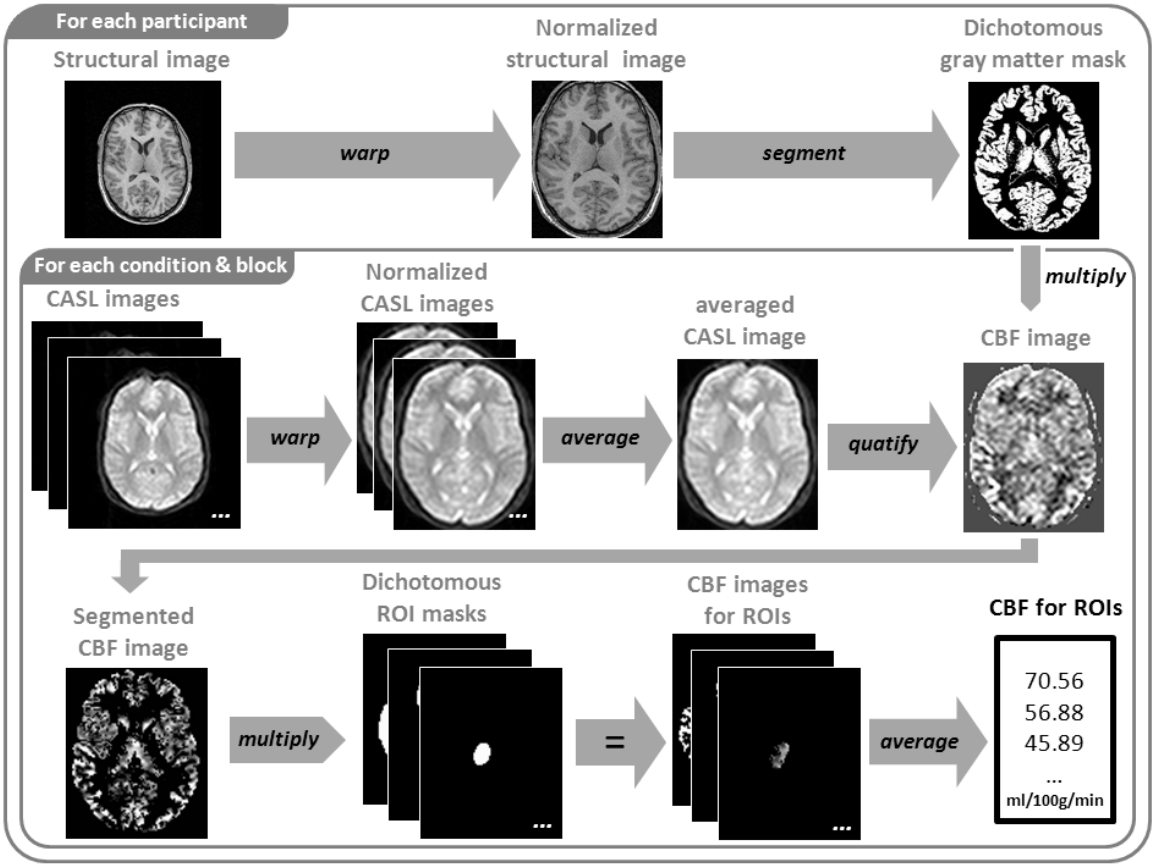

Figure 2.2.5 Overview of data processing steps to obtain CBF for individual ROIs

Realigning and co-registering steps were omitted in this schematic depiction. For each experimental condition and measurement block per participant, the CBF of 45 ROIs was obtained for each hemisphere after quantification on the basis of dichotomous gray matter and ROI masks.

After quantification, T_1 images were segmented and converted into dichotomous gray matter masks. These gray matter masks were multiplied with the CBF images which resulted in CBF maps for gray matter. *Primary ROIs* consisted of regions of the limbic lobe, and the subcortical gray because these structures are likely to be involved in fast cognitive stress effects (Dedovic, et al., 2009; Sutanto, van Eekelen, Reul, & de Kloet, 1988). However, since glucocorticoid binding sites are distributed throughout the entire brain (Sanchez, Young, Plotsky, & Insel, 2000) *secondary ROIs* consisted of all regions in

the frontal, temporal, parietal, and occipital lobe, and central region. *Primary* and *secondary ROIs* together consisted of 45 regions (independent variable REGION) as defined based on published templates (Tzourio-Mazoyer et al., 2002), and were used to create dichotomous ROI masks. ROIs were grouped by their superordinate lobe or area location to classify them according to their anatomical relationship - see MARINA (Walter et al., 2003) toolbox or Appendix A for region labels. Finally, the ROI masks were multiplied with the gray matter CBF images and the mean rCBF for each hemisphere (independent variable HEMISPHERE) in each ROI was calculated intra-individually (see Figure 2.2.5).

In addition, images for the voxel-based result presentations were generated by spatially smoothing the unsegmented CBF images of each acquisition block with a 6×6×12mm full width at half maximum kernel.

2.2.4 Manipulation checks

Acute HPA axis activity was obtained through three saliva samples per session to check if the pharmacological manipulation succeeded. Participants provided their first sample upon arrival, the second before entering the MRI scanning room, and the third after the last MRI sequence (independent variable TIME). All samples were immediately frozen for biochemical analysis. Salivary cortisol was analyzed with an immunoassay with fluorescence detection (see Dressendorfer, Kirschbaum, Rohde, Stahl, & Strasburger, 1992). Intra- and inter-assay variability was less than 10 and 12% respectively, and this reliability was suited for further statistical analyses.

2.2.5 Statistical analyses

2.2.5.1 Manipulation check

For Study 1, the pharmacological manipulation was assessed via an analysis of variance (ANOVA) with the variables INTERVENTION (cortisol, placebo) and measurement TIME (arrival, before MRI, after MRI) in a mixed between-subject factorial design.

2.2.5.2 ROI analyses

A ROI based approach decreased the likelihood of false-positive results during the brain wide result exploration.

Study 1 assessed individual rCBF averages of each ROI by performing Analyses of Covariance (ANCOVA) in order to avoid multiple t-tests between the ROIs, control for the compounding error rates, and increase the statistical power of the analyses. Baseline rCBF (-7 to 0 min before cortisol infusion) were intra-individually subtracted from the remaining three CASL measurement blocks to obtain the absolute change of rCBF relative to baseline of each ROI. This accounted for naturally occurring personal baseline differences between participants which, in Study 1, reached from 61.12 to 91.44 ml/100g/min in global gray matter CBF. Baseline corrected rCBF values were used for all further ANCOVA.

A separate ANCOVA was performed for each anatomical lobe or area of the *target* and *exploratory ROIs,* entering the factors INTERVENTION (cortisol, placebo)*,* MEASUREMENT BLOCK (0 - 7 min, 10 - 17 min, 20 - 27 min post infusion), REGION (according to ROIs), and HEMISPHERE (left, right). This led to two ANCOVAs for the *target ROIs* (limbic lobe with 7 ROIs, and subcortical gray with 6 ROIs), and five ANCOVAs for the *exploratory ROIs* (frontal lobe with 13 regions; central region with 3 regions; occipital lobe with 7 regions; parietal lobe with 5 regions; and temporal lobe with 4 regions). In all ANCOVAs a Huynh–Feldt correction of the degrees of freedom was performed whenever appropriate. Significant effects (alpha < 0.05) were further analyzed using Dunn's Multiple Comparison Procedure (Dunn, 1961) as posthoc analyses and the critical differences (ψ) for $p < .05$, $p < .01$, and the number of comparisons (*C*) are stated. For the interaction, INTERVENTION x MEASUREMENT BLOCK x REGION, for example, three comparisons per ROI were observed, namely the difference between cortisol and placebo in the three post intervention CASL measurement blocks. The number of comparisons (C) for testing a significant effect in the ANCOVA of the subcortical gray ROIs would then be 18 (3 CASL measurement blocks * 6 ROIs). All the ANCOVA analyses contained the individual CASL baseline perfusion of the gray matter CBF images as a covariate in order to reduce unexplained statistical variance (i.e. error variance) that can be attributed to differences in baseline perfusion.

The presentation of results will be limited to significant ($p < .05$) intervention related effects only and according degrees of freedom (df_{effect}; df_{error}), and the effect size measure *partial* η^2 (Cohen, 1988) are reported. All statistical analyses were performed with SPSS for Windows (Version 17, SPSS Inc.).

2.2.5.3 Voxel based analyses

A voxel-based analysis was set up for the primary ROIs within the framework of the general linear model (Friston, Holmes, et al., 1995), which is employed in SPM8. The voxel based analysis is much less sensitive to statistical effects than the ROI analyses, yet it is used to only visualize the localization of the effects of the main ROI analyses. Therefore, it is not meant to substitute ROI analyses, but it is to compliment the visualization of its results. The reasoning for this visualization is the theoretical possibility that an effect that is located on the border of two neighbouring ROIs is cut in half during the ROI definition procedure. The effect can then either (1) lose its power and not show up statistically (a statistical dilution), or on the contrary (2) it might be strong enough to induce a statistical effect into (the border region of) a ROI which in reality harbours no effect at all (a statistical wash-in). Cases of split effects (wash-in) would be more difficult to interpret but they are possible and need to be explored and excluded as possible sources for false-positive ROI effects.

The mean (unsegmented and smoothed) CBF images were employed in random effects full factorial models. Statistical parametric maps (SPMs) were calculated for CBF changes for the interaction INTERVENTION x MEASUREMENT BLOCK. The interaction contrasts were set up to account for inter-individual differences in the CASL baseline by subtracting the between-group baseline effect from the three post-intervention CASL measurement blocks. The significance threshold was set to $P<0.01$ (uncorrected) at the voxel level in order to visualize and confirm the location of all results of the ROI analyses. To minimize the contribution of extra cerebral voxels, an absolute CBF threshold of 5ml/100g/min was employed.

2.3 RESULTS

2.3.1 Manipulation check

The cortisol intervention was successful in all participants ($F_{(2,48)}$ = 5.066, p = .015, η^2_{part} = .174) with significant salivary cortisol increases directly after the MRI measurements in the cortisol but not in the placebo group (significant increases, for cortisol condition: 2.6 nmol/l).

2.3.2 Primary ROIs

Cortisol infusion significantly effected rCBF in regions of the subcortical gray, which is expressed in a significant three way interaction between INTERVENTION, MEASUREMENT BLOCK, and REGION (Table 2.1). Posthoc analyses ($\psi_{5\%}$ = 7.07

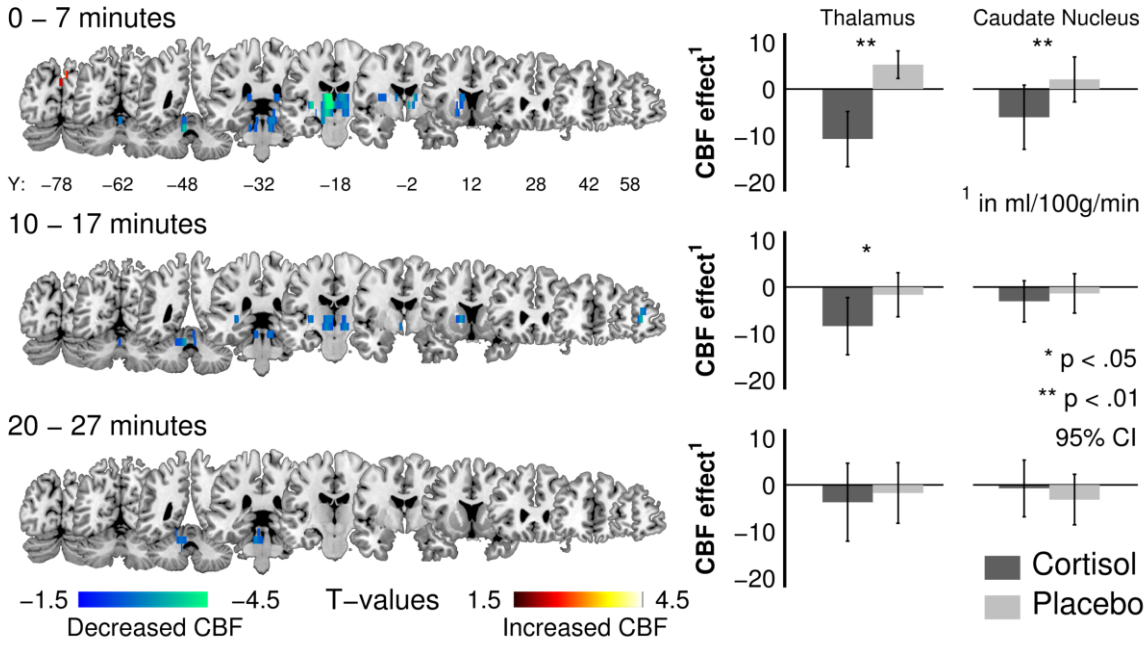

Figure 2.3.1 Cortisol induced rCBF changes (Study 1)

Left: Locally distinct bilateral perfusion decrements in the thalamus and caudate nucleus (baseline corrected), after the intravenous infusion of cortisol (4 mg). **Right:** Bilaterally averaged rCBF for significant ROI comparisons for all post-infusion measurement blocks (95% confidence interval (CI)). The cortisol induced perfusion decrease is significant in the first measurement block after glucocorticoid infusion (0 – 7 minutes) for the thalamus and caudate nucleus. The effect remains significant during the second post-infusion measurement block (10-17 minutes) in thalamus but returns back to baseline for both ROIs in the third block (20-27 minutes).

ml/100g/min; $\psi_{1\%}$ = 8.16 ml/100g/min; C = 18) further decomposed this effect as a significant bilateral perfusion decrease of 15.92 ml/100g/min in the thalamus during the first seven minutes after cortisol infusion compared to placebo (see Figure 2.3.1).

Table 2.3.1 ANCOVA results for all anatomical groups of Study 1, separated according to primary and secondary region of interests (ROIs)

		primary ROIs		secondary ROIs				
		limbic lobe	sub-cortical gray	frontal lobe	tempor. lobe	parietal lobe	occipital lobe	central region
INTERVENTION	df	1;23	1;23	1;23	1;23	1;23	1;23	1;23
	F	1.905	.366	.163	2.678	.573	3.120	.529
	p	.181	.551	.690	.115	.457	.091	.474
INTERVENTION *	df	6;138	5; 115	12;276	3;69	4;92	6;138	2;46
REGION	F	.721	1.5622	.279	.590	1.948	1.334	.675
	p	.599	.203	.936	.592	.133	.258	.457
INTERVENTION *	df	2;46	2;46	2;46	2;46	2;46	2;46	2;46
MEASUREMENT	F	.306	2.364	.500	.117	1.017	.278	1.149
BLOCK	p	.738	.111	.610	.890	.370	.759	.326
INTERVENTION *	df	1;23	1;23	1;23	1;23	1;23	1;23	1;23
HEMISPHERE	F	1.805	2.203	5.914	.010	.109	6.976	.532
	p	.192	.151	**.023**	.920	.744	**.015**	.473
	η^2_{part}			.205			.233	
INTERVENTION *	df	12;276	10;230	24;552	6;138	8;184	12;276	4; 92
MEASUREMENT	F	1.309	2.447	1.223	.348	.528	.890	.349
BLOCK * REGION	p	.228	**.020**	.276	.859	.782	.536	.788
	η^2_{part}		.096					
INTERVENTION *	df	6;138	5;115	12;276	3;69	4;92	6; 138	2;46
REGION *	F	.678	.313	1.409	.991	1.861	3.121	.346
HEMISPHERE	p	.606	.831	.170	.374	.124	**.017**	.709
	η^2_{part}						.119	
INTERVENTION *	df	2;46	2;46	2;46	2;46	2;46	2;46	2;46
MEASUREMENT	F	1.926	.277	.261	.073	4.158	.578	.241
BLOCK *	p	.157	.760	.771	.930	**.022**	.565	.787
HEMISPHERE	η^2_{part}					.153		
INTERVENTION *	df	12;276	15;345	24;552	6;138	8;184	12;276	4;92
MEASUREMENT	F	1.480	1.311	1.209	.623	1.221	.657	.616
BLOCK * REGION *	p	.181	.231	.242	.651	.292	.738	.652
HEMISPHERE								

Result overview of significant region of interest ANCOVA analyses: degrees of freedom (df), F-values (F), p-values (p), partial eta-squared (η^2_{part}), temporal lobe (tempr. lobe). Significant effects are found in the subcortical gray, frontal lobe, parietal lobe, and occipital lobe.

The cortisol induced perfusion decrement remained in the second measurement block (7.56 ml/100g/min) but disappeared in the third in which the thalamic perfusion values receded back to baseline levels. Posthoc analyses further revealed a significant bilateral perfusion decrease of 8.61 ml/100g/min in the caudate nucleus during the first seven minutes after the cortisol infusion compared to placebo. The voxel based visualizations in Figure 2.3.1 supports the notion that the localization of these effects was anatomically plausible and that it was not due to wash-in effects of neighboring ROIs. No other significant INTERVENTION related effects were found for the remaining subcortical regions or any other primary ROIs.

2.3.3 Secondary ROIs

Three further anatomical regions revealed significant effects (Table 2.3.1). A significant interaction INTERVENTION x HEMISPHERE was found for the frontal lobe ROIs and for the occipital lobe ROIs. The subsequent Dunn's comparisons for the frontal lobe ROIs ($\psi_{5\%}$ = 1.39 ml/100g/min; $\psi_{1\%}$ = 1.74 ml/100g/min; C = 4) revealed a significant perfusion decrease of 1.66 ml/100g/min in the right frontal hemisphere after the cortisol

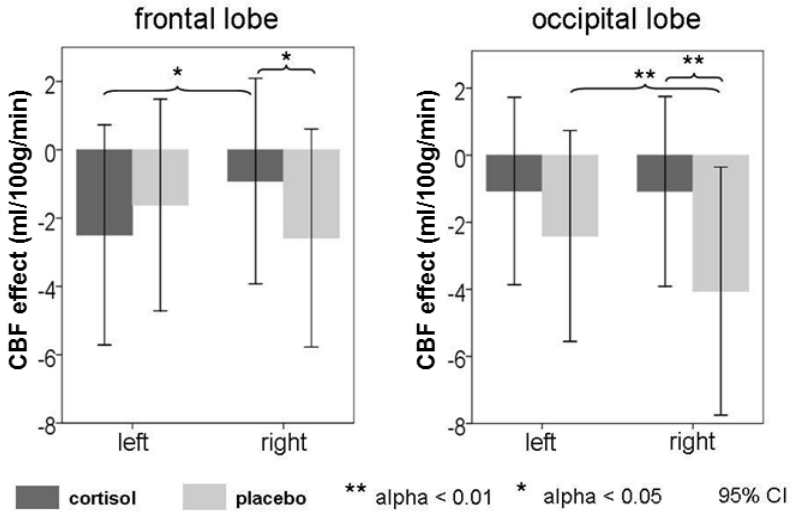

Figure 2.3.2 CBF in the frontal and occipital lobe for the interaction INTERVENTION x HEMISPHERE

95% confidence interval (CI). Cortisol (dark gray) maintained the CBF closer to baseline levels in the frontal and occipital lobe. This effect became significant in the right hemispheres because in the occipital lobe the CBF of the right hemisphere decreased most in the placebo group (light gray), and in the frontal lobe the left hemisphere decreased more than the right hemisphere.

injection, compared to placebo. In the left frontal hemisphere, cortisol led to no significant perfusion change compared to placebo (see Figure 2.3.2). This interaction rests on a significantly higher perfusion of the right compared to the left frontal hemisphere (1.57 ml/100g/min) in the cortisol group. The Dunn's comparisons for the occipital lobe ROIs ($\psi_{5\%}$ = 0.98 ml/100g/min; $\psi_{1\%}$ = 1.22 ml/100g/min; C = 4) revealed a significantly higher perfusion of the cortisol group compared to the placebo group in the right (2.97 ml/100g/min) (Figure 2.3.2). However a significant lower perfusion of the right compared to the left occipital hemisphere (1.64 ml/100g/min) in the placebo group led to the interaction.

The above described interaction in the occipital lobe, however, is not unconstrained because of a significant three-way interaction INTERVENTION x REGION x HEMISPHERE (see Table 2.1). The Dunn's comparisons for this effect ($\psi_{5\%}$ = 3.60

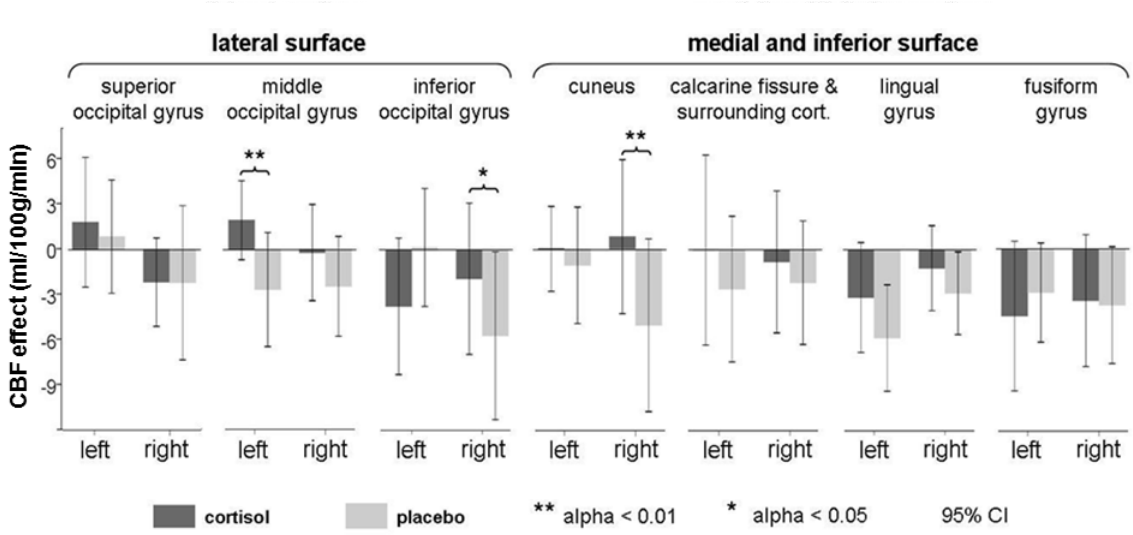

Figure 2.3.3 CBF in the occipital lobe for the Interaction INTERVENTION x REGION x HEMISPHERE

The cortisol (dark gray) induced relative preservation of CBF levels in the right hemisphere (Figure 2.3.2) in fact rests on effects in the inferior occipital gyrus and the cuneus (95% confidence interval, CI). In addition, in the middle occipital gyrus this effects is not present in the right but in the left hemisphere.

ml/100g/min; $\psi_{1\%}$ = 4.21 ml/100g/min; C = 14) revealed that the effect of INTERVENTION and HEMISPHERE were different between REGION. The middle occipital lobe (lateral surface) displayed an intervention effect in the left (4.61 ml/100g/min) but not in the

right (2.70 ml/100g/min) hemisphere, whereas the inferior occipital gyrus (lateral surface) displays the effect in the right (3.79 ml/100g/min) but not in the left (3.33 ml/100g/min), as well as the cuneus (medial and inferior surface), which displays the effect in the right (5.85 ml/100g/min) but not in the left (1.09 ml/100g/min) hemisphere (see Figure 2.3.3). All the remaining regions of the occipital lobe showed no significant effect with INTERVENTION. The lack of significant higher order interactions concerning measurement block also signifies that the perfusion differences in the frontal and occipital lobes stretch across all post intervention CASL measurement blocks.

The secondary ANCOVAs have also revealed a significant three-way interaction INTERVENTION x MEASUREMENT BLOCK x HEMISPHERE in the parietal lobe (Table 2.1). The subsequent Dunn's comparisons ($\psi_{5\%}$ = 1.57 ml/100g/min; $\psi_{1\%}$ = 1.91 ml/100g/min; C = 6) revealed divergent effect patterns in the three CASL measurement blocks. In the first seven minutes after intervention, a significant perfusion increase of 1.84 ml/100g/min in the cortisol relative to the placebo group was found in the right hemisphere but not in the left. Ten to seventeen minutes after intervention, no significant perfusion difference between cortisol and placebo groups could be quantified. In the last measurement blocks, (20-27 minutes after intervention) the cortisol group significantly increased perfusion

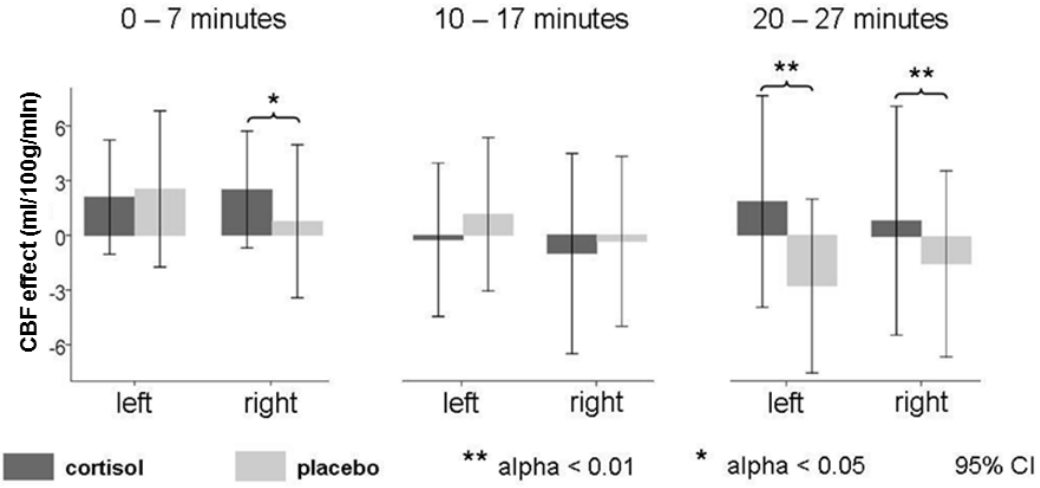

Figure 2.3.4 CBF in the parietal lobe for the interaction INTERVENTION x MEASUREMENT BLOCK x HEMISPHERE

Cortisol (dark gray) induced differences are found unilaterally on the right side during the first measurement block, but bilaterally during the last measurement block (95% confidence interval, CI).

relative to the placebo group in both the left (4.64 ml/100g/min) and right (2.37 ml/100g/min) hemisphere (see Figure 2.3.4). This three-way interaction can, therefore, be attributed to the different effects of INTERVENTION on the hemispheres and between the CASL measurement blocks.

2.3.4 Covariate

The CASL baseline covariate led to no significant effects in any of the performed ANCOVAs; therefore, the covariate only cleared up unexplained variance and did not carry significant INTERVENTION effect variance in itself. Thus, the effects of intervention (cortisol, placebo) are unrelated to pre-infusion effects of the baseline that are due to naturally occurring inter-individual differences.

2.4 DISCUSSION

Study 1 was a first exploratory assessment of cortisol induced CBF changes in the human brain, and a number of previously unreported effects were found. The magnitude and timeframe (< 15 minutes; and disappearance/wash-out of the effect after 20 minutes) of a majority of those effects excludes currently known genomic mechanisms of cortisol action and points towards non-genomic cortisol mechanisms as a source for these CBF effects. The results also infer regionally specific influences on CNS activity. Effects in the subcortical gray region are particularly interesting because of their ability to direct and to modulate neuronal traffic to and from the cortex. The following discussion will, therefore, focus mainly on the possible implications of the subcortical findings.

2.4.1 Primary and Secondary ROIs

Cortisol infusion led to a bilateral perfusion decrease in the thalamus, after the cortisol and relative to the placebo intervention (Figure 2.3.1). This effect is largest in the first seven minutes after the cortisol intervention and decreases in the ten to seventeen minutes after the cortisol intervention, before CBF measurements returned back to baseline. The thalamus has not been reported to display non-genomic effects after an intravenous administration of cortisol. However, quick modulating effects of cortisol on thalamic functioning seem reasonable as a part of stress related coping processes. The

thalamic nuclei are generally believed to serve as an early relay station for most afferent and efferent signaling to or from the cortex (S.M. Sherman & Guillery, 2006). Recently, more evidence accumulated that suggests that the thalamus plays a more pronounced role as a mediator and modulator for a majority of cortico-cortical bound transmissions (S.M. Sherman & Guillery, 2006). Unfortunately, the spatial resolution of the present CASL images does not justify a more distinct localization of the thalamus effect, which would allow separating functionally distinct thalamic nuclei. However, three neurological processes that include the thalamus, and have been studied under stress interventions, might be involved in early stress related coping responses. The following paragraphs will continue by discussing each as a possible underlying mechanism for the intervention related results.

2.4.1.1 Thalamo-cortical processes

The neural correlates of vigilance and sustained attention have been largely localized in the right parietal, prefrontal lobe and the thalamus, with the thalamus as a mediator to cortical attention networks (Portas et al., 1998; Sarter, Givens, & Bruno, 2001). In addition, Steriade (1990) draws a thalamo-cortical network in which a decreased perfusion in the nucleus reticularis thalami is connected to an increase in cortical activity in the frontal cortex. This pattern of deactivation in the thalamus and activation in frontal lobe structures would be in line with the presented results. The effect INTERVENTION x HEMISPHERE (Figure 2.3.2) further supports the interpretation of the thalamus effect as a process in the attention networks because the frontal lobe shows an expected relative perfusion increase in its right hemisphere. This pattern can also be interpreted in light of EEG studies in which increased cortisol levels were found to increase (or maintain) cortical activity in the right hemisphere, which is generally attributed to negative affect, avoidance, and anxious arousal in humans (Hewig et al., 2008).

In the parietal lobe, this hemispheric asymmetry is only present in the first seven minutes after the intervention, whereas the later effect bilaterally increases CBF in the last CASL measurement block compared to placebo (Figure 2.3.4). Finally, the effects in the frontal lobe and occipital lobe stretch across all post-intervention CASL measurement blocks and suggests that cortisol continuously alters frontal and occipital perfusion for

longer periods of time. The timeframe of these effects imply non-genomic cortisol mechanisms. However, later effects (> 20 minutes) may also contain genomic actions. It seems likely that frontal, parietal, and occipital (Figure 2.3.3) effects are aimed at maintaining an increased adaptation to stress through an increased avoidance or vigilance, which includes increased perfusion of areas attributed to the visual processing in the cortisol, compared to the placebo group. Early effects of cortisol on thalamic mechanisms may, therefore, have an impact on attention, vigilance, or approach motivation.

2.4.1.2 Thalamo-striatal network

A prominent projection from the thalamus reaches to the basal ganglia, wherein several thalamic nuclei are recognized as the primary origin of thalamo-striatal and thalamo-neostriatal pathways. Overlapping territories exist between thalamic regions innervated by the output nuclei of the basal ganglia and thalamostriatal projection neurons, which suggests the presence of feedback mechanisms between these two brain regions (for a general overview see Packard & Knowlton, 2002; Ulrich, 2007). The rapid, non-genomic cortisol effect in the caudate nucleus during the first seven minutes after the intervention (Figure 2.3.1) might suggest that the thalamo-neostriatal projections have been effected.

Several functions of the caudate nucleus are under investigation or have already been established that might be important for coping with stressors. For one, the caudate nucleus mediates a form of learning and memory in which stimulus-response associations or habits are incrementally acquired (Packard & Knowlton, 2002). Moreover, activation in the caudate nucleus is associated with performance of an implicitly learned sequence, but not when participants are explicitly told the sequence beforehand and can, therefore, consciously anticipate the location of the upcoming stimulus (Packard & Knowlton, 2002). If such processes were influenced by cortisol, the results of Study 1 would suggest that stimulus-response learning may be decreased during early coping in stressful situations.

The caudate nucleus is a potential mediator site for learned habits or procedures, but it also plays a role in the ability to shift cognitive sets or switch between tasks in response to the environment (Robbins, 2007). The ability to readily switch between

learned stimulus-response associations are a necessary component of many complex executive tasks such as planning, problem solving, and strategizing. The observed perfusion decrease in the caudate nucleus (Figure 2.3.1) could also suggest that in an early part of stress coping, task switching or attention shifting abilities might be inhibited. Decreased task switching or attention shifting may be an adequate primary stress response in order to maintain the focus of attention at a potentially harmful, yet unclear situation.

2.4.1.3 Processes of emotional appraisal

The thalamic paraventricular nucleus (PVT) is activated by stress and it projects to forebrain structures which implies its role in processing stress-related information (Spencer, Fox, & Day, 2004). PVT lesions in air puff stressed Wistar rats were shown to increase Fos (protooncogene that leads to prolonged functional changes in neurons) expression patterns in the central amygdala which are normally elicited by an acute psychological stressor (Spencer, et al., 2004). However, the results failed to quantify CBF effects in the amygdala. The lack of perfusion differences in PVT effect sites weakens a possible involvement of this structure in the results.

The apparent plausibility of some of the above mentioned thalamic processes needs to be put into perspective because the present results cannot support one over the other and have yet to be replicated. Study 2 (Chapter III) applied an almost identical design in an independent sample in order to replicate the main CBF results of Study 1.

2.4.2 Other findings

There were no significant intervention related effects in the limbic lobe ANCOVA, which is contrary to findings in current literature concerning glucocorticoid effects on the hippocampus (e.g. Grillon, Smith, Haynos, & Nieman, 2004; J. J. Kim & Diamond, 2002; van Stegeren, 2009). The lack of studies that utilize intravenous cortisol interventions in humans makes it difficult to assess if the previously reported stress mediated effects in the limbic lobe are solely tied to experimental tasks or experimental context, or if they are indeed caused by cortisol alone. These differences in experimental findings need to

also be examined in terms of differences in applied MRI sequences. CASL measurements, as compared to BOLD measures, do not quantify deoxygenated blood but instead quantify absolute CBF changes. It is not yet fully understood how much CBF and BOLD signals can be directly compared, since both share different attributes (Goense & Logothetis, 2010). Furthermore, CASL is able to quantify slow changes in blood flow that are not easily measurable with BOLD. Therefore, if rapid, non-genomic effects of cortisol find their expression through longer lasting, low frequency changes on CBF, then BOLD cannot be easily used to detect them. Using BOLD, rapid, non-genomic changes may also show up at different regions (e.g. regions next to the thalamus) due to the inferior functional localization of BOLD (see remarks on "Advantages of CASL" in section 2.1.3.1).

2.4.3 Conclusion

The aim of this study was to identify brain regions that are affected early after intravenous cortisol administration. Within the first seven minutes after intravenous infusion, cortisol (4 mg) induced a significant bilateral perfusion decrement in the thalamus and caudate nucleus (among other areas), relative to baseline and placebo. These results provide a first indicator that rapid and non-genomic glucocorticoid mechanisms are active in the human brain and that these actions can be investigated by using MRI measurements. The lack of non-genomic findings in the imaging study of Lovallo and colleagues (2009)(see chapter 1.2.3) seems, therefore, to be related to their experimental setting or imaging sequence and not to the absence of such effects.

The subcortical structures that were affected by the intravenous infusion, in particular the thalamic nuclei, have the potential to exert global effects on the entire brain by altering functional brain states and processing routines. In fact, if the changes in thalamic nuclei are indeed related to coping with stress and are not a mere reflection of negative feedback processes of the HPA axis, then their functional effects must influence neuro-electrical discharge patterns in the cerebral cortex. The obtained subcortical results, therefore, also indicate that rapid, non-genomic cortisol effects may be observed during electrophysiological measurements, such as during an EEG or a magnetoencephalogram. This hypothesis was further investigated by applying an almost identical experimental procedure in Study 3 (Chapter IV) while measuring EEG.

In conclusion, it seems likely at this point that non-genomic cortisol effects in the thalamus and caudate nucleus influence *thalamo-cortical* or *thalamo-striatal* processes that are associated with attention or vigilance and also might involve mechanisms that are engaged in the ability to switch between tasks or shift attention, depending on environmental demands.

However, prior to additional electrophysiological investigations into the possibility of rapid cortisol effects on brain functioning, the existence of rapidly induced subcortical cortisol effects must first be further confirmed. Therefore, Study 2 (Chapter III) was designed in order to replicate such effects in a separate, but identically screened, sample of participants.

RAPID EFFECTS OF CORTISOL ON THE PERFUSION OF THE HUMAN THALAMUS

CHAPTER III

ABSTRACT

The stress hormone cortisol acts on the central nervous system in order to support adaptation and time-adjusted coping processes. There is only limited knowledge about rapid, non-genomic cortisol effects on *in vivo* neuronal activity in humans. The earlier presented and first explorative investigation into cortisol induced effects on the CBF in humans (Chapter II) found that cortisol significantly affected blood flow within 15 minutes after intravenous administration. These effects are intriguing but require further replication in order to further establish these rapid cortisol actions. Therefore, an independent but almost identical placebo-controlled and double-blinded study in healthy men (N=9) was conducted in order to replicate the main findings of the study presented in Chapter II. Cerebral blood flow was again assessed using continuous arterial spin labeling as a magnetic resonance imaging sequence and the rapid bilateral perfusion decrements in the thalamus were replicated. Other effects in regions that had been affected by cortisol, such as the caudate nucleus and regions in frontal, occipital, and parietal lobe, were not replicated. In conclusion, cortisol may indeed act on the perfusion of the thalamic relay via a rapid, non-genomic mechanism, implying profound effects on global signal processing.

3.1 INTRODUCTION

The stress hormone cortisol acts on the human brain in order to support adaptation and time-adjusted coping processes to present or anticipated stressors. The results of Study 1 (Chapter II) provided coherent evidence for the existence of rapid cortisol induced CBF effects on the thalamus and caudate nucleus. The findings from Study 1 provide first neuroimaging support that earlier reports on rapid, non-genomic cortisol effect in humans (Kuehl, et al., 2010; Richter, et al., 2011) may indeed involve mechanisms that affect the functioning of the human brain. However, an important feature of acquiring scientific knowledge is that a result needs to be repeatable (Ravetz, 1971).

In fact, Karl Popper, who (among others) shaped much of today's scientific reasoning, made the following statement:

> *"We do not take even our own observations quite seriously, or accept them as scientific observations, until we have repeated and tested them. Only by such repetitions can we convince ourselves that we are not dealing with a mere isolated 'coincidence', but with events which, on account of their regularity and reproducibility, are in principle inter-subjectively testable."*
>
> (1959, p. 23)

Thus, since the results of Study 1 are indeed unique and have not been reported before, it is of much importance to replicate (at least in principle) the observed cortisol induced effects on the human brain. Therefore, identical experimental procedures (compared to Study 1) were applied to an independent sample of participants in Study 2, with the aim of replicating the effects of cortisol on the subcortical gray region.

3.2 METHODS

3.2.1 Participants

In Study 2, nine (mean age = 23.22 years, SD = 1.86 years), right-handed, psychologically and physiologically healthy, and non-smoking men participated. Prior to the MRI measurements, informed consent was obtained and all participants underwent a screening interview to determine if they were suitable for MR imaging. Exclusion criteria included cerebrovascular or cardiovascular diseases, psychiatric disorders, medication (including glucocorticoid containing substances), smoking at any point in life, other than normal BMI, as well as any acute or chronic diseases. The study was approved by the ethics committee of Rhineland-Palatinate and was in accordance with the ethical guidelines of the Declaration of Helsinki.

3.2.2 Experimental Procedure

In Study 2, participants (N = 9) were measured twice, one week apart and at exactly the same time of day, in a within-subject design. Repeated measurements in the same participants are advantageous since they reduce naturally occurring inter-group variance. Participants received cortisol and placebo in a randomized yet balanced order to control sequence effects. All experimental procedures were identical to study 1. However, since the perfusion effects in Study 1 may have been (at least in parts) attributable to the task during the break, in Study 2, participants were told that they had been assigned to a waiting control group and they were asked to use all breaks to rest (see Figure 3.2.1). This resting condition was used to control possible task-related influences that may have contributed to the results of Study 1. After the MRI measurement was finished the participants completed final questionnaires, and after the second MRI session they were

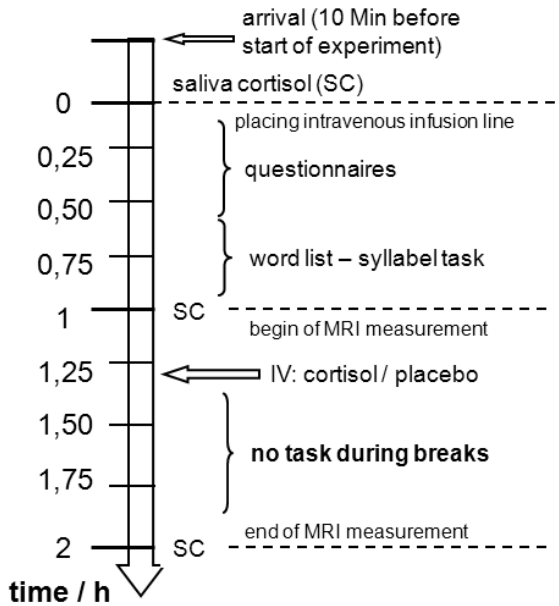

Figure 3.2.1 Overview of the general experimental procedure of Study 2

compensated for their participation (100€) and informed about whether they had received cortisol or placebo.

3.2.3 MRI measurements

In Study 2, the ROI analysis was hypotheses driven, in order to replicate the main findings of Study 1. Therefore, the only ROIs examined were the thalamus and caudate nucleus (*replication ROIs*). All other MRI measurement related procedures and processing steps, such as acquisition (equipment and parameters), imaging sequence (see Figure 3.2.2) and Data Processing (image processing – see Figure 2.2.5) were identical to Study 1.

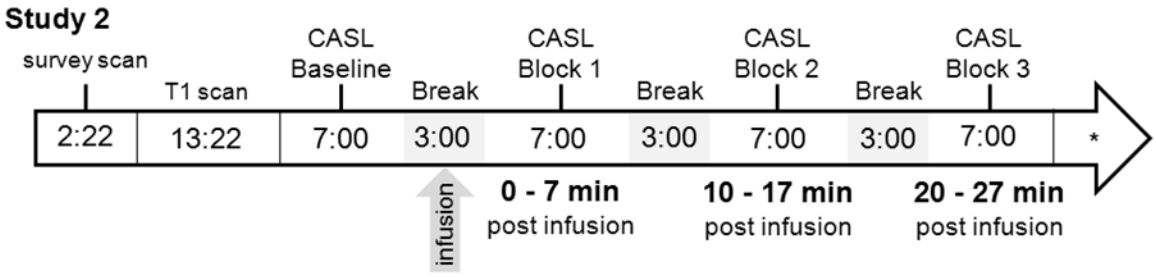

Figure 3.2.2 Order of measurements and duration (in minutes) of Study 2

(*) The experimental measurements were succeeded by an M_0 measurement (3:25 minutes) and a T_2-weighted anatomical measurement (2:54 minutes) to further control for physiological abnormalities. Other than in Study 1, participants were asked to not perform the previously practiced task. Instead they were asked to use the breaks to rest. The time that each participant spent in the MR-scanner was about 58 minutes in total. After all MRI measurements were finished, the participants provided their final saliva sample for the manipulation check.

3.2.4 Manipulation check

Acute HPA axis activity was obtained through three saliva samples per session to check if the pharmacological manipulation succeeded. Participants provided their first sample upon arrival, the second before entering the MRI scanning room, and the third after the last MRI sequence (independent variable TIME). All samples were immediately frozen for biochemical analysis. Salivary cortisol was analyzed with an immunoassay with fluorescence detection (see Dressendorfer, et al., 1992). Intra- and inter-assay variability

was less than 10 and 12% respectively, and this reliability was, therefore, suited for further statistical analyses.

3.2.5 Statistical analyses

3.2.5.1 Manipulation check

For Study 2, the pharmacological manipulation was assessed via ANOVA with the INTERVENTION (cortisol, placebo) and measurement TIME (arrival, before MRI, after MRI) in a repeated-measures factorial design.

3.2.5.2 Power Analyses

A Post-hoc power analysis was performed for Study 1 and Study 2 using G*POWER (Buchner, Erdfelder, Faul, & Lang, 2009) in order to determine the likelihood of Study 2 to replicate the empirical effect (of the subcortical gray) that was found in Study 1. Therefore, the empirical effect INTERVENTION x REGION x MEASUREMENT BLOCK of the subcortical gray areas in Study 1 was used to determine the post-hoc statistical power (1-β) for both studies. For Study 1, post-hoc power was determined for lambda (ʎ) = 14.47 and for Study 2 for ʎ = 20.04 (See Appendix B for detailed calculations and results). Because Study 2 applied a repeated measurement design, its power (1-ß) was higher (0.84) compared to Study 1 (0.72). However, the interaction INTERVENTION x REGION x MEASUREMENT BLOCK found no significant ($\alpha = 0.071$) results for Study 2 during a first (here not further presented) explorative analysis. Therefore, statistical analyses of Study 2 were performed using one-tailed planned comparisons for only subcortical gray ROIs that showed a significant effect in Study 1.

3.2.5.3 ROI analyses

In Study 2, raw perfusion values of the bilateral thalamus and caudate nucleus ROIs are assessed via one-tailed, paired student t-tests of the baseline and the remaining three CASL measurement blocks (applying Bonferoni-Holm (1979) procedure to corrected for multiple tests). No baseline correction was necessary since the repeated measurements avoided significant baseline differences between the cortisol and placebo conditions.

3.3 RESULTS

3.3.1 Manipulation check

The cortisol intervention was successful in Study 2 in all participants ($F_{(2,16)}$ = 3.830, p = .044, η^2_{part} = .324) with significant salivary cortisol increases directly after the MRI measurements in the cortisol, but not in the placebo group (significant increases for cortisol conditions: 4.12 nmol/l).

3.3.2 Replication ROIs

Cortisol infusion significantly decreased the bilateral perfusion of the thalamus by 13.45 ml/100g/min during the first seven minutes (Figure 3.3.1) compared to placebo (see Table 3.1). No significant differences between the cortisol and placebo conditions were found in the baseline measurement, and no significant effects of the cortisol infusion were found during the second and third measurement blocks and in the caudate nucleus.

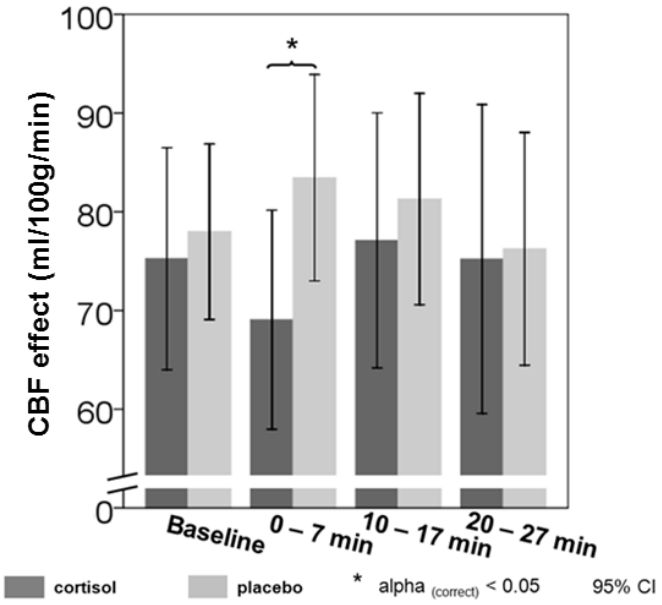

Figure 3.3.1 rCBF in the bilateral thalamus for Study 2

Cortisol (dark gray) induced a bilateral perfusion decrease in the thalamus during the first measurement block (0 - 7 minutes) after the infusion. This result replicates the thalamic perfusion decrease during the first measurement block of Study 1 (Figure 2.3.1).

Table 3.3.1 T-test results for replication ROIs (Study 2)

ROI	cortisol - placebo	t	df	p	p^1 for α < 5 %
thalamus L & R					
Baseline	-3.700	-0.842	8	.212	0.0100
0 – 7 min	-13.453	- 3.329	8	.005*	0.0063
10 – 17 min	-3.760	- 0.753	8	.236	0.0167
20 – 27 min	- 0.768	-0.110	8	.457	0.0500
caudate nucleus L & R					
Baseline	-5.990	-1.469	8	.090	0.0083
0 – 7 min	- 6.763	-1.625	8	.071	0.0071
10 – 17 min	-4.090	-0.850	8	.210	0.0125
20 – 27 min	-0.459	-0.125	8	.451	0.0250

[1]critical p-value of Bonferoni-Holm correction for eight student t-tests. *significant for corrected p <.05

3.4 DISCUSSION

Study 2 is a N = 9 double-blinded, repeated-measurement replication of Study 1 with only minor changes in the experimental procedure (no tasks during breaks). The focus was on to what extent the cortisol induced CBF changes in the thalamus and caudate nucleus can be replicated.

Indeed, Study 2 replicated the bilateral perfusion decrease in the thalamus within the first seven minutes after cortisol infusion with a much smaller sample. This strongly supports the main findings of Study 1 (Chapter II) suggesting that cortisol acts via a rapid, non-genomic mechanism on basal regulatory processes in the brain. The bilateral decrease in the thalamus of 13.45 ml/100g/min (Figure 2.3.1) makes up an effect of 17.9 % relative to baseline perfusion.

However, effects of cortisol on the caudate nucleus show a descriptive, yet not significant, decrease in perfusion. This discrepancy cannot likely be caused by the lack of statistical power in Study 2, but may be specific to the particular sample and possibly due to increased error variances (a number of effects were promising in their descriptive

tendencies). It may therefore be possible that glucocorticoids have additional, smaller, but here not significant effects that may include the caudate nucleus and the secondary ROIs of Study 1 (secondary ROIs see chapter 2.2.3). Nevertheless, the replication of cortisol induced effects on the thalamus was crucial for further investigations into cortisol effects on brain functioning. It seems now likely that cortisol may induce measurable effects on neuronal functioning that can be measured with the EEG (Study 3 – Chapter IV).

RAPID EFFECTS OF CORTISOL ON THE ELECTROPHYSIOLOGY OF THE HUMAN BRAIN

CHAPTER IV

ABSTRACT

Cortisol is an adrenal steroid hormone that is increasingly released during stress. It modulates a variety of psychobiological processes to support adaptation and coping with challenging situations. A number of experimental investigations have focused on how cortisol affects the functioning of the central nervous system via genomic mechanisms, but little is known about cortisol's *in vivo* functional effects on the human brain. The first of two neuroimaging studies that were specifically designed to investigate rapid cortisol actions in humans, and that were presented in Chapter II and III, found a rapid perfusion decrease in the bilateral thalamus. Since the functioning of thalamic nuclei is of utmost importance for the entire brain, cortisol induced effects on the thalamus also imply functional effects on the cortex. Therefore, a placebo-controlled and double-blinded study in healthy men (N=14) was conducted to investigate and confirm the effects of 4 mg cortisol on electrophysiological activity, occurring within 15 minutes after intravenous administration. Electrophysiological activity was assessed via the electroencephalogram and revealed large global effects on the spectral power of spontaneous oscillations and on global markers of signal strength and map complexity. These results suggest that cortisol acts by reducing neuronal background activity in order to possibly improve the processing of coping relevant stimulus-response contingencies.

4.1 INTRODUCTION

Cortisol is increasingly released during stress and modulates a variety of psychobiological processes to support adaptation and coping with challenging situations. How cortisol affects the functioning of the CNS via genomic mechanisms has been often investigated, however little is known about cortisol's *in vivo* functional effects on the human brain. Chapter II and Chapter III have presented the first neuroimaging studies that were specifically designed to investigate rapid hemodynamic aspects of cortisol actions in the human brain. Both studies found a rapid perfusion decrease in the bilateral thalamus, which is an indication that cortisol may have adjusted the neuronal demand by inducing metabolic changes. However, hemodynamic changes only reflect a crude measure of neuronal activity because changes in blood supply are only a reflection of energy demand but hold no information about the content or rhythm of the ongoing electrical discharges that constitute neuronal processing. In fact, the pattern of the neuronal action potentials may change without a need to (immediately) adjust metabolic supplies which would trigger hemodynamic changes. Thus, MR-imaging is only an indirect measure of neural activity.

The *actual* neuronal activity in the brain induces electrical fields (by accumulated action potentials of several thousand neurons) that extend to the surface of the scalp, where they give rise to a specific topographical distribution. These resulting scalp potential maps can be sampled accurately if a sufficient amount of recording sites (e.g. electrodes) covers the head surface. The measurement of these scalp potentials, for example via EEG, holds a specific advantage: neuronal activity is recorded directly and with a very high temporal resolution. The best-known temporal characteristic of EEG is its ability to assess the electrical field activity of the prominent rhythmic oscillations in different frequency ranges. In addition to observing the oscillatory EEG rhythms, the spatial analysis of the EEG also reveals a meaningful temporal characteristic of the scalp potentials. Instead of continuous smooth transitions between the electrical field potential configurations, continuous EEG recordings are characterized by sharp topographical transitions that separate discrete segments of electrical stability. These periods of stable electric field maps are called functional microstates and they have been proposed to

reflect individual information processing steps. These microstates are under discussion to be the basic building blocks of the content of consciousness (e.g. Lehmann, Ozaki, & Pal, 1987).

Conducting EEG measurements during the intravenous infusion of cortisol would, therefore, provide extended information about when, where, and possibly how neuronal activity is being influenced. That electrophysiological effects are even likely to exist is implied by the observed perfusion effect in the thalamus, as reported in Chapter II and Chapter III. Thalamic nuclei affect the entire brain and have been causally linked to EEG activity numerous times (e.g. de Munck et al., 2007; Feige et al., 2005; Goncalves et al., 2006; Laufs et al., 2003; Moosmann et al., 2003). However, the ability to spatially localize neuronal activity with EEG measurements is limited, and it is critical to understand that neuronal events that originate from subcortical regions, such as the thalamus, cannot be directly detected (but have to be theoretically inferred) in adults.

Investigating cortisol induced effects on the rhythmic EEG properties can help to identify yet another aspect of glucocorticoid action in the human brain (even if statements about causal relationships between hemodynamic and electrophysiological are not easily possible). Therefore, a placebo-controlled and double-blinded study in healthy men (N=14) was conducted to investigate and confirm the effects of 4 mg of cortisol on EEG activity, occurring within 15 minutes after intravenous administration. In particular, signal strength, map complexity, and spectral power of resting EEG were used as global markers for electrophysiological activity. Similar to Study 1 and Study 2 (Chapter II and Chapter III), special care was taken to assure that the acquisition conditions of Study 3 were optimal for uncovering cortisol effects during EEG measurements. As in Study 2, participants were measured twice, receiving cortisol and placebo, in order to further assure adequate data quality.

4.2 METHODS

4.2.1 Participants

Fourteen right-handed and healthy men (mean age = 24.50 years, SD = 2.14 years) participated in the experiment. Prior to the EEG measurements, all participants underwent a screening interview to determine if they met the same criteria as participants for the MRI measurements of Study 1 and 2 (Chapter II and III). Informed consent was obtained for all participants. Exclusion criteria included cerebrovascular or cardiovascular diseases, psychiatric disorders, medication (including glucocorticoid containing substances), smoking at any point in life, other than normal BMI, as well as any acute or chronic diseases. The study was approved by the ethics committee of Rhineland-Palatinate and was in accordance with the ethical guidelines of the Declaration of Helsinki.

4.2.2 Experimental Procedure

Participants were measured twice, one week apart, and at exactly the same time of day, in a within-subject design. The general experimental procedures and intervention (4 mg cortisol), were identical to Study 1 and 2, however, participants were seated in a psychophysiological laboratory and prepared for EEG measurements (Figure 4.2.1). Again, the repeated measurements of the same participants increased the statistical value of the results. During the EEG measurements, participants kept their eyes open (O) or closed (C) in an intra- and inter-individually balanced order that alternated between and within the individual EEG measurement blocks (per condition – starting blocks with O…C…O…C… or C…O…C…O…). As in Study 2, in the second break participants

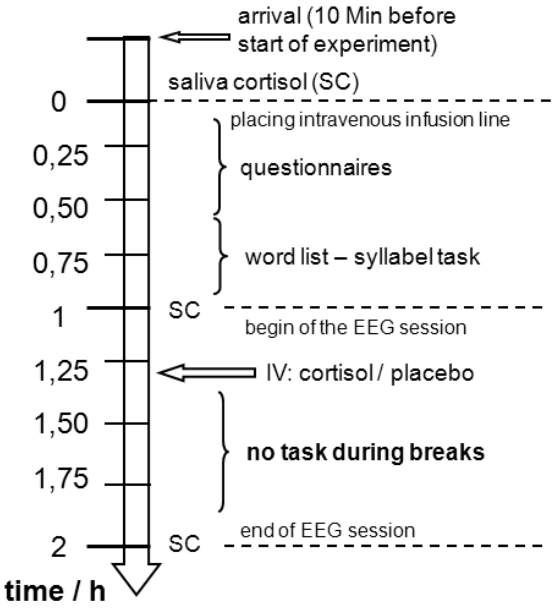

Figure 4.2.1 Overview of the general experimental procedure of Study 3

were told that they had been randomly assigned to a waiting control group and were asked to use all following breaks to rest (Figure 4.2.2). After EEG-measurements were finished the participants completed final questionnaires, and after the second measurement they were compensated for their participation (100€) and informed about whether they had received cortisol or placebo.

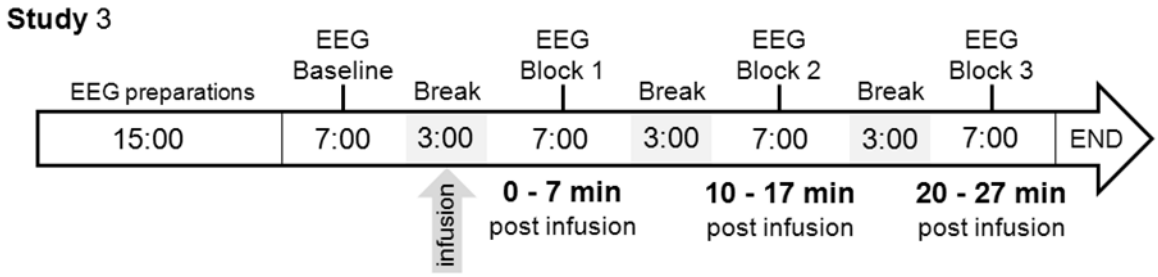

Figure 4.2.2 Order of measurements and duration (in minutes) for Study 3

Other than in Study 1 and Study 2, participants were initially prepared for EEG measurements. This also familiarized them to the experimental set-up. As in Study 2, participants were asked not to perform the previously practiced task. The time that each participant spent in the EEG-measurement was about 52 minutes in total. After all MRI measurements were finished, the participants provided their final saliva sample for the manipulation check.

4.2.3 EEG measurements

EEG was recorded continuously by 32 Ag-AgCl pin-type active electrodes (Brain-amp: Brain Products, Munich). The electrodes – FP(1, 2), F(3, z, 4), FC(7, 2, 4, 8), T(7, 1, 2, 8), C(3, z, 4), CP(5, 1, 2, 6), P(7, 3, z, 4, 8), O(1, z, 2), A(1, 2) - were mounted according to the 10–20 system (Chatrian, Lettich, & Nelson, 1988), and referenced to FCz. Impedances of the EEG electrodes were below 10 kOhm. The highpass-filter was set to 0.0159 Hz (24 dB/octave rolloff), and the lowpass-filter was set to 250 Hz. The signals were digitized at 1000 Hz and stored for offline analysis.

4.2.4 EEG pre-processing

The EEG was re-referenced to mathematically linked mastoids, then re-filtered (band pass: 1-40 Hz; 48 db) to minimize noise and drifts that were present in some data

channels, and re-sampled to 250 Hz. Continuous EEG recordings were segmented into non-overlapping 4 second epochs for each measurement block and visually inspected.

Epochs with non-stereotyped artifacts (e.g. electrode cable movements, swallowing, etc.) were rejected from further analyses (mean across blocks for cortisol and placebo: 5.2 segments and 5.7 segments; total range across blocks for cortisol and placebo: 17, and 20 segments), whereas epochs containing repeatedly occurring, stereotyped ocular and heart beat related artifacts were corrected using infomax ICA (Bell & Sejnowski, 1995; Jung, Makeig, Humphries, et al., 2000; Makeig, Bell, Jung, & Sejnowski, 1996). Following this procedure, ocular and heart beat artifact corrected data was created via ICA back-projection (average removed components per participant: cortisol condition - 5.82; placebo condition - 5.58).

4.2.4.1 Independent Component Analysis for EEG

The statistical decomposition of multi-channel EEG signals has become a frequently used approach to gain a better understanding and recognition of various types of processes that are reflected in the EEG (Onton, Westerfield, Townsend, & Makeig, 2006). Independent Component Analysis (ICA) is such an approach and is a linear blind source decomposition (i.e. separation) technique that is able to reveal the underlying statistical sources of mixed signals (Debener, et al., 2010). The term *blind* implies that ICA can separate data into source signals even though not much is known about those sources. The application of ICA to EEG signals, that consists of various brain and non-brain contributions, has become popular, as (1) it provides a powerful way to remove artifacts from EEG data (Jung, Makeig, Humphries, et al., 2000; Jung, Makeig, Westerfield, et al., 2000), and (2) it helps to disentangle otherwise mixed brain signals (Makeig et al., 2002). In some areas of EEG research, such as simultaneous EEG-fMRI measurements and their integration, these two characteristics significantly fostered the progress in that field (Debener, Ullsperger, Siegel, & Engel, 2006).

Rational behind ICA

ICA is related to more conventional methods for decomposing sources of large data sets, such as Principle Component Analyses (PCA) or Factor Analysis (FA). However,

whereas ICA finds independent signal sources, PCA and FA find only uncorrelated signal sources (see Figure 4.2.3 for an illustration). This distinction is crucial and can be further understood with a simple example.

Imagine the situation at a cocktail party in which two people are in a room talking to each other and their voices are recorded by two microphones. When examining each individual voice, it would become apparent that the amplitude of one voice at any given point in time is unrelated to the amplitude of the other voice at that time. The reason why the amplitudes of different voices are unrelated is that they are generated by unrelated physical processes (i.e. different people). Therefore, one key strategy to separate voice mixtures into their constituent voice components is to look for unrelated time-varying signals within signal mixtures. With this strategy, the extracted signals are unrelated, just as the voices are unrelated, and therefore, the extracted signals are the individual voices. Now, if only uncorrelated signal sources would be extracted, then the decomposed signals would simply be a new set of voice mixtures that are composed of uncorrelated, but mixed signals of different speakers (example adjusted from Stone, 2004).

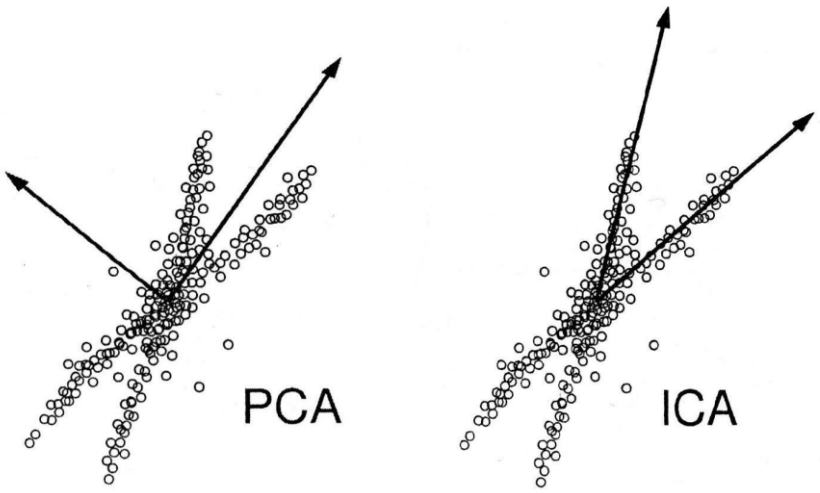

Figure 4.2.3 Difference between uncorrelated (PCA) and independent (ICA) assumptions (illustration Bergmeir, 2005) If two independent processes, which result into the data distribution of the above scatter plot, are not orthogonal to each other, then the ICA will result in better data decomposition. In the PCA (left side), the decomposed data of non-orthogonal signal sources will lead to a solution that mixes signals of different sources.

The property of being unrelated is of fundamental importance, because it can be used to separate not only mixtures of sounds, but also mixtures of almost any type (e.g. ongoing EEG). The informal notion that voices are *unrelated* can be captured in terms of statistical independence. If two or more signals are statistically independent of each other, then the value of one signal provides no information regarding the value of the other signals. For independent signal sources, the assumption that signals from different physical processes are uncorrelated is still true, but the opposite assumption that uncorrelated signals are from different physical processes is not. This is because lack of correlation is a weaker property than independence. In summary, independence implies a lack of correlation, but a lack of correlation does not imply independence (rational from Stone, 2004).

Therefore, the decomposition into independent source signals during ICA is superior to the decomposition into uncorrelated source signals during PCA or FA and is more applicable for identifying *independent* neuronal processes in on-going EEG signals.

Assumptions of ICA

The previously applied example of decomposing voices during a cocktail party is somewhat idealized and lacks external validity. Two people rarely make up a cocktail 'party', and usually a vast amount of background noise is present (loud ceiling ventilators, music, cocktail-shakers, etc.). During a 'real' cocktail party it would certainly be much harder, if not impossible, to follow any single conversation by listening to the recorded sounds of only two microphones. This is because the two microphones would pick up sounds from all sources (even though to different degrees). Similarly, during neuronal processing in the brain, a large number of simultaneous components constitute the measured EEG signal that is recorded by a limited amount of recording sites on the scalp. In a recent summary on how to apply ICA during EEG analyses Debener and colleagues (2010) summarized the assumptions that need to be met in order for the ICA to reliably decompose a large number of sources. They also provide recommendations for how to best meet these assumptions for EEG recordings. Indeed, the *real* cocktail party example remains a good illustration of the proper usage of ICA for the EEG signal. The following assumptions and implications are stated for EEG:

More Sensors than Sources.

In order to solve the cocktail party problem, there must be at least as many microphones in the room as there are sources of sound. During the cocktail party, one can simply assign one microphone per person and add more for other sources (music, etc.) However, with real biological signals (e.g. EEG), the number of sources that constitute the signal are unknown and, therefore, the number of required recording sites cannot be easily determined. This becomes an issue if several independent, but non-stereotypical artifacts are part of the EEG signal. Each artifact would be identified as an independent component and very quickly the available amount of recording sites on the scalp (microphones) would be used up. In the case in which there are more EEG signal sources than electrodes on the scalp, the ICA algorithm will try to pool sources that are most similar to each other into one component.

One strategy to minimize the problem of too many EEG signal sources is to reject non-stereotypical artifacts (that would bind their own source component), such as gross head movement, cable movement, or swallowing. These contributors to the EEG normally occur only a limited number of times during the recording and are not of particular interest for the experiment. Therefore, the EEG data in Study 3 that was submitted to ICA was pruned from epochs containing non-stereotypical artifacts. In contrast, more common and frequent EEG artifacts such as eye- or eye-lid movements remained in the data and were removed via back projection that included these artifact components (see chapter 4.2.4.2).

Spatial Stationarity.

The location of the sources is not allowed to change relative to the location of the microphones since that would change the source composition that is being picked up by each individual microphone. In other words, neither the guests of the party, nor the microphones would be allowed to change their positions over time. Even though neuronal sources (i.e. party guests) are not likely to shift in the brain, the recording sites (i.e. microphones) are. This assumption is an issue for EEG recordings because the electrode cap may move due to a bad fit, touch, facial expressions, pulling, or head movements. Therefore, electrode movements should be avoided or kept at a minimum in

order to facilitate a good ICA decomposition. In addition, single channel drifts also violate this assumption because they distort the *true* underlying signals and add to data complexity.

A strategy for reducing data complexity that is recommended by Debener and colleagues (2010) is the removal of channel drifts. These drift are usually due to wide filter settings that lead to high amplitude drifts in the < 1 Hz frequency range. These drifts are often caused by electrode potentials or sweating. The removal of low frequency drifts in the EEG data of Study 3 was achieved by applying a high-pass filter of 1 Hz (48 db). In addition, spatial stationarity of EEG data in Study 3 was preserved by taking particular care of properly placing and adjusting the electrode caps and informing participants that the movement of their jaw or scratching their scalp during the EEG measurement blocks would influence data quality (and they were asked to avoid these movements if possible).

Linear Mixing.

The signals that are received by each microphone are assumed to be an instantaneous linear mixture of all the source signals. For the cocktail party example, this may become be a problem if the room is very large as it takes time for sound to travel across a distance. The result is that microphones that are placed farther away would pick up a signal from a source slightly later than those microphones nearby. For EEG measurements, however, the electrophysiological signals are very fast, due to the laws of conductance and, therefore, the assumption of an instantaneous arrival of all signals to the recording sites seems very well met. For this reason no particular care had to be taken during the data acquisition of Study 3 in order to fulfill this requirement.

Independence of Sources.

If during the cocktail party two cocktail mixers are used perfectly simultaneously and in perfect synchrony, would the ICA be able to decompose the recoded signal into two independent sounds? This is also becoming an issue for EEG data, since the independence of all neuronal activity is not very plausible. A number of neuronal networks have much in common with each other and functional coupling or connectivity between even distant cortical regions can be assumed. This problem, however, appears

more serious than it is since, as long as two sources are not perfectly coupled during the recording, some degree of temporal independence can be assumed. This amount of partial independence, i.e. only partial connectivity, seems to be sufficient for the ICA to achieve a good result for the signal decomposition. Debener and colleagues (Debener, Hine, Bleeck, & Eyles, 2008) even report that ICA can also deal with artifacts that appear to be perfectly phase-locked to certain event-related potentials (ERPs). In addition, ICA is very successful in recovering regionally distinct dipole patterns of the brain, which suggests that the cortical brain regions involved may not be perfectly simultaneous enough in order to cause significant issues with the signal decomposition. Therefore, it seems safe to believe that this assumption is met also for Study 3.

Non-Gaussian Distribution.

Debener and colleagues (2010) point out that this assumption appears to be impossible to test for EEG signals. That is, the assumption that (at least some) sources of the EEG must not contribute a perfectly Gaussian distribution. They state that mixed signals such as EEG data are often characterized by Gaussian distributions, which can be explained by the central limit theorem. This theorem, they summarize, states that: "the sum of a number of independent random variables is characterized by a more Gaussian distribution than that of the independent variables. The opposite interpretation is however not justified: Just because we are recording a signal with a Gaussian distribution we cannot infer that this signal consists of a mixture of non-Gaussian sources" (Debener, et al., 2010, p. 142). For that reason, as with the independence assumption, it seems impossible to tell whether this assumption is reasonable for EEG data. They conclude, however, that "given the practical value of ICA and the quality of many ICA decompositions, we conclude that the assumptions of independence and non-Gaussian distribution seem to be reasonably plausible for EEG data" (Debener, et al., 2010, p. 142).

In summary, the assumptions that need to be met in order to assure a good ICA outcome seem very well established by the experimental procedure of Study 3. The signal decomposition of the 32 recording sites of Study 3 are well suited to identify epochs containing repeatedly occurring, stereotyped ocular and heart beat related artifacts using

ICA. However, since it cannot be assured that the number of true source signals did not exceed 32, which would lead to an under-complete decomposition (mixing some of the neuronal sources into one component), the ICA decomposition of Study 3 was not suited to reliably distinguish or analyze neuronal source generators on their dipole level. Therefore, the ICA decomposition was just used to remove well defined and easy to identify artifact components (see section 4.1.4.2).

ICA calculation

Well written books on the mathematical details and differences between different ICA applications have been published (e.g. Hyvarinen, Karhunen, & Oja, 2001; Stone, 2004). However, the following paragraphs will rely on the excellent chapter from Debener and colleagues (2010) that provides specifically meaningful insight by describing the basic ICA model in the context of EEG data.

In principle, the authors explain that the ICA decomposes multi-channel EEG recordings into a weighted (linear) mixture of different processes or signal sources. If a recorded EEG is 2-D data matrix X consisting of a number of channels (rows) and time points (columns), then the outcome of the ICA is a square matrix W of the size of the number of channels. W enables the modeling, or recovery, of the independent component activity time courses, A, such that

$$A = WX \tag{2}$$

The matrix A is revealed by matrix multiplication of W with the raw data matrix X, and has the same size as X. Now, however, A refers to independent components (ICs), not channels, and the columns represent the activity profiles from ICs that are maximally temporal independent from each other. The recorded data X can be fully reconstructed through a method called back-projection, i.e. by multiplication of the inverse of W with A (Figure 4.2.4). Thus, W^{-1} is known as the mixing matrix:

$$X = W^{-1}A \tag{3}$$

Terminologically, the left part of this equation (equation 3) is usually referred to as the channel or signal space, because the values stored in X have a proper physical unit (micro volts for EEG recordings). The right part of the equation however is called the source space and its values are arbitrarily scaled. Being arbitrary scaled, however, does not mean that sign and magnitude information is lost, but only that the sign and magnitude information are distributed between W^{-1} and A.

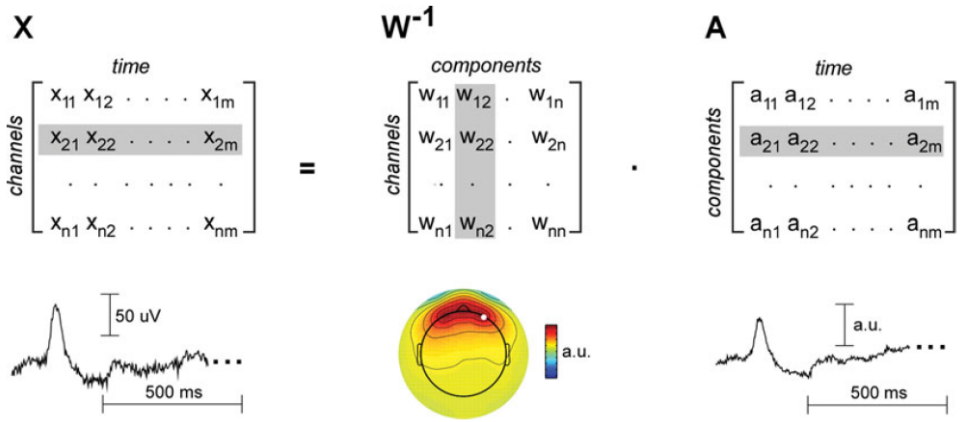

Figure 4.2.4 Linear decomposition of multi-channel EEG data (X)

Inverse weights (W^{-1}) represent the spatial pattern of each source time course. Matrix-multiplication of W with the maximally independent time courses (in A) results in the mixed channel data; this process is called back-projection. For illustration purposes, one component/channel vector is highlighted in grey and shown below the corresponding matrices (description and illustration adapted from, Debener, et al., 2010).

For each independent component (IC), the rows of matrix W^{-1} contain the weights at each recording channel. Each row can therefore provide the topographical information for an IC, which is nothing else than the contribution of each channel to the respective IC time course stored in A. This topographical contribution can be plotted as a topographical map. In summary, A reflects the activity changes over time, and W^{-1} stores the spatial weights that apply equally to all time points. This is also illustrated in Figure 4.2.4.

For the EEG data pre-processing of Study 3, an Infomax ICA (Bell & Sejnowski, 1995; Makeig, et al., 1996) was applied, which integrates a self-organizing learning algorithm in order to maximize the information contained in the ICs. Infomax ICA was

found to produce robust decompositions of EEG signals (Jung, Makeig, Humphries, et al., 2000) and is also the most widely used for EEG data analyses (Debener, et al., 2010).

4.2.4.2 EEG artifact removal using ICA

One or several ICs can be back-projected into the signal space in order to obtain and evaluate the actual contribution that they have on the raw signal. The back-projection produces results in the signal space and, therefore, possesses the proper physical units. In fact, ICs that were identified to contain artifacts can be removed by performing a back-projection of all but those artifact components. This can be practically achieved by zeroing out the columns (in W^{-1}) or the rows (in A) of those ICs. Figure 4.2.5 provides a good illustration of the principle of applying back-projection for artifact removal in EEG data. The comparison of the eye blink topographies before and after artifact correction (top left and right topographies) demonstrates that the eye-blink has been corrected from the EEG data. An analysis of the electrophysiological signal at the position of the eye-blinks would have not been possible prior to the ICA artifact correction.

The apparent advantages of using ICA for artifact removal, however, come at a cost. To date, no established and tested procedure exists that can automatically identify only ICs that contain artifact contributions to the EEG signal. The identification of artifact ICs must either occur manually or through semi-automatic procedures (e.g. Viola et al., 2009) but (both times) neither misses nor false-alarms can be fully avoided. There are many issues that are raised by this subjectivity of IC-selection, but the danger of overcorrecting the data appears to be the most practically concerning. During IC selection, it is easy to categorize a component as an artifact, whereas in reality it contains a true EEG signal. The consequences for an EEG experiment can be dire, if small but relevant effects of the experimental intervention are excluded in several participants or (even worse) between different conditions (which would lead to no or false findings).

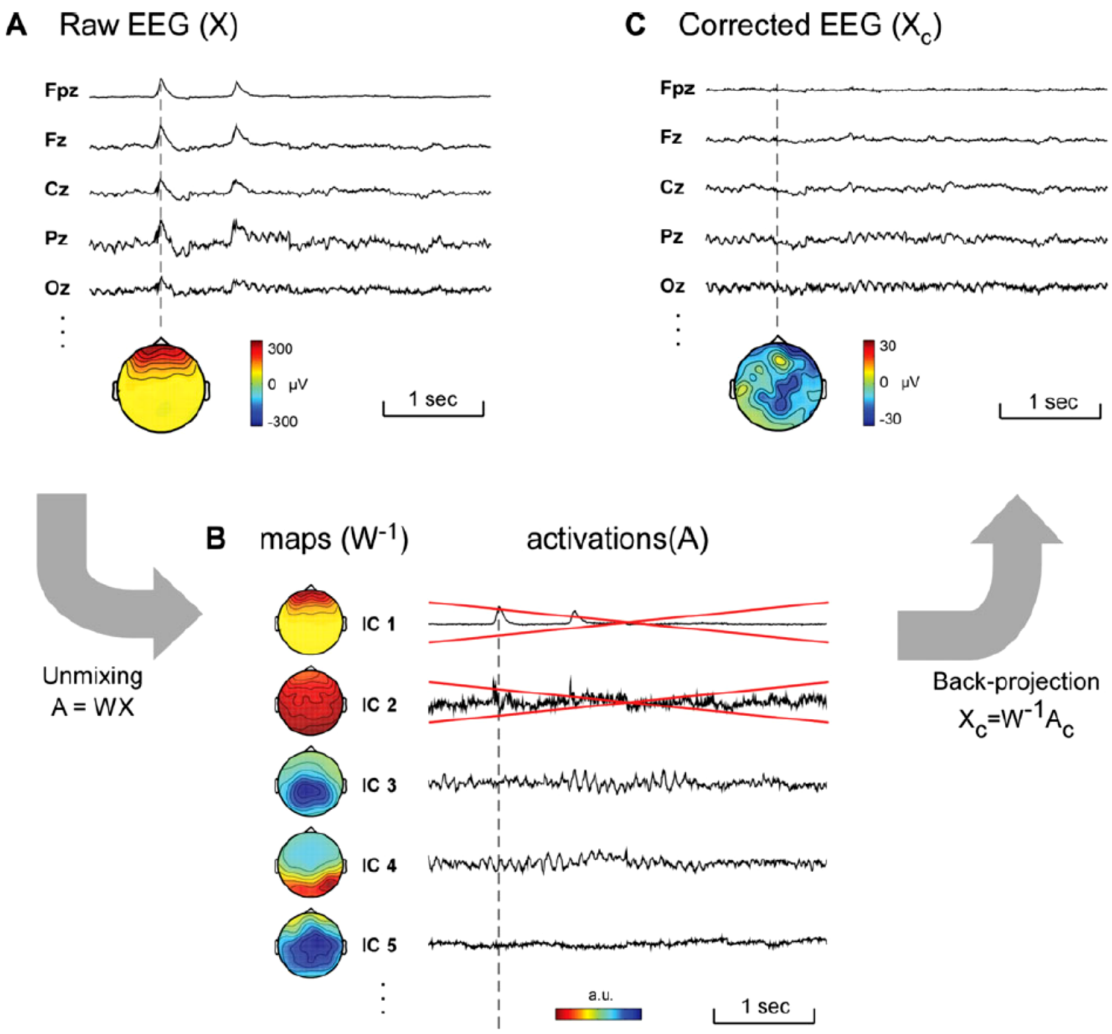

Figure 4.2.5 Illustration of artifact removal by means of ICA

A: Selection of EEG channels shows ongoing EEG with two eye blinks at fronto-polar channels. **B:** Unmixing of the EEG data results in independent components (ICs). Each IC can be described on the basis of a topographical map and a time course of activation. **C:** The back-projection of all but the first (eye-blink) and second (noise) IC results in artifact corrected EEG data (description and illustration adapted from Debener, et al., 2010).

In order to minimize the issues of IC artifact selection in Study 3, only ICs that could be clearly identified to be different from brain activity patterns were excluded from the EEG signal. To aid and guide the IC selection process, a number of clearly defined artifact criteria were used. These criteria were also proposed by Debener and colleagues (2010) and are illustrated in Figure 4.2.6. Only four very common and easy to identify artifact components were excluded from the EEG signal in Study 3:

(i) Eye blinks can often be easily identified by their characteristic frontal topography (W^{-1}) and time course (A) (Viola, et al., 2009). Since this kind of artifact also occurs very frequently and affects even the EEG signal during eyes closed conditions (rolling eye-balls while the eyes are closed), its removal in Study 3 was essential in order to obtain large segments of consecutive, artifact free EEG data for the further statistical analyses.

(ii) Lateral eye movements (usually represented by just one IC) also have a very characteristic time course and topography, and often correlate with the horizontal electro-occulogram (HEOG). The removal of this IC was not as essential for Study 3 but it clearly added to the data quality.

(iii) Muscle (or electromyogram – EMG) activity can often be identified by clear topographies that represent different muscle groups. However, the distinction between muscle activity and channel noise may not always be straight forward, and the two can be mistaken for each other. Noise can appear just at a single electrode, but it can also be more distributed in cases of issues with multiple cable leads or electrode malfunctions. In Study 3, both artifact sources were excluded, since there was no reason to include either one of them. Therefore, their exact distinction was not necessary and their removal greatly improved the spectral plausibility of the succeeding spectral analyses.

(iv) Electrical heartbeat activity is often represented in one (or even two) IC(s). The characteristic R peaks of the heartbeat signal are likely to go undetected in the mixed channel signal, but ICA decomposition is able to provide a clear unmixing. Its asymmetric topography is highly characteristic for this component, and its spectral properties are posed to influence measures such as posterior EEG alpha asymmetry (Debener, et al., 2010). For that reason, it was crucial to exclude this artifact during the artifact correction of Study 3, in order to avoid artifact related shifts in spectral power and spectral topographies.

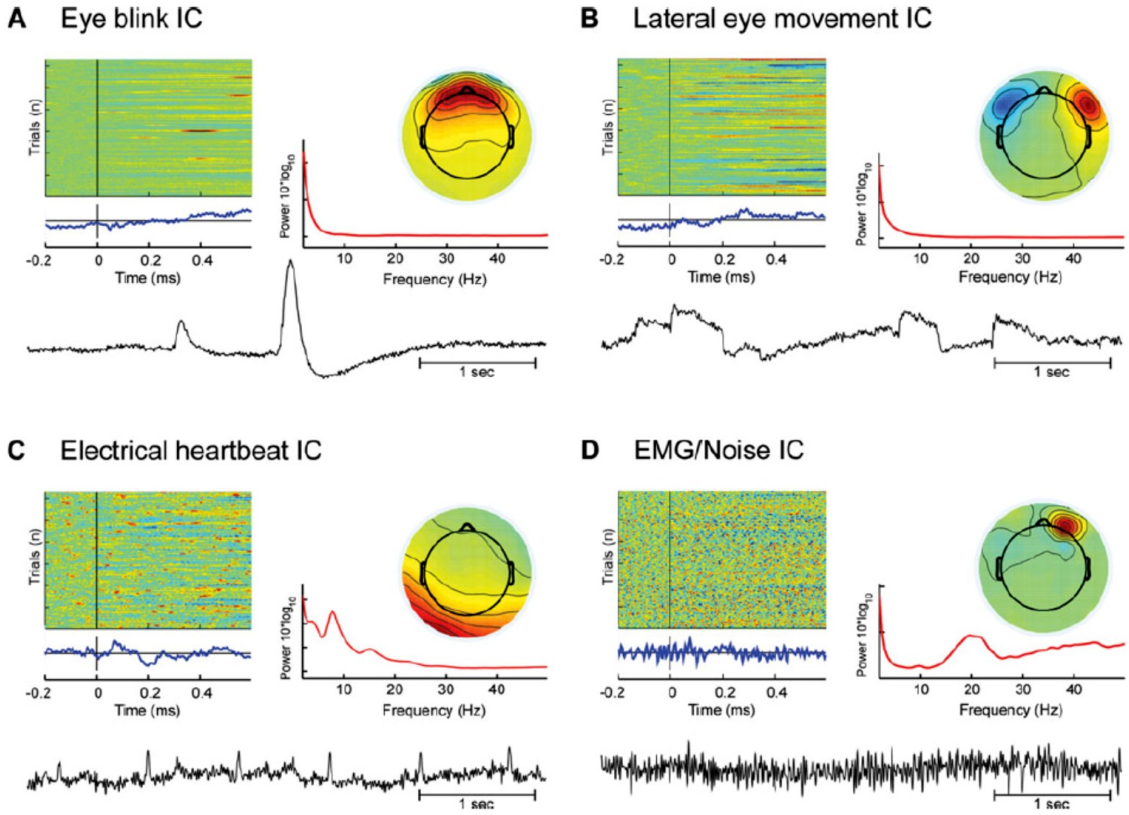

Figure 4.2.6 Typical artifacts as identified by ICA

Shown are the IC maps of the single-trial activity as an image, the time domain average (i.e. ERP, in blue) and the spectrum (red), along with a representative section of ongoing activity (below) – each for the artifact: A: Eye blink; B: Lateral eye movement; C: Heartbeat; D: Same for muscle/noise activity. (illustration from, Debener, Thorne, Schneider, & Viola, 2010)

By applying ICA artifact correction in Study 3, it was possible to obtain very large and coherent sections of EEG that were cleared from (nearly) all ocular, muscle, heart-beat, and noise artifacts. The only sections of EEG that were excluded from all analyses contained infrequent and non-stereotypical artifacts, such as cable movements, and these segments amounted, on average, to less than 5 % per measurement block and participant. More traditional artifact correction procedures would have resulted in a much greater loss of data since all segments that contain an artifact are not corrected but excluded from all analyses. For participants that showed a large number of eye-blink or eye-movement related artifacts, for example, a traditional data correction would have in some cases led to the exclusion of more than 60 % of EEG data. The ICA artifact correction maintained almost the entire EEG signal and, therefore, was a much better

representation of the neuronal processing than would have been achieved by just excluding all artifacts. Therefore, ICA data correction improved the quality for the analysis of global markers of EEG activity that are negatively influenced by a large number of non-consecutive EEG data segments (see section 4.2.5.2).

4.2.5 EEG Analyses

Study 1 and Study 2 revealed cortisol induced effects on the thalamus, implying fundamental and global changes on EEG. Therefore, effects of cortisol infusion were assessed for global field power (GFP; spatial standard deviation) which quantifies global signal strength, and for global map dissimilarity (GMD; the spatial square root of the mean of the squared differences, between two maps) which measures map complexity (for a closer decription, see section 4.2.5.1 and 4.2.5.2, or, Koenig & Gianotti, 2009; Lehmann, et al., 1987). Scalp potential fields with pronounced peaks and steep gradients result in high GFP (i.e. high signal strength), while GFP is low in maps with flat appearance and shallow gradients. GMD is 0 when two maps are equal (i.e. low map complexity), and maximally reaches 2 when the maps have the same topography with reversed polarity. GFP and GMD were obtained from each data point or consecutively paired data points (for GMD) of the artifact corrected epochs, and averaged separately for each measurement block resulting in a single value per block and participant.

Spectral power density [μV^2/Hz] was calculated applying fast Fourier transformation (FFT) to the artifact corrected epochs of 4 seconds, resulting in a maximum resolution of 0.25 Hz. All epochs overlapped (10% at each end) to compensate the differential weighting of data points (Dumermuth & Molinari, 1987) and were extracted through a Hanning window which was specified to diminish the signal 10% at each end, to prevent spurious estimates of spectral power (Bloomfield, 1976). The resulting spectral epochs were averaged and Ln-transformed (Gasser, Bacher, & Mocks, 1982) and spectral power density for the frequency bands 4-8 Hz, 8-12 Hz, and 12-30 Hz (independent variable FREQUENCY) were created for each electrode. Electrodes at the location F, FC, C, CP, P and O (independent variable CAUDALITY) were averaged according to coronal rows on the scalp to include them as the topographical factor CAUDALITY

(frontal, fronto-central, central, centro-parietal, parietal, occipital) during statistical analyses.

The post infusion measurements of spectral power density, GFP and GMD (0-7 min, 10-17 min, 20-27 min), were baseline corrected intra-individually by subtracting the pre-infusion measurement (-7 – 0 min) – the baseline corrected values are used for ANOVA. The artifact screening, re-referencing, and ICA were performed with Brain Vision Analyzer 2.0 (BrainProducts, München, Germany), FFT (applying '*pwelch'* function), GFP- and GMD-analyses were performed in MATLAB.

4.2.5.1 Global Field Power

Global field power (GFP) is a descriptor of the global strength of a scalp potential at one point in time across all recording sites (i.e. electrodes) of an EEG. GFP quantifies the strength of the measured electrophysiological activity of all involved electrodes and, therefore, constitutes a measure of global (i.e. across the whole head) scalp potential field strength. It is equivalent to the computation of the standard deviation of the field potential (Koenig & Gianotti, 2009) and is defined as

$$GFP = \sqrt{\frac{\sum_{i=1}^{N}(u_i - \bar{u})^2}{N}} \tag{4}$$

where u_i is the voltage of the map u at the electrode i, $\bar{u}$ is the average voltage of all electrodes of the map u, and N is the number of electrodes of the map u. GFP is reference independent but through the subtraction of the averaged signal from the individual potential, an average reference is implicitly contained. GFP can be seen as a spatial standard deviation that is calculated on a sampling point by sampling point basis.

Koenig and Gianotti (2009) point out that scalp potential fields with steep gradients (i.e. a large voltage difference between distant recording sites) and pronounced peaks and troughs, which they describe as "hilly" maps, result in a high GFP value. On the other side, shallow gradients of a flat and shallow appearing electrical fields result in a low GFP value. Figure 4.2.7 illustrates this by plotting the electrical scalp potentials of an EEG during low and high GFP.

Figure 4.2.7 also illustrates that the calculation of GFP for continuous EEG data leads to a single GFP value per data point that can also be plotted as a function of time. The GFP and its rational can also be demonstrated another way. When the potentials of two recording sites are plotted into a state (vector) space (as seen in Figure 4.2.8), the

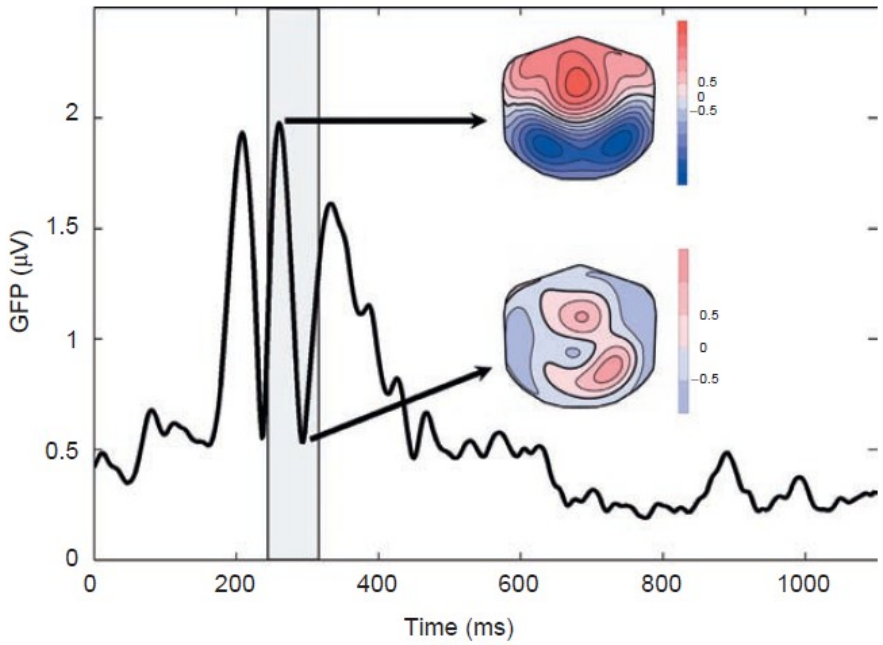

Figure 4.2.7 Global Field Power during high and low gradient scalp potentials

Curve of Global field power (GFP, y-axis in µV) over time (x-axis) for ERP data. The scalp field map during high GFP (at 226 ms) shows a much steeper gradient than the field map during shallow gradients (292 ms) (illustration from, Koenig & Gianotti, 2009).

Euclidean distance u of this point (vector) from the origin is the *sum* of the squared potentials of both recording sites (e.g. C3, P3). Now, the GFP has been defined as the root of the *mean* of the squared potentials, and the only difference between the distance u and GFP is thus a constant factor$\sqrt{N}$ by which the GFP is smaller than u. Now, if instead of using only two recording sites, the number is increased to N, the state space display would then change from two to N-dimensional. The computation of u, however, would still be defined as the root of the sum of all squared potentials of all N electrodes and this would still remain proportional to the GFP by factor of $\sqrt{N}$ (Koenig & Gianotti, 2009).

Interpretation of the GFP in Study Three

Since the GFP is a numerical expression for the gradients (i.e. hilliness) and, therefore, the amplitude of a recorded EEG topography, it is a very good expression of the global signal strength of the EEG. This logic does not only apply on the level of a single data point but can also be extended to a number of consecutive data points. That is, in an EEG segment (e.g. 10 seconds with 2500 data points) in which the signal is generally very hilly due to large amplitudes, the GFP will on average also be higher than in segments that contain shallower, or low amplitude signals. This way the general (or averaged) hilliness (amplitude) of a section of EEG can be assessed. Of course, even if the averaged GFP of an EEG segment may be very high, there are even a number of data points representing low GFP. However, it is still possible to compare the averaged GFP signal of several EEG segments in order to draw a conclusion about how much they differ (on average) in their inherent signal strength (i.e. amplitudes). This rational was applied to assess the signal strength of the EEG measurement block in Study 3.

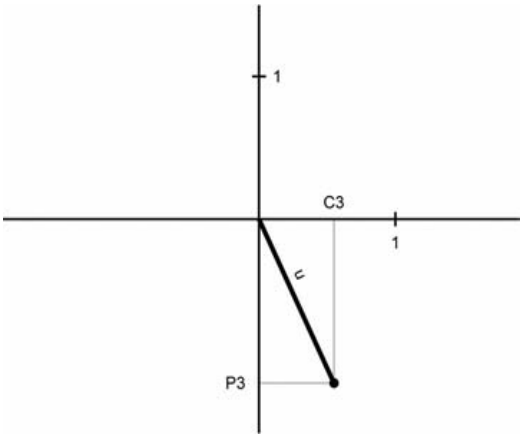

Figure 4.2.8 Electrode potentials of two recording sites (C3, P3) plotted into a state-space diagram.

(Koenig & Gianotti, 2009)

By calculating the averaged GFP of each measurement block in Study 3, it was possible to examine if cortisol, on average, influences the EEG signal strength. However, due to the GFP averageing, it is not possible to infer that a cortisol induced change affected EEG throughout the entire segment. Changes in the average can, for example, also occur if an effect is large, but temporally narrow. Therefore, the applied analysis of EEG signal strength in Study 3 is meaningful in order to establish if there is indeed an effect, but more temporally destinct GFP calculations would be necessary in order to further characterize the temporal nature of that effect. For a first explorative investigation into cortisol induced effects on the EEG, such temporal distinctions are not necessary.

4.2.5.2 Global Map Dissimilarity

Another meaningful way to assess global EEG characteristics, besides the measurement of signal strength through the GFP (section 4.2.5.1), is to quantify how homogeneous (or heterogeneous) EEG scalp topographies are across time. One can assume that two identical neuronal processes that are active just at two different points in time will produce two identical EEG topographies at the scalp recording sites. In comparison, neurological processes that are different from each other will lead to two different EEG scalp topographies. These two statements are generally true and by assessing the EEG map similarity of same or different neurological processes, it would be possible to quantify the amount of neuronal processing similarity. However, since the EEG measured at the scalp is a mixture of electrical potentials, the reverse statement would be invalid. Due to the inverse problem (Hopfiner, Khoe, & Song, 2005), one cannot infer that two identical topographical maps must be the result of two identical neurological processes. In other words, identical topographical maps are a necessary but not a sufficient requirement to infer identical neuronal processes. Now, what does it mean if two topographical maps are identical?

With no other assumptions made, identical topographical maps do not contain much information other than the general possibility that there *may* be two identical neuronal processes active. Information like that is not very valuable. On the contrary, when two maps are different from each other, it is impossible that all neuronal processes that constitute these signals are identical. Therefore, even if the topographical map *similarity* holds no valid information, the topographical map *dissimilarity* allows definite statements about whether or not neuronal processes are absolutely different from each other.

The above stated rational was used in Study 3 in order to assess the influence of a cortisol infusion on the dissimilarity of topographical EEG maps. In other words, the assessment of map dissimilarity allowed inferences in regards to how cortisol influences the dissimilarity of neuronal processes. Increased dissimilarity scores would signal very heterogeneous and diverse neuronal processing, whereas smaller dissimilarity scores would indicate the necessary requirements for more equal neuronal processing (and increase the likelihood, but not guaranty, that identical neuronal processes are indeed at

play). Map dissimilarity scores appear very helpful to assess global EEG brain states, but how can they be reliably quantified?

Calculating Map Dissimilarity

In general, the similarity or dissimilarity of two topographies can be easily assessed by the computation of a difference map. The rationale behind this is that if two experimental conditions differ in some neuronal sources, then the difference map between the scalp field maps of the two conditions equals the scalp field map produced by those sources that differ between the two conditions. This reasoning concerning difference maps is theoretically sound but does not truly represent a measure of topographical map *dissimilarity*. It merely represents a crude measure of difference, irrespective of topographical changes. The reason for this is that there needs to be a distinction made between changes in total map amplitude and amplitude independent changes in the spatial distribution. In other words, two cases are possible that can lead to a difference map, but their implications are quite different (Koenig & Gianotti, 2009):

(i) The difference in a map can occur because all active sources changed their strength in a proportional manner. Therefore, the maps of the two conditions would only differ by a global scaling factor. When this scaling is eliminated, the potentials of the difference map should become zero at all electrodes. In practice, such a difference map would not imply differences in the amount of involved signal sources or their individual contribution, but solely in their amplitude.

(ii) The difference in a map can occur because some sources changed their strength in a manner that was disproportional to the strength of the other sources. Therefore, map differences exist although possible differences in scaling have been eliminated by map normalization. Such a difference would imply a ‘real’ change in topography due to the change of the amount of signal sources or due to a shift in the amount of their individual contribution to the resulting scalp potential.

The above mentioned distinctions between the possible characteristics of difference maps point out the necessity to normalize the maps prior to subtraction in order to infer real topographical map differences. The map normalization can be achieved by dividing the potential values at each electrode of a given map by its GFP (section 4.2.5.1). This procedure is somewhat similar to the computation of relative power, where the power spectrum is normalized by the total power (Koenig & Gianotti, 2009).

With a similar rational as presented earlier for GFP calculation (Figure 4.2.8) difference maps and their map normalization have a simple geometrical representation in the state space. Figure 4.2.9 illustrates how two electrodes of one map (at time t1) are plotted into the state space together with the same electrodes at a later time (at time t2). The two maps are represented by two points in the state space, and it becomes clear that they differ in their GFP because their length relative to the origin is different. Normalizing

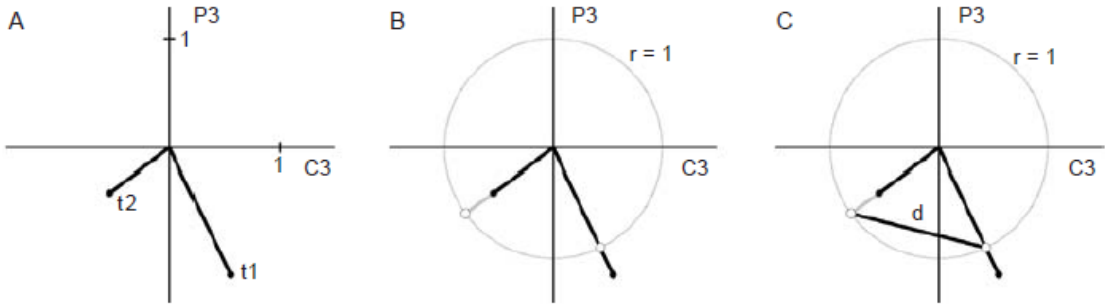

Figure 4.2.9 Potentials of two electrodes at two different time points and their dissimilarity plotted into a state-space diagram

A: Potentials of two electrodes C3 and P3 at two different time points (t1, t2). They are mapped into the state-space and form two vectors. **B:** Their vectors are normalized by projection on the unit circle. **C:** The global map dissimilarity (GMD) is defined as the distance d between the endpoints of two normalized vectors (illustration and description adapted from, Koenig & Gianotti, 2009).

the maps makes them equidistant to their origin and they both project onto the unit circle (Koenig & Gianotti, 2009). If the two maps were to only differ in their total strength (i.e. amplitude) but not in their topography, then the normalization would project them at exactly the same point of the circle. Their difference would be fully explained by a difference in their GFP, and this corresponds to the first case (i) described above.

However, if as in Figure 4.2.9 the normalization projects the maps at t1 and t2 onto different points of the unit circle, then their differences cannot be simply explained by differences in their GFP. In fact, their difference can also be attributed to an additional change in topographies which corresponds to the second case (ii) described above. The distance d between the two projections on the unit circle is "the amplitude-independent measure of map difference and corresponds to the GFP of the difference of the normalized maps" (Koenig & Gianotti, 2009, p. 45). Lehmann and Skrandies (1980) introduced this measure as the global map dissimilarity (GMD) and defined it as

$$GMD = \sqrt{\frac{1}{N}\sum_{i=1}^{N}\left\{\frac{u_i - \bar{u}}{\sqrt{\sum_{i=1}^{N}\frac{(u_i-\bar{u})^2}{N}}} - \frac{v_i - \bar{v}}{\sqrt{\sum_{i=1}^{N}\frac{(v_i-\bar{v})^2}{N}}}\right\}^2} \quad (5)$$

where u_i is the voltage of map u at the electrode i, v_i is the voltage of map v at the electrode i, $\bar{u}$ is the average voltage of all electrodes of map u, $\bar{v}$ is the average voltage of all electrodes of map v, and N is the total number of electrodes. The GMD (distance d in Figure 4.2.9c) is 0 when two maps are equal, and GMD can maximally reach 2 (equals the diameter of the unit circle) for the case where the two maps point in the opposite direction, i.e. have the same topography with reversed polarity (Koenig & Gianotti, 2009). As with the GFP, the calculation of GMD is identical for N electrodes which would then be the distance d in an N-dimensional state space.

Similar to the GFP, the logic of the GMD does not solely apply to the comparison of only two topographical maps, thus in Study 3 the GMD was also calculated for large segments of consecutive EEG data. GMD was calculated pair-wise (comparisons of data points 1-2, 2-3, 3-4 … etc.) for all K consecutive data points in each measurement block of the EEG, resulting into $K - 1$ GMD values.

Influences of the Artifact Correction

In prior investigations that used GMD calculations, topographical maps have been reported to be relatively stable for about 60-100 ms. These stable map topographies have

been termed *microstates* (e.g. Lehmann, et al., 1987). The GMD between two data points within such a microstate are expected to be close to 0, whereas the GMD between different microstates is much closer to 2. For this reason, it was crucial that the EEG artifact correction was conducted using ICA back-projection. A more traditional artifact correction may have excluded a large number of data sections and would have led to a large number of 'sharp edges' between (apparently) consecutive maps (which would in turn have resulted in large GMD values). In fact, these differences would have not been due to physiological processes, but simply due to the artifact correction. ICA artifact correction avoided this problem all together by keeping large parts of the data in its consecutive integrity, and only excluding infrequent non-stereotypical artifacts which would have led to higher (and faulty) GMD in the first place (e.g. the topography of muscle activity or channel noise is very different from 'normal' EEG maps).

Interpretation of GMD in Study Three

As for the GFP, all GMD values of one EEG measurement block were averaged into one single GMD value to assess the general (or averaged) map dissimiliarity of a section of EEG. This averaging generalized all changes in GMD and more advanced statements on the temporal charateristics (i.e. distribution) were not possible. However, this approach is perfectly able to assess global and longer lasting effects of cortisol on the electrophysiological potentials recorded by the EEG. An increase in the GMD average of an EEG measurement block, relative to a baseline, would infer that the topographical maps have changed much more often or to a much larger extent. A GMD decrease, relative to a baseline, on the other hand, would infer that the neuronal processing during this measurement block did not alter as often or as much as during baseline. Such statements may be somewhat crude for the discription of distinct effect mechanisms, but they are valuable to estabablish whether or not cortisol induces any kind of measurable effect.

4.2.6 Manipulation check

Acute HPA axis activity was obtained through three saliva samples per session to check if the pharmacological manipulation succeeded. Participants provided their first

sample upon arrival, the second before entering the MRI scanning room, and the third after the last MRI sequence (independent variable TIME). All samples were immediately frozen for biochemical analysis. Salivary cortisol was analyzed with an immunoassay with fluorescence detection (see Dressendorfer, et al., 1992). Intra- and inter-assay variability was less than 10 and 12% respectively, and this reliability was suited for further statistical analyses.

4.2.7 Statistical Analyses

4.2.7.1 Manipulation check

For Study 3, the pharmacological manipulation was assessed via 2 x 3 ANOVA with the INTERVENTION (cortisol, placebo) and acquisition TIME (arrival, before MRI, after MRI) in a repeated-measurements factorial design.

4.2.7.2 Signal strength, spectral power, map complexity

The baseline corrected global EEG measures of GMD and GFP were submitted each to a separate 2 x 3 ANOVA, entering the factors INTERVENTION (cortisol, placebo), and MEASUREMENT BLOCK (0 - 7 min, 10 - 17 min, 20 - 27 min post infusion) as repeated measures. The baseline corrected and Ln-transformed spectral power density measures were submitted to a 2 x 3 x 6 x 3 ANOVA, entering the factors INTERVENTION (cortisol, placebo), MEASUREMENT BLOCK (0 - 7 min, 10 - 17 min, 20 - 27 min post infusion), CAUDALITY (frontal, fronto-central, central, centro-parietal, parietal, occipital) and FREQUENCY (4-8 Hz, 8-12 Hz, 12-30 Hz) as repeated measures.

A Huynh–Feldt correction of the degrees of freedom was performed whenever appropriate. Significant effects (alpha < 0.05) were further analyzed using Dunn's Multiple Comparison Procedure (Dunn, 1961) as posthoc analyses and the critical differences (ψ) for $p < .05$, $p < .01$, and the number of comparisons (C) are stated. The presentation of results will be limited to significant ($p < .05$) intervention related effects only, and the effect size measure *partial* η^2 (Cohen, 1988) are reported.

4.3 RESULTS

4.3.1 Manipulation check

After the inspection of the salivary cortisol measurements, a descriptive increase in the cortisol levels (after the MRI measurement) could only be observed in thirteen of fourteen participants. The intervention in these thirteen participants was successful ($F_{(2,24)}$ = 9.064, p = .001, η^2_{part} = .411) and only these participants entered into EEG analyses. In these participants, salivary cortisol significantly increased directly after the EEG measurements in the cortisol but not in the placebo condition (significant mean increase in cortisol condition: 3.7 nmol/l).

4.3.2 Signal strength, spectral power, map complexity

Cortisol infusion significantly decreased the signal strength ($F_{(1,12)}$ = 41.009, p < .001, η^2_{part} = .774) and the spectral power density ($F_{(1,12)}$ = 18.215, p < .001, η^2_{part} = .603) as established by the significant main effect of INTERVENTION. Since spectral power is mathematically linked to signal strength, the decrease in GFP is reflected in the spectral power decrease across all bands (Figure 4.3.1, A, B). The interaction INTERVENTION x FREQUENCY that would signify an effect between the different frequency bands and the intervention (placebo or cortisol) showed no significant effect ($F_{(2,24)}$ = 0.726, p > .40). However, effects were significantly different between the frequency bands in the frontal topographical region because the interaction INTERVENTION x FREQUENCY x CAUDALITY became significant ($F_{(1,12)}$ = 8.150, p < .001, η^2_{part} = .404). A subsequent post-hoc analysis ($\psi_{5\%}$ = 0.226; $\psi_{1\%}$ = 0.262; C = 48) established that this effect was due to differences between the frequency bands in the frontal lobe during the placebo condition. The main effect INTERVENTION always remained significant (see Figure 4.3.2), however there were significant effects of the spectral power of the placebo condition in that the 8-12 Hz frequency band was significantly lower compared to both the 3-8 Hz and 12-30 Hz frequency band. The interaction INTERVENTION x FREQUENCY x CAUDALITY became significant because this effect was absent in the cortisol condition (Figure 4.3.2).

The measures of map complexity (GMD) significantly decreased after infusion in the cortisol compared to the placebo condition (Figure 4.3.1 C) across all measurement

blocks ($F_{(1,12)}$ = 6.532, p < .05, η^2_{part} = .352). This indicates a less dissimilar topography in the cortisol, compared to the placebo condition.

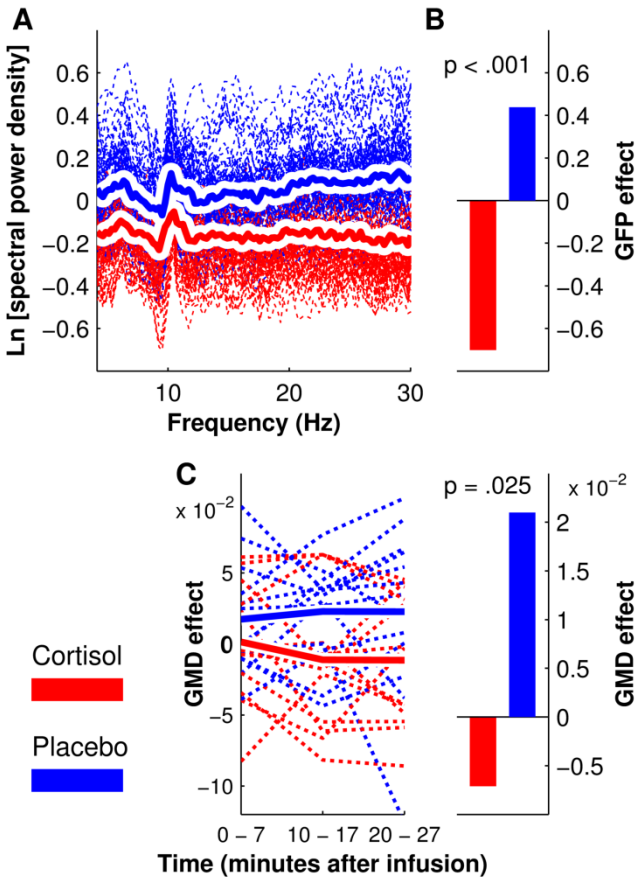

Figure 4.3.1 Effects of cortisol infusion on global EEG markers (Study 3)

A: Ln-transformed and baseline corrected FFT power spectra for all post-infusion measurement blocks, electrodes, and participants (dashed lines), with the average for cortisol (solid red line) and placebo (solid blue line) conditions. The cortisol induced decrease in spectral power stretches across all frequency bins (3-30 Hz). **B:** Baseline corrected signal strength (GFP) effect, averaged for all participants and post-infusion measurements for cortisol (red) and placebo (blue) conditions. The decrease in signal strength matches the effect in the spectral power. **C - left:** Baseline corrected global map complexity (GMD), for all post-infusion measurement blocks (0-7 minutes, 10-17 minutes, 20-27 minutes) displayed for each participant (dashed lines) and averaged for cortisol (solid red line) and placebo (solid blue line) conditions. **C - right**: Baseline corrected map complexity (GMD) averaged across all participants and post-infusion measurements for cortisol (red) and placebo (blue) conditions. GMD significantly decreased after the infusion of cortisol.

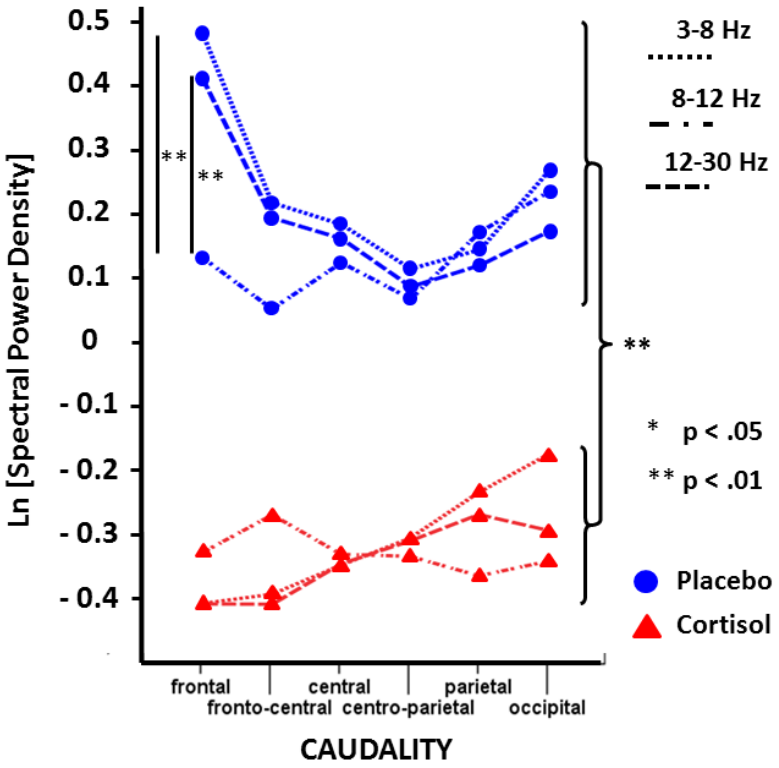

Figure 4.3.2 Three-way interaction INTERVENTION x FREQUENCY x CAUDALITY for Ln-transformed spectral power density scores (Study 3)

Baseline corrected spectral power density of all frequency bands was significantly different between cortisol (red – triangles) and placebo (blue – circles) conditions. However, in frontal regions the 8-12 Hz frequency band (dash-dotted lines) was significantly lower than the 3-12 Hz (dotted lines) and 12-30 Hz (dashed lines) bands in the placebo condition, but not in the cortisol condition.

4.4 DISCUSSION

Chapter IV reports on a placebo controlled and double-blinded EEG study in which 13 participants received intravenous cortisol (4mg) and placebo infusions in a randomized but balanced order of a within-subject design. Cortisol infusion significantly decreased the spectral power, the signal strength (GFP), and the map complexity (GMD) rapidly and for all post-infusion measurement blocks. The timeframe of these EEG effects (especially during the first two measurement blocks) gives reason to exclude currently known genomic mechanisms of cortisol action and points towards non-genomic cortisol mechanisms as a source for these effects. Since spectral power is mathematically linked

to signal strength, the decrease in signal strength is reflected in the spectral power decrease across all bands (Figure 4.3.1, A, B). This relationship is a convincing explanation for why channel position (CAUDALITY) led to no significant changes in the main cortisol effect of the spectral analyses.

The cortisol induced effects on EEG infer the existence of global and profound effects on neuronal activity that were not evident from the hemodynamic changes of Study 1 and Study 2. The decrease in signal strength after cortisol infusion across all recording sites may reflect a general protective mechanism of the CNS that is intended to suppress background processing in favor of more relevant stimuli response contingencies. That a decrease in signal strength may indeed be related to the ability to better process afferent signals has first been shown through evidence that the spontaneous EEG activity before an external event considerably influences the response to that event. In animals and humans, Basar and colleagues (e.g. Basar, Rahn, Demiralp, & Schurmann, 1998), among others, demonstrated an inverse relationship between spontaneous EEG and evoked potentials (e.g. the visual or auditory evoked potential; VEP, AEP), namely between the amplitude of the pre-stimulus EEG and the evoked potential to that stimulus. For example, the spectral power in the theta and alpha frequency bands showed a significant negative correlation with the subsequent VEPs and AEPs (Basar, et al., 1998; Rahn & Basar, 1993a, 1993b) with effect sizes larger than 10 %. Even if in those studies the correlation was higher for the theta band, a general processing advantage by decreasing the signal strength of all bands can be reasonably assumed.

In addition, the decrease in global map complexity (map dissimilarity) also suggests that the modes of stimuli processing may have been affected, i.e. streamlined, towards a more homogenous focus. Random and spontaneous cognitions, which would increase the map complexity over time, may have been suppressed in favor of exploring the environment for stress relevant stimuli. In the placebo condition the global map complexity increases and likely reflects enhanced spatial disarray as a result of an increase in spontaneous cognitions.

The absence of a real life stressor in Study 3 also suggests that the cortisol induced reduction in signal strength and map complexity may represent a general and unspecific (preparatory) response that is appropriate for a large variety of situations. After all, in real

life, cortisol levels of healthy adults are not expected to increase (other than due to diurnal rhythms) in the absence of a stressor. Therefore, the observed effects in Study 3 (and in fact in Study 1 and Study 2) may be unspecific but, at the same time, advantageous enough that they may represent one of the most fundamental ways of an organism to respond to challenges (or uncertainties). During genuine and natural stress responses (appearance of stressor – stress appraisal – stress-coping) this down tuning may even be overshadowed by increased processing of the stressor, yet, the unspecific down-tuning of background may make all the difference in regards to a successful coping outcome. In that sense, reducing signal strength and streamlining neural processing may keep the brain as a whole from a state of "processing overload".

The decrease in signal strength across all recoding sites indeed points towards a central contribution of subcortical areas (e.g. the thalamic nuclei). However, these effects may also be related to changes on the neuronal cell membranes and require further replication, ideally using simultaneous EEG-MRI measurements to enable EEG informed MRI analyses or visa verse (i.e. prediction of EEG from MRI; or prediction of MRI from EEG). That the main effect of the intervention for signal strength was also superimposed by a significant effect between the frequency bands at frontal recording sites in the placebo condition is not of much importance in regards to the general interpretation of the EEG findings. However, it is possible that the effect in frontal regions is yet another indicator that during the placebo condition, cognitions and ruminations increased compared to the cortisol condition. This interpretation seems feasible since the effect is in part carried by a spectral power increase of the beta band which is recognized to reflect cognitive processes (e.g.Ray & Cole, 1985).

In conclusion, the results of Study 3 suggest that cortisol profoundly affects the electrophysiological functioning of neuronal cells via a rapid and non-genomic mechanism that reduces global signal strength and map complexity and therefore, may improve the processing of stress relevant stimulus response contingencies.

GENERAL DISCUSSION

CHAPTER V

This thesis provides coherent evidence for rapid, large scale effects of glucocorticoids on the functioning of the CNS. Three placebo-controlled and double-blinded intravenous infusion studies found that infusions similar to naturally occurring (4 mg) cortisol boosts may exert effects on the human brain within 15 minutes. Using CASL as an MRI sequence, Studies 1 and 2 (Chapter II and III) identified rapid bilateral cortisol-induced thalamic perfusion decrements. Study 3 (Chapter IV) indicated the existence of global and functionally relevant changes in the EEG after cortisol infusion.

Study 1 (N = 26) established a rapid and bilateral perfusion decrease of 15.92 ml/100g/min in the thalamus within the first few minutes after cortisol infusion (19 % decrease relative to the absolute average baseline). Study 2 (N = 9) replicated this effect in the bilateral thalamus during the first seven minutes after infusion by quantifying a perfusion decrease of 13.45 ml/100g/min (or 17.9 % relative to baseline). However, Study 2 could not replicate the perfusion effect in the second measurement block (10-17 minutes post-infusion). This may be caused by sample specific increases in error variance since the statistical power in Study 2 was actually higher than in Study 1 and a number of ROIs showed close to statistically significant effects which makes it is possible that glucocorticoids have additional, smaller, but here-unreported effects that may include the caudate nucleus and the secondary ROIs of Study 1 (Chapter 2.3.3). Another replication attempt on another group of participants would likely clear up this uncertainty. Nevertheless, the timeframe of the CBF effects that were found by Study 1 and 2 give reasons to exclude currently known genomic mechanisms of cortisol action and points towards non-genomic cortisol mechanisms as a source for these CBF effects.

Hemodynamic effects of glucocorticoids on the thalamus have not yet been reported after pharmacological infusions in humans. A recent study from Wang (J. Wang et al., 2005), however, established a perfusion increase in the thalamus after a psychological stress challenge (mental arithmetic task) in healthy adults that is known to lead to endogenous cortisol secretion. Importantly, the blinded pharmacological cortisol infusion of all three presented studies mimics just one aspect of a genuine (psycho-physiological) stress manipulation (that would involve emotional, cognitive, ANS, and endocrine activation) and, therefore, prevents a direct comparison to Wang's results. The only study that reported rapid effects on the thalamus after glucocorticoid infusion was

by Ferris and Stolberg (2010) who described the existence of a BOLD effect during the first five minutes after glucocorticoid infusion in rats. However, this effect was not further evaluated nor discussed.

Thalamic nuclei play a crucial role in the adaptation to challenges by modulating thalamocortical and corticocortical communication (Guillery & Sherman, 2002; S. M. Sherman, 2007; S. M. Sherman & Guillery, 2002; Theyel, Llano, & Sherman, 2010). The spatial resolution of the CASL CBF images unfortunately does not justify a reliable localization of functionally distinct thalamic nuclei. In general, however, thalamic functioning has been tied to processes of attention, consciousness, and arousal (Newman, 1995; Portas, et al., 1998; Sarter, et al., 2001), and sensorimotor integration and anticipation (Brunia, 1999; Newman, 1995). Thalamic functioning has been causally linked to EEG activity (Hughes & Crunelli, 2005; Lopes da Silva, 1991; Nunez, Wingeier, & Silberstein, 2001; Steriade, et al., 1990) and, therefore, constitutes a possible origin for glucocorticoid induced effects on EEG.

The EEG results of Study 3 (N = 13) established rapid, widely distributed and long lasting changes in signal strength and map complexity of EEG resting activity (Figure 4.3.1) which have also not previously been reported after cortisol infusion. Relative to baseline and for all three post-infusion measurements (up to 27 minutes post infusion), signal strength and map complexity decreased in the cortisol compared to the placebo condition. The early onset of the effects on EEG also implies the action of non-genomic cortisol mechanisms. However, it is theoretically possible that later effects (> 20 minutes) may in part be supplemented through genomic mechanisms.

The cortisol induced decrease in EEG signal strength suggests that cortisol acts on global cortical functioning by dampening global brain activity patterns instead of influencing an isolated region or process. This effect may support adaptation to environmental challenges because it moderates the cortical processing-load that typically increases during a stressful situation (stressors are known to increase cognitive and emotional processing; see, Pruessner et al., 2010), thereby protecting the brain as a whole from a state of processing over-load. A down-tuning of non-relevant *background* processing may deliberate cognitive resources and ultimately improve the processing of potentially important and demand specific sensory inputs. Shifts of cognitive operating

capacities may result in faster detection of stimulus-response contingencies such as a recent report on trace eyeblink conditioning implies (Kuehl, et al., 2010). Furthermore, it may result in a relative enhanced (less inhibition) processing of startling danger signals (Richter, et al., 2011). In addition, decreases in map complexity in the cortisol condition indicate an enhanced spatial similarity of neuronal activity and indicate a more focused processing.

Future studies may reach beyond the here-implemented exploratory design by focusing on relevant behavioral or physiological measurements that characterize the suggested glucocorticoid induced functional stream-lining. For example, the down-tuning of non-relevant background activation may improve signal-to-noise ratios for visual evoked potential or auditory evoked potentials of the EEG. It also remains to be shown if the cortisol induced thalamic effects are indeed linked to the changes in signal strength and map complexity, but the apparent implications for understanding normal (and eventually pathological) stress responses in humans makes this worth further investigation. In summary, the observed glucocorticoid induced changes on EEG suggest a rapid, non-genomic neuro-modulatory effect that streamlines global neuronal functioning towards effective adaptation to stressors.

The immediate biological interpretation of the results must remain in the context of a pharmacological glucocorticoid infusion. During a genuine (natural) stress response, a vast array of additional endocrine, ANS, and cognitive aspects are triggered and result in behavioral patterns that are characteristic for coping with stress. It is theoretically possible that these genuine stress responses counteract (i.e. cover-up) the pharmacological glucocorticoid actions. However, the lack of studies that apply cortisol infusions in humans makes it difficult to conclusively assess if such counteracting takes place and which particular aspects of experimental interventions (i.e. aspects of a genuine stressor) are necessary to elicit effects in brain regions other than the thalamus. In addition, a growing number of evidence is accumulating which suggests that men and women might utilize different psychological and physiological coping mechanisms (e.g. J. Wang, et al., 2007). It may therefore be possible that the reported effects of cortisol are specific to men, which demands for replication studies in women.

The physiological origins of the observed changes in CBF can be twofold. For one, glucocorticoids may hypothetically act on the vascular resistance on the levels of arterioles which would influence the post arteriole blood flow (Gros et al., 2007). A second and more plausible origin for glucocorticoid induced changes in CBF is its effect on neuronal cell activity (by influencing neuronal cell metabolism). A glucocorticoid mediated decrease in neuronal activity would decrease metabolic needs and cause reduced CBF. The specific endocrine pathways by which glucocorticoids can rapidly and non-genomically influence such changes in neuronal cell activity, however, remain still under investigation (for an overview of possible pathways in animal models see, Groeneweg, et al., 2011).

The observed changes in EEG signal strength and map complexity must be related to changes in neuronal activity, however, the effect cannot be statistically linked to changes in the thalamus since both effects were assessed separately and in different participants. Therefore, the induced changes in signal strength and map complexity may also be linked to direct glucocorticoid-action on individual neuronal cells. Simultaneous EEG-MRI measurements seem well suited to further investigate the interaction of cortisol induced electrophysiological and hemodynamic effects.

In contrast to previous research in humans, the three here-presented studies were specifically designed to explore rapid, non-genomic CNS effects of cortisol. The relatively modest infusions of 4 mg cortisol are within a plausible physiological range (for a discussion on plausible ranges see, Richter, et al., 2011) and are much lower than in other investigations. It is reasonable to assume that until systematic dose escalation studies have found otherwise, non-physiological doses of glucocorticoids lead to non-physiological effects on the CNS. In addition, all three studies were designed to avoid mental stress (e.g. extended waiting period after placing intravenous infusion line), ANS activation, and arousal, while employing a double-blinded design; therefore, minimizing influences of potentially confounding variables. Furthermore, effects of glucocorticoid infusion were measured under resting conditions, i.e. a physiological baseline (Gusnard & Raichle, 2001), which avoided any event-related (evoked) experimental stimulation that could cover-up or counteract pharmacological glucocorticoid actions. Non-invasive methods, such as CASL, were used to avoid psychological stress from the application of

tracer substances. In addition, the strength of CASL sequences is their ability to accurately assess absolute CNS perfusion during resting conditions (i.e. intrinsic, non-event-related activation) which distinguishes them from more commonly applied BOLD fMRI protocols (see, Raichle & Snyder, 2007 for advantages of resting state analyses).

The identification of non-genomic cortisol effects in humans provides a valuable first insight into how glucocorticoids affect the early stages of the stress response which adds to our general ability to more fully understand the normal human stress response and eventually its pathological extremes.

In conclusion, the presented results are the first to coherently suggest that a physiologically plausible amount of cortisol profoundly affects functioning and perfusion of the human CNS *in vivo* by a rapid, non-genomic mechanism. The observed changes in neuronal functioning suggest that cortisol may act on the thalamic relay of non-relevant background as well as on task specific sensory information in order to facilitate the adaptation to stress challenges.

APPENDIX A

	regions of interest (ROI)
primary ROIs	
subcortical gray	amygdala
	caudata nucleus
	insula
	lenticular nucleus, putamen
	lenticular nucleus, pallidum
	thalamus
limbic lobe	temporal pole: superior temporal gyrus
	temporal pole: middle temporal gyrus
	anterior cingulate and paracingulate gyri
	median cingulate and paracingulate gyri
	posterior cingulate gyrus
	hippocampus
	parahippocampal gyrus
secondary ROIs	
frontal lobe	lateral surface, superior frontal gyrus, dorsolateral
	lateral surface, middle frontal gyrus
	lateral surface, inferior frontal gyrus, opercular part
	lateral surface, inferior frontal gyrus, triangular part
	medial surface, superior frontal gyrus, medial
	medial surface, supplementary motor area
	medial surface, paracentral lobule
	orbital surface, superior frontal gyrus, orbital part
	orbital surface, superior frontal gyrus, medial part
	orbital surface, middle frontal gyrus, orbital part
	orbital surface, inferior frontal gyrus, orbital part
	orbital surface, gyrus rectus
	orbital surface, olfactory cortex
temporal lobe	lateral surface, superior temporal gyrus
	lateral surface, henschl gyrus
	lateral surface, middle temporal gyrus
	lateral surface, inferior temporal gyrus
central region	precentral gyrus
	postcentral gyrus
	rolandic operculum
parietal lobe	lateral surface, superior parietal gyrus
	lateral surface, inferior parietal, but supramarginal & angular gyri
	lateral surface, angular gyrus
	lateral, supramarginal gyrus
	medial surface, precuneus
occipital lobe	lateral surface, superior occipital gyrus
	lateral surface, middle occipital gyrus
	lateral surface, inferior occipital gyrus
	medial and inferior surface, cuneus
	medial and inferior surface, calcarine fissure & surrounding cortex
	medial and inferior surfaces, lingual gyrus
	medial and inferior surfaces, fusiform gyrus

APPENDIX B

A Post-hoc power analysis was performed for Study 1 and Study 2 using G*POWER (Buchner, et al., 2009) with the option '*Generic F test*' that returns exact power values after entering the degrees of freedom for the effect and error terms, and the non-centrality parameter lambda (ʎ). The decrees of freedom and ʎ for Study 1 and 2 were determined for the ANOVA interaction INTERVENTION x REGION x MEASUREMENT BLOCK following the forms of Rasch and colleagues (2010).

For both studies, the factor INTERVENTION had two levels (p), REGION had six levels (q) (see Appendix A), and MEASUREMENT BLOCK had three levels (r). Both studies also contained a forth factor, HEMISPHERE, with another two levels (t). However, in Study 1, INTERVENTION was a between subject variable (group variable), whereas Study 2 applied a completely within subject design.

Study 1

The number of participants (n) per group was 13 and the empirical F-value equaled 2.447 (see Table 2.3.1).

Equation	Calculation
$df_{effect} = (p-1) \cdot (q-1) \cdot (r-1)$	$df_{effect} = (2-1) \cdot (6-1) \cdot (3-1) = 10$
$df_{error} = p \cdot (q-1) \cdot (r-1) \cdot (n-1)$	$df_{error} = 2 \cdot (6-1) \cdot (3-1) \cdot (13-1) = 240$
$n_{obs} = p \cdot q \cdot r \cdot n$	$n_{obs} = 2 \cdot 6 \cdot 3 \cdot 13 = 468$
$f^2 = \frac{df_{effect} \cdot (F_{empirical} - 1)}{n_{obs}}$	$f^2 = \frac{10 \cdot (2.447 - 1)}{468} = 0.030918$
$\lambda = f^2 \cdot n_{obs}$	$\lambda = 0.030918 \cdot 468 = 14.47$

Entering ʎ = 14.47, df_{effect} = 10 and df_{error} = 240 in G*POWER (*Generic F test*) results in:

Critical F = 1.8702953

β error probability = 0.2790652

Power (1-β error probability) = 0.7209348

Study 2

The number of participants (n) was 9 in total and the assumed effect variance was Ω^2 = 3 %, which is close to (but slightly larger than) the empirical effect of Study 1 (see above).

Equation	Calculation
$df_{effect} = (p-1) \cdot (q-1) \cdot (r-1)$	$df_{effect} = (2-1) \cdot (6-1) \cdot (3-1) = 10$
$df_{error} = (p-1) \cdot (q-1) \cdot (r-1) \cdot (n-1)$	$df_{error} = (2-1) \cdot (6-1) \cdot (3-1) \cdot (9-1) = 80$
$n_{obs} = p \cdot q \cdot r \cdot t \cdot n$	$n_{obs} = 2 \cdot 6 \cdot 3 \cdot 2 \cdot 9 = 648$
$\Phi^2 = \frac{\Omega^2}{1-\Omega^2}$	$\Phi^2 = \frac{0.03}{1-0.03} = 0.030927$
$\lambda = \Phi^2 \cdot n_{obs}$	$\lambda = 0.03927 \cdot 648 = 20.04123$

Entering ʎ = 20.041, df_{effect} = 10 and df_{error} = 80 in G*POWER (*Generic F test*) results in:

Critical F = 1.9512203

β error probability = 0.1537089

Power (1-β error probability) = 0.8462911

The statistical power, i.e. the probability to correctly accept the alternative hypothesis, is much larger in Study 2 than in Study 1. In other words, the probability to falsely accept the null hypothesis (beta-error) is larger in Study 1 than it is in Study 2. Therefore, Study 2 may well find all statistical effects that were uncovered with the statistical analyses of Study 1. It is also important to note, that the small effect sizes are related to the statistical effect of the entire interaction INTERVENTION x REGION x MEASUREMENT BLOCK. The statistical effects within the (e.g. subcortical) ROIs would be much larger when calculated based on individual post-hoc comparisons.

REFERENCES

Alsop, D. C., & Detre, J. A. (1996). Reduced transit-time sensitivity in noninvasive magnetic resonance imaging of human cerebral blood flow. *J Cereb Blood Flow Metab, 16*(6), 1236-1249.

Basar, E., Rahn, E., Demiralp, T., & Schurmann, M. (1998). Spontaneous EEG theta activity controls frontal visual evoked potential amplitudes. *Electroencephalogr Clin Neurophysiol, 108*(2), 101-109.

Bell, A. J., & Sejnowski, T. J. (1995). An information-maximization approach to blind separation and blind deconvolution. *Neural Comput, 7*(6), 1129-1159.

Bergmeir. (2005). Independent Component Analysis Retrieved April, 20th 2011, from http://www.informatik.uni-ulm.de/ni/Lehre/SS05/HauptseminarMustererkennung/ausarbeitungen/Bergmeir.pdf

Bloomfield, P. (1976). *Fourier Analysis of Time Series: An Introduction*. New -york: John Wiley and Sons, Inc.

Brunia, C. H. (1999). Neural aspects of anticipatory behavior. *Acta Psychol (Amst), 101*(2-3), 213-242.

Buchner, A., Erdfelder, E., Faul, F., & Lang, A.-G. (2009). G*Power (Version 3.1.2). Düsseldorf: Universität Düsseldorf. Retrieved from http://www.psycho.uni-duesseldorf.de/abteilungen/aap/gpower3/

Chatrian, G. E., Lettich, E., & Nelson, P. L. (1988). Modified nomenclature for the "10%" electrode system. *J Clin Neurophysiol, 5*(2), 183-186.

Cohen, J. (1988). *Statistical power analysis for the behavioral sciences*. Hilldale, New York: Erlbaum.

Coirini, H., Marusic, E. T., De Nicola, A. F., Rainbow, T. C., & McEwen, B. S. (1983). Identification of mineralocorticoid binding sites in rat brain by competition studies and density gradient centrifugation. *Neuroendocrinology, 37*(5), 354-360.

Cullinan, W. E., Herman, J. P., Battaglia, D. F., Akil, H., & Watson, S. J. (1995). Pattern and time course of immediate early gene expression in rat brain following acute stress. *Neuroscience, 64*(2), 477-505.

Dallman, M. F. (2005). Fast glucocorticoid actions on brain: back to the future. *Front Neuroendocrinol, 26*(3-4), 103-108.

de Kloet, E. R., Joels, M., & Holsboer, F. (2005). Stress and the brain: from adaptation to disease. *Nat Rev Neurosci, 6*(6), 463-475.

de Kloet, E. R., Oitzl, M. S., & Joels, M. (1999). Stress and cognition: are corticosteroids good or bad guys? *Trends Neurosci, 22*(10), 422-426.

De Kloet, E. R., Veldhuis, H. D., Wagenaars, J. L., & Bergink, E. W. (1984). Relative binding affinity of steroids for the corticosterone receptor system in rat hippocampus. *J Steroid Biochem, 21*(2), 173-178.

De Kloet, E. R., Vreugdenhil, E., Oitzl, M. S., & Joels, M. (1998). Brain corticosteroid receptor balance in health and disease. *Endocr Rev, 19*(3), 269-301.

de Munck, J. C., Goncalves, S. I., Huijboom, L., Kuijer, J. P., Pouwels, P. J., Heethaar, R. M., & Lopes da Silva, F. H. (2007). The hemodynamic response of the alpha rhythm: an EEG/fMRI study. *Neuroimage, 35*(3), 1142-1151.

Debener, S., Hine, J., Bleeck, S., & Eyles, J. (2008). Source localization of auditory evoked potentials after cochlear implantation. *Psychophysiology, 45*(1), 20-24.

Debener, S., Thorne, J., Schneider, T. R., & Viola, F. C. (2010). Using ICA for Analyses of Multi-Channel EEG Data. In M. Ullsperger & S. Debener (Eds.), *Simultaneous EEG and FMRI* (pp. 138-150). Oxford: Oxford University Press.

Debener, S., Ullsperger, M., Siegel, M., & Engel, A. K. (2006). Single-trial EEG-fMRI reveals the dynamics of cognitive function. *Trends Cogn Sci, 10*(12), 558-563.

Dedovic, K., Duchesne, A., Andrews, J., Engert, V., & Pruessner, J. C. (2009). The brain and the stress axis: the neural correlates of cortisol regulation in response to stress. *Neuroimage, 47*(3), 864-871.

Detre, J. A., Leigh, J. S., Williams, D. S., & Koretsky, A. P. (1992). Perfusion imaging. *Magn Reson Med, 23*(1), 37-45.

Dressendorfer, R. A., Kirschbaum, C., Rohde, W., Stahl, F., & Strasburger, C. J. (1992). Synthesis of a cortisol-biotin conjugate and evaluation as a tracer in an immunoassay for salivary cortisol measurement. *J Steroid Biochem Mol Biol, 43*(7), 683-692.

Dryden, T., & Fitch, P. (2000). Recovering Body and Soul from Post-Traumatic Stess Disorder Retrieved April 2nd, 2011, from http://www.amtamassage.org/articles/3/MTJ/detail/1817

Dumermuth, G., & Molinari, L. (1987). Spectral analysis of the EEG. Some fundamentals revisited and some open problems. *Neuropsychobiology, 17*(1-2), 85-99.

Dunn, O. J. (1961). Multiple comparison among means. *Journal of the American Statistical Association, 56*, 52-64.

Duong, T. Q., Kim, D. S., Ugurbil, K., & Kim, S. G. (2001). Localized cerebral blood flow response at submillimeter columnar resolution. *Proc Natl Acad Sci U S A, 98*(19), 10904-10909.

Edelman, R. R., Siewert, B., Darby, D. G., Thangaraj, V., Nobre, A. C., Mesulam, M. M., & Warach, S. (1994). Qualitative mapping of cerebral blood flow and functional localization with echo-planar MR imaging and signal targeting with alternating radio frequency. *Radiology, 192*(2), 513-520.

Evanson, N. K., Herman, J. P., Sakai, R. R., & Krause, E. G. (2010). Nongenomic actions of adrenal steroids in the central nervous system. *J Neuroendocrinol, 22*(8), 846-861.

Feige, B., Scheffler, K., Esposito, F., Di Salle, F., Hennig, J., & Seifritz, E. (2005). Cortical and subcortical correlates of electroencephalographic alpha rhythm modulation. *J Neurophysiol, 93*(5), 2864-2872.

Ferris, C. F., & Stolberg, T. (2010). Imaging the immediate non-genomic effects of stress hormone on brain activity. *Psychoneuroendocrinology, 35*(1), 5-14.

Friston, K. J., Ashburner, J., Frith, C., Poline, J. B., Heather, J. D., & Frackowiak, R. S. J. (1995). Spatial registration and normalization of images. *Hum Brain Mapp 2*, 165–189.

Friston, K. J., Holmes, A. P., J., W. K., J.-P., P., C.D., F., & Frackowiak, R. S. J. (1995). Statistical parametric maps in functional imaging: a general linear approach. *Hum Brain Mapp, 2*, 189-210.

Gasser, T., Bacher, P., & Mocks, J. (1982). Transformations towards the normal distribution of broad band spectral parameters of the EEG. *Electroencephalogr Clin Neurophysiol, 53*(1), 119-124.

Goense, J., & Logothetis, N. K. (2010). Physiological Basis of the BOLD Signal. In M. Ullsperger & S. Debener (Eds.), *Simultanous EEG and fMRI* (1st ed., pp. 21-45). Oxford, New York: Oxford University Press.

Goncalves, S. I., de Munck, J. C., Pouwels, P. J., Schoonhoven, R., Kuijer, J. P., Maurits, N. M., . . . Lopes da Silva, F. H. (2006). Correlating the alpha rhythm to BOLD using simultaneous EEG/fMRI: inter-subject variability. *Neuroimage, 30*(1), 203-213.

Grillon, C., Smith, K., Haynos, A., & Nieman, L. K. (2004). Deficits in hippocampus-mediated Pavlovian conditioning in endogenous hypercortisolism. *Biol Psychiatry, 56*(11), 837-843.

Groeneweg, F. L., Karst, H., de Kloet, E. R., & Joels, M. (2011). Rapid non-genomic effects of corticosteroids and their role in the central stress response. *J Endocrinol*.

Gros, R., Ding, Q., Armstrong, S., O'Neil, C., Pickering, J. G., & Feldman, R. D. (2007). Rapid effects of aldosterone on clonal human vascular smooth muscle cells. *Am J Physiol Cell Physiol, 292*(2), C788-794.

Guillery, R. W., & Sherman, S. M. (2002). The thalamus as a monitor of motor outputs. *Philos Trans R Soc Lond B Biol Sci, 357*(1428), 1809-1821.

Gusnard, D. A., & Raichle, M. E. (2001). Searching for a baseline: functional imaging and the resting human brain. *Nat Rev Neurosci, 2*(10), 685-694.

Haller, J., Mikics, E., & Makara, G. B. (2008). The effects of non-genomic glucocorticoid mechanisms on bodily functions and the central neural system. A critical evaluation of findings. *Front Neuroendocrinol, 29*(2), 273-291.

Hermes, M., Hagemann, D., Britz, P., Lieser, S., Bertsch, K., Naumann, E., & Walter, C. (2009). Latent state-trait structure of cerebral blood flow in a resting state. *Biol Psychol, 80*(2), 196-202.

Hermes, M., Hagemann, D., Britz, P., Lieser, S., Rock, J., Naumann, E., & Walter, C. (2007). Reproducibility of continuous arterial spin labeling perfusion MRI after 7 weeks. *MAGMA, 20*(2), 103-115.

Herscovitch, P., & Raichle, M. E. (1985). What is the correct value for the brain--blood partition coefficient for water? *J Cereb Blood Flow Metab, 5*(1), 65-69.

Hewig, J., Schlotz, W., Gerhards, F., Breitenstein, C., Lurken, A., & Naumann, E. (2008). Associations of the cortisol awakening response (CAR) with cortical activation asymmetry during the course of an exam stress period. *Psychoneuroendocrinology, 33*(1), 83-91.

Holm, S. (1979). A Simple Sequentially Rejective Multiple Test Procedure. *Scandinavian Journal of Statistics, 6*, 65-70.

Hopfiner, J. B., Khoe, W., & Song, A. (2005). Combining Electrophyiology with Structural and Functional Neuroimaging: ERPs, PET, MRI, and fMRI. In T. Handy (Ed.), *Event-Related Potentials* (pp. 345-379). Cambridge: The MIT Press.

Hsieh, P. F., & Watanabe, Y. (2000). Time course of c-FOS expression in status epilepticus induced by amygdaloid stimulation. *Neuroreport, 11*(3), 571-574.

Hughes, S. W., & Crunelli, V. (2005). Thalamic mechanisms of EEG alpha rhythms and their pathological implications. *Neuroscientist, 11*(4), 357-372.

Hyvarinen, A., Karhunen, J., & Oja, E. (2001). *Independent Component Analysis*. New York: John Wiley & Sons, Inc.

Ikeda, J., Nakajima, T., Osborne, O. C., Mies, G., & Nowak, T. S., Jr. (1994). Coexpression of c-fos and hsp70 mRNAs in gerbil brain after ischemia: induction threshold, distribution and time course evaluated by in situ hybridization. *Brain Res Mol Brain Res, 26*(1-2), 249-258.

Joels, M., & de Kloet, E. R. (1994). Mineralocorticoid and glucocorticoid receptors in the brain. Implications for ion permeability and transmitter systems. *Prog Neurobiol, 43*(1), 1-36.

Jung, T. P., Makeig, S., Humphries, C., Lee, T. W., McKeown, M. J., Iragui, V., & Sejnowski, T. J. (2000). Removing electroencephalographic artifacts by blind source separation. *Psychophysiology, 37*(2), 163-178.

Jung, T. P., Makeig, S., Westerfield, M., Townsend, J., Courchesne, E., & Sejnowski, T. J. (2000). Removal of eye activity artifacts from visual event-related potentials in normal and clinical subjects. *Clin Neurophysiol, 111*(10), 1745-1758.

Kim, J. J., & Diamond, D. M. (2002). The stressed hippocampus, synaptic plasticity and lost memories. *Nat Rev Neurosci, 3*(6), 453-462.

Kim, S. G. (1995). Quantification of relative cerebral blood flow change by flow-sensitive alternating inversion recovery (FAIR) technique: application to functional mapping. *Magn Reson Med, 34*(3), 293-301.

Kim, S. G., Jin, T., & Fukuda, M. (2010). Spatial Resolution of fMRI Techniques. In S. Ulmer & O. Jansen (Eds.), *fMRI - Basics and Clinical Applications* (pp. 15-22). Heidelberg: Springer.

Kim, T., & Kim, S. G. (2005). Quantification of cerebral arterial blood volume and cerebral blood flow using MRI with modulation of tissue and vessel (MOTIVE) signals. *Magn Reson Med, 54*(2), 333-342.

Koenig, T., & Gianotti, L. R. R. (2009). Scalp field maps and their characterization. In C. M. Michel, T. Koenig, D. Brandeis, L. R. R. Gianotti & J. Wackermann (Eds.), *Electrical Neuroimaging* (pp. 25-47). Cambridge: Cambridge University Press.

Kuehl, L. K., Lass-Hennemann, J., Richter, S., Blumenthal, T. D., Oitzl, M., & Schachinger, H. (2010). Accelerated trace eyeblink conditioning after cortisol IV-infusion. *Neurobiol Learn Mem, 94*(4), 547-553.

Kwong, K. K., Chesler, D. A., Weisskoff, R. M., Donahue, K. M., Davis, T. L., Ostergaard, L., . . . Rosen, B. R. (1995). MR perfusion studies with T1-weighted echo planar imaging. *Magn Reson Med, 34*(6), 878-887.

Laufs, H., Kleinschmidt, A., Beyerle, A., Eger, E., Salek-Haddadi, A., Preibisch, C., & Krakow, K. (2003). EEG-correlated fMRI of human alpha activity. *Neuroimage, 19*(4), 1463-1476.

Lee, S. P., Silva, A. C., & Kim, S. G. (2002). Comparison of diffusion-weighted high-resolution CBF and spin-echo BOLD fMRI at 9.4 T. *Magn Reson Med, 47*(4), 736-741.

Lehmann, D., Ozaki, H., & Pal, I. (1987). EEG alpha map series: brain micro-states by space-oriented adaptive segmentation. *Electroencephalogr Clin Neurophysiol, 67*(3), 271-288.

Lehmann, D., & Skrandies, W. (1980). Reference-free identification of components of checkerboard-evoked multichannel potential fields. *Electroencephalogr Clin Neurophysiol, 48*(6), 609-621.

Lopes da Silva, F. (1991). Neural mechanisms underlying brain waves: from neural membranes to networks. *Electroencephalogr Clin Neurophysiol, 79*(2), 81-93.

Lovallo, W. R., Robinson, J. L., Glahn, D. C., & Fox, P. T. (2009). Acute effects of hydrocortisone on the human brain: An fMRI study. *Psychoneuroendocrinology*.

Makara, G. B., & Haller, J. (2001). Non-genomic effects of glucocorticoids in the neural system. Evidence, mechanisms and implications. *Prog Neurobiol, 65*(4), 367-390.

Makeig, S., Bell, A. J., Jung, T. P., & Sejnowski, T. J. (1996). Independent component analysis of electroencephalographic data. In D. Touretzky, M. Mozer & M. Hasselmo (Eds.), *Advances in Neural Information Processing Systems* (Vol. 8, pp. 145–151). Cambridge: MIT Press.

Makeig, S., Westerfield, M., Jung, T. P., Enghoff, S., Townsend, J., Courchesne, E., & Sejnowski, T. J. (2002). Dynamic brain sources of visual evoked responses. *Science, 295*(5555), 690-694.

McEwen, B. S., & Sapolsky, R. M. (1995). Stress and cognitive function. *Curr Opin Neurobiol, 5*(2), 205-216.

Mikics, E., Kruk, M. R., & Haller, J. (2004). Genomic and non-genomic effects of glucocorticoids on aggressive behavior in male rats. *Psychoneuroendocrinology, 29*(5), 618-635.

Moosmann, M., Ritter, P., Krastel, I., Brink, A., Thees, S., Blankenburg, F., . . . Villringer, A. (2003). Correlates of alpha rhythm in functional magnetic resonance imaging and near infrared spectroscopy. *Neuroimage, 20*(1), 145-158.

Newman, J. (1995). Thalamic contributions to attention and consciousness. *Conscious Cogn, 4*(2), 172-193.

Nishi, M., Takenaka, N., Morita, N., Ito, T., Ozawa, H., & Kawata, M. (1999). Real-time imaging of glucocorticoid receptor dynamics in living neurons and glial cells in comparison with non-neural cells. *Eur J Neurosci, 11*(6), 1927-1936.

Nunez, P. L., Wingeier, B. M., & Silberstein, R. B. (2001). Spatial-temporal structures of human alpha rhythms: theory, microcurrent sources, multiscale measurements, and global binding of local networks. *Hum Brain Mapp, 13*(3), 125-164.

Oguz, K. K., Golay, X., Pizzini, F. B., Freer, C. A., Winrow, N., Ichord, R., . . . Melhem, E. R. (2003). Sickle cell disease: continuous arterial spin-labeling perfusion MR imaging in children. *Radiology, 227*(2), 567-574.

Onton, J., Westerfield, M., Townsend, J., & Makeig, S. (2006). Imaging human EEG dynamics using independent component analysis. *Neurosci Biobehav Rev, 30*(6), 808-822.

Packard, M. G., & Knowlton, B. J. (2002). Learning and memory functions of the Basal Ganglia. *Annu Rev Neurosci, 25*, 563-593.

Popper, K. (1959). *The Logic of Scientific Discovery*. New York, NY: Routledge Classics.

Portas, C. M., Rees, G., Howseman, A. M., Josephs, O., Turner, R., & Frith, C. D. (1998). A specific role for the thalamus in mediating the interaction of attention and arousal in humans. *J Neurosci, 18*(21), 8979-8989.

Pruessner, J. C., Dedovic, K., Pruessner, M., Lord, C., Buss, C., Collins, L., . . . Lupien, S. J. (2010). Stress regulation in the central nervous system: evidence from structural

and functional neuroimaging studies in human populations - 2008 Curt Richter Award Winner. *Psychoneuroendocrinology, 35*(1), 179-191.

Rahn, E., & Basar, E. (1993a). Enhancement of visual evoked potentials by stimulation during low prestimulus EEG stages. *Int J Neurosci, 72*(1-2), 123-136.

Rahn, E., & Basar, E. (1993b). Prestimulus EEG-activity strongly influences the auditory evoked vertex response: a new method for selective averaging. *Int J Neurosci, 69*(1-4), 207-220.

Raichle, M. E., & Snyder, A. Z. (2007). A default mode of brain function: a brief history of an evolving idea. *Neuroimage, 37*(4), 1083-1090; discussion 1097-1089.

Rasch, B., Friese, M., Hofmann, W., & Naumann, E. (2010). *Quantitative Methoden* (3rd ed. Vol. 2). Heidelberg: Springer.

Ravetz. (1971). *Scientific Knowledge and its Social Problems*. Oxford: Clarendon Press.

Ray, W. J., & Cole, H. W. (1985). EEG alpha activity reflects attentional demands, and beta activity reflects emotional and cognitive processes. *Science, 228*(4700), 750-752.

Richter, S., Schulz, A., Zech, C. M., Oitzl, M. S., Daskalakis, N. P., Blumenthal, T. D., & Schachinger, H. (2011). Cortisol rapidly disrupts prepulse inhibition in healthy men. *Psychoneuroendocrinology, 36*(1), 109-114.

Robbins, T. W. (2007). Shifting and stopping: fronto-striatal substrates, neurochemical modulation and clinical implications. *Philos Trans R Soc Lond B Biol Sci, 362*(1481), 917-932.

Roberts, D. A., Rizi, R., Lenkinski, R. E., & Leigh, J. S., Jr. (1996). Magnetic resonance imaging of the brain: blood partition coefficient for water: application to spin-tagging measurement of perfusion. *J Magn Reson Imaging, 6*(2), 363-366.

Robertson, N. M., Schulman, G., Karnik, S., Alnemri, E., & Litwack, G. (1993). Demonstration of nuclear translocation of the mineralocorticoid receptor (MR)

using an anti-MR antibody and confocal laser scanning microscopy. *Mol Endocrinol, 7*(9), 1226-1239.

Sanchez, M. M., Young, L. J., Plotsky, P. M., & Insel, T. R. (2000). Distribution of corticosteroid receptors in the rhesus brain: relative absence of glucocorticoid receptors in the hippocampal formation. *J Neurosci, 20*(12), 4657-4668.

Sapolsky, R. M. (1996). Stress, Glucocorticoids, and Damage to the Nervous System: The Current State of Confusion. *Stress, 1*(1), 1-19.

Sarter, M., Givens, B., & Bruno, J. P. (2001). The cognitive neuroscience of sustained attention: where top-down meets bottom-up. *Brain Res Brain Res Rev, 35*(2), 146-160.

Selye, H. (1936). A Syndrome produced by Diverse Nocuous Agents. *Nature, 138*, 32.

Selye, H. (1950). Stress and the general adaptation syndrome. *Br Med J, 1*(4667), 1383-1392.

Sherman, S. M. (2007). The thalamus is more than just a relay. *Curr Opin Neurobiol, 17*(4), 417-422.

Sherman, S. M., & Guillery, R. W. (2002). The role of the thalamus in the flow of information to the cortex. *Philos Trans R Soc Lond B Biol Sci, 357*(1428), 1695-1708.

Sherman, S. M., & Guillery, R. W. (2006). *Exploring the Thalamus and Its Role in Cortical Function* (2nd ed.). Cambridge, Massachusetts: The MIT Press.

Spencer, S. J., Fox, J. C., & Day, T. A. (2004). Thalamic paraventricular nucleus lesions facilitate central amygdala neuronal responses to acute psychological stress. *Brain Res, 997*(2), 234-237.

Steriade, M., Gloor, P., Llinas, R. R., Lopes de Silva, F. H., & Mesulam, M. M. (1990). Report of IFCN Committee on Basic Mechanisms. Basic mechanisms of cerebral rhythmic activities. *Electroencephalogr Clin Neurophysiol, 76*(6), 481-508.

Stone, J. V. (2004). *Independent component analysis: a tutorial introduction*. Cambridge, MA: MIT Press.

Sutanto, W., van Eekelen, J. A., Reul, J. M., & de Kloet, E. R. (1988). Species-specific topography of corticosteroid receptor types in rat and hamster brain. *Neuroendocrinology, 47*(5), 398-404.

Theyel, B. B., Llano, D. A., & Sherman, S. M. (2010). The corticothalamocortical circuit drives higher-order cortex in the mouse. *Nat Neurosci, 13*(1), 84-88.

Tzourio-Mazoyer, N., Landeau, B., Papathanassiou, D., Crivello, F., Etard, O., Delcroix, N., . . . Joliot, M. (2002). Automated anatomical labeling of activations in SPM using a macroscopic anatomical parcellation of the MNI MRI single-subject brain. *Neuroimage, 15*(1), 273-289.

Ulrich-Lai, Y. M., & Herman, J. P. (2009). Neural regulation of endocrine and autonomic stress responses. *Nat Rev Neurosci, 10*(6), 397-409.

Ulrich, B. (2007). Sensaationelle Entdeckung - Steinlaus Endlich Gefunden Retrieved April 15th, 2011, from http://www.tu-dresden.de/biw/geotechnik/geologie/zulazuwei/steinlaus.htm

van Stegeren, A. H. (2009). Imaging stress effects on memory: a review of neuroimaging studies. *Can J Psychiatry, 54*(1), 16-27.

Viola, F. C., Thorne, J., Edmonds, B., Schneider, T., Eichele, T., & Debener, S. (2009). Semi-automatic identification of independent components representing EEG artifact. *Clin Neurophysiol, 120*(5), 868-877.

Walter, B., Blecker, C., Kirsch, P., Sammer, G., Schienle, A., Stark, R., & Vaitl, D. (2003). *MARINA: An esay to use tool for creation of MAsks for Region of INterest Analyses.*

Paper presented at the 9th International Conference on Functional Mapping of the Human Brain, New York, NY.

Wang, J., Korczykowski, M., Rao, H., Fan, Y., Pluta, J., Gur, R. C., . . . Detre, J. A. (2007). Gender difference in neural response to psychological stress. *Soc Cogn Affect Neurosci, 2*(3), 227-239.

Wang, J., Rao, H., Wetmore, G. S., Furlan, P. M., Korczykowski, M., Dinges, D. F., & Detre, J. A. (2005). Perfusion functional MRI reveals cerebral blood flow pattern under psychological stress. *Proc Natl Acad Sci U S A, 102*(49), 17804-17809.

Wang, Z., Aguirre, G. K., Rao, H., Wang, J., Fernandez-Seara, M. A., Childress, A. R., & Detre, J. A. (2008). Empirical optimization of ASL data analysis using an ASL data processing toolbox: ASLtbx. *Magn Reson Imaging, 26*(2), 261-269.

Webster, J. C., & Cidlowski, J. A. (1999). Mechanisms of Glucocorticoid-receptor-mediated Repression of Gene Expression. *Trends Endocrinol Metab, 10*(10), 396-402.

Williams, D. S., Detre, J. A., Leigh, J. S., & Koretsky, A. P. (1992). Magnetic resonance imaging of perfusion using spin inversion of arterial water. *Proc Natl Acad Sci U S A, 89*(1), 212-216.

Wong, E. C., Buxton, R. B., & Frank, L. R. (1998). Quantitative imaging of perfusion using a single subtraction (QUIPSS and QUIPSS II). *Magn Reson Med, 39*(5), 702-708.

Ye, F. Q., Mattay, V. S., Jezzard, P., Frank, J. A., Weinberger, D. R., & McLaughlin, A. C. (1997). Correction for vascular artifacts in cerebral blood flow values measured by using arterial spin tagging techniques. *Magn Reson Med, 37*(2), 226-235.

EIDESSTATTLICHE ERKLÄRUNG

Hiermit erkläre ich, dass ich diese vorliegende Dissertation selbstständig verfasst und keine anderen als die angegebenen Quellen als Hilfsmittel verwendet habe. Zudem wurde die Arbeit an keiner anderen Universität zur Erlangung eines akademischen Grades eingereicht.

Trier, April 2011

Florian Strelzyk